COMPARISON OF THE OPTICAL POTENTIAL METHOD AND THE DISTORTED WAVE BORN APPROXIMATION METHOD IN ELECTRON – ATOM ELASTIC SCATTERING

By

KARIUKI PETER KINUTHIA
M. Sc. (PHYSICS)

I84/25565/2011

A Thesis is Submitted in Partial Fulfillment of the Requirements for the Award of the Degree of Doctor of Philosophy in the School of Pure and Applied Sciences of Kenyatta University

November, 2015

DECLARATION

This thesis is my original work and has not been presented for award of a degree in any other University.

Signature …… Date ……

Peter Kinuthia Kariuki (I84/25565/2011)

Department of Physics

We confirm that the candidate, under our supervision, carried out the work reported in this thesis.

Signature …… Date ……

Dr. C. S. Singh

Department of Physics

Kenyatta University

Signature …… Date ……

Prof. J. Okumu

Department of Physics

Kenyatta University

DEDICATION

This thesis is dedicated to my family, especially my daughter Sheila, and to all who have made this work possible.

ACKNOWLEDGEMENTS

I start by thanking our heavenly Father from whom all good things come. I am grateful to my Supervisor, Dr. C. S. Singh, for suggesting the problem and for his guidance. I also thank my supervisor Prof. J. Okumu for his helpful insights. I thank my dear parents, the late Dominic Kariuki and my mom, Lois Njoki, for the physics genes. I thank my lovely wife Annie, son Eugene, and daughter Sheila for their great company during the course of my studies. Finally financial assistance from the School of pure and Applied Sciences at Kenyatta University through the Dean's grant is also gratefully acknowledged.

TABLE OF CONTENTS

Chapter 2

Literature Review

Chapter 3

Methodology

Chapter 4

Results and Discussion

Chapter 5

Conclusions and Recommendations

LIST OF FIGURES

Page

LIST OF TABLES

Page

SYMBOLS

$f(\theta)$	Scattering amplitude
χ	Total wavefunction of the scattering electron
u_l	Radial wavefunction of the scattering electron
δ_l	Phase shift corresponding to u_l
σ	Integral cross section
H	Total Hamiltonian of the electron-atom system
H_T	Target atom Hamiltonian
E	Total energy of the electron-atom system
E'	Energy of the scattering electron
Ψ	Total wavefunction of the electron-atom system
$\wp_{oi}$	Exchange operator
A	Antisymmetrization operator
V	Electron-atom interaction potential
U_{opt}	The optical potential
U_{st}	The static potential
U_{ex}	Exchange potential
U_{pol}	Polarization potential
U_{abs}	Absorption potential
K	Kinetic energy operator
k	Momentum of the scattering electron
Δ	Average excitation energy

Y_{lm}	Spherical harmonic
P_l	Legendre polynomial
$P_{n_a l_a}$	Radial wavefunction of target atom
Z	Atomic number of the target atom
N	Number of electrons in the target atom
j_l	Spherical Bessel function
n_l	Spherical Neumann function
$\rho(r)$	Electron-charge density

ABBREVIATIONS

LS	Lippmann-Schwinger Equation
T-Matrix	Transition Matrix Element
OP	Optical Potential Method
DWBA	First order distorted wave Born approximation method
DWSB	Second order distorted wave Born approximation method
3CCO	Three state Coupled-Channels Optical Method
XPS	X-ray Photoelectron Spectroscopy
AES	Auger-Electron Spectroscopy
DCS	Differential Cross Section
ICS	Integral Cross Section
TCS	Total Cross Section
CCC	Convergent Close Coupling Method
ECS	Exterior Complex Scaling

ABSTRACT

The optical potential (OP) method has been widely used in electron-atom elastic scattering since for a given distorting potential, a solution valid to all orders of perturbation series can be obtained. The first-order distorted-wave Born approximation (DWBA) is only valid to first order. However by use of a distorting potential that accurately models the electron-atom interaction, the DWBA method can yield quite reliable results for elastic scattering and possibly for inelastic scattering as well. In this study, elastic differential cross sections (DCS) and integral cross sections (ICS) have been calculated using the OP method and the DWBA method for the alkali atoms sodium and potassium at intermediate electron-impact energies $E = 7 - 200eV$. In both methods, and for both atoms, distorting potentials in the form of the sum of the static potential, the local Furness-McCarthy exchange potential, a non-local polarization potential involving discrete excited states of the atoms, and a local absorption potential, have been used. For the sodium atom the 3p, 3d, 4s, and 4p, excited states were used in the polarization potential, while for the potassium atom 4p, 5p, 3d, and 5s, excited states were used. Exchange effects have also been incorporated in the distorted-wave Born approximation method through the exchange T-Matrix element. In doing so, the frozen-core approximation has been applied which allows for exchange between the incident electron and the valence atomic electron, as well as the core electrons. For both sodium and potassium the present differential cross sections in the OP and DWBA calculations are in very good agreement with various experimental DCS at small scattering angles at all electron-impact energies considered. This indicates that the optical potential used describes adequately polarization effects which influence small-angle scattering. It is found that the difference between the DWBA and OP methods increases with decrease in electron-impact energy. This difference is as a result of the exchange T-matrix element in the DWBA calculations. The difference between the two methods decreases as the distorting potential becomes more accurate (complete) as the DWBA calculations converge to the OP results. Comparison with available experimental and theoretical results shows the need to use a complex distorting potential to account for loss of flux into inelastic channels.

CHAPTER 1

INTRODUCTION

1.1 Background

Knowledge of electron-atom elastic-scattering is important for the development of theoretical models for quantitative analysis in Auger-electron spectroscopy (AES), X-ray photoelectron spectroscopy (XPES), electron microprobe analysis (EMA), and analytical electron microscopy (AEM) (Jablonski *et al.*, 2004). Since the development of quantum mechanics close to a century ago, many attempts have been made to formulate different approaches for solving electron-atom scattering problems that yield results in agreement with experimental data which has consistently been made available over a wide range of energies and for a variety of target atoms.

Electron-atom collision is a many-body problem. The Schrödinger equation which governs scattering processes has a known analytical solution only for a two-body problem. The implication of this is that even the simplest case of electron-hydrogen scattering, which is a three-body problem, can only be solved approximately. Some of the perturbative approaches that have been developed include the Born approximation, first and second order distorted wave Born approximations (DWBA and DWSB respectively), and the optical potential method (OP). Non – perturbative approaches include the close coupling approximation (CC), coupled-channels optical method (CCO), convergent close-coupling method (CCC), R-matrix (RM) method, and the exterior complex scaling (ECS) method.

When an electron collides with a target atom, scattering of the projectile electron may occur without loss of energy by the electron, giving rise to elastic scattering, or the atom may absorb energy from the projectile leading to excitation and ionization of the atom. This is known as inelastic scattering. The theoretical approach that has been widely used to study elastic scattering of electrons by atoms at the intermediate energy range above the ionization threshold of the atom, is the optical potential method which was first formulated by Mittlemann and Watson (1959). In this method the many-body elastic scattering problem is converted to a one-body problem of the projectile moving in a complex non-local potential. The formal optical potential involves a first order term that can be determined exactly, and a complex second order term in the form of an infinite sum over inelastic states which can only be evaluated approximately (Joachain, 1975). The complex model optical potential obtained consists of a static potential which is the average of the Coulomb potential experienced by the scattering electron, an exchange potential which is a consequence of the Pauli exclusion principle, the polarization potential resulting from the polarization of the target charge cloud in the presence of the projectile electron, and the absorption potential that accounts for removal of the projectile electrons from the elastic channel due to inelastic processes.

As noted by Yaqiu *et al*. (2011), the most straight forward theoretical approach that has produced reliable results for inelastic processes is the first order distorted wave Born approximation (DWBA) especially at high electron impact energies. Various DWBA formulations exist (Itikawa, 1986). In using the DWBA the form of the distorting potentials adopted is vital. In principle the choice of the distorting potential is rather arbitrary but various forms, such as the ground state average of the projectile – target potential, or a linear combination with the excited state average of the interaction potential, have been found to yield good agreement with experimental results (Itikawa, 1986). The DWBA method has an

advantage over the OP method in that it can be used to study elastic as well as inelastic processes. However for a given effective potential while the DWBA method is accurate to first order of perturbation theory, the OP method is valid to infinite order (Madison *et al*., 1995). With a judicious choice of a distorting potential, the DWBA method is likely to yield elastic electron-atom scattering data comparable to the OP method. It may also be possible to apply such a potential in the DWBA method to improve the method's description of electron-atom excitation and ionization processes (Balashov *et al*., 1989).

Both the OP and DWBA methods give reliable electron-atom collision data using relatively modest computational resources. While the OP method involves solving the Schrödinger equation in coordinate space, the DWBA method involves solving the equation in momentum space. The OP and DWBA methods are thus related to the R-matrix and CCC methods respectively which are two of the most sophisticated methods in current use. In the R-matrix method (Zatsarinny and Bartschat, 2013), configuration space is divided into an inner region, where exchange between the projectile and target electrons as well as correlation effects are significant, and an outer region, where such effects are negligible. In the inner region, the electron-atom compound system is treating using fairly well-developed atomic structure methods such as the configuration interaction (CI) approach. In the outer region, the problem is one of an electron moving in a long-range local potential.

In the CCC method (Fursa and Bray, 2012) the Lippmann-Schwinger equation, which is equivalent to Schrödinger's equation expressed as an integral equation in momentum space with the appropriate boundary conditions, is solved non-iteratively using matrix inversion techniques. In this method, the discrete and continuum target states are expanded in an

associated Laguerre polynomial basis and while a distorting potential is usually used to speed-up convergence of the solution, the results are independent of the potential. Both the R-matrix and CCC methods involve use of considerable computational resources since they typically require a large number of target states to bring about convergence. The goal of electron-atom collision theory is to calculate the probability that a projectile electron will be scattered in a particular direction either elastically or inelastically. These probabilities are called differential cross sections (DCS). The probability that a collision occurs irrespective of the scattering angle is called the integral cross sections (ICS) and is obtained by integrating the DCS over all scattering angles.

1.2 Problem Statement and Justification

We have compared the optical potential (OP) and first order distorted wave Born approximation (DWBA) methods in elastic scattering of intermediate-energy electrons by the alkali atoms of sodium and potassium. This study is justified on the following grounds:

i. The OP and DWBA methods have been widely applied in the study of elastic scattering and inelastic scattering respectively. However there has been no systematic study to compare both these methods for the elastic scattering process in which both are applicable.

ii. Alkali atoms such as sodium and potassium have a relatively simple atomic structure and are adequately described using the Hartree – Fock approximation. However numerous theoretical approaches for calculation of scattering cross sections have yielded results that are not in complete agreement with absolute measurements. This indicates the need for continued work to better understand how these systems interact

with energetic electrons especially at intermediate energies above the ionization threshold.

1.3 Research Questions

The study seeks to answer the following research questions:

i. How is the Transition matrix (T-matrix) element for elastic electron-alkali atom scattering in the OP method different from that in the DWBA method?
ii. How does use of different T-matrix elements and various distorting potentials affect the DCS and ICS?
iii. What aspects of the T-matrix elements and distorting potentials have the most significance in the determination of the DCS and ICS?
iv. How do the OP and DWBA DCS and ICS compare with other calculations and measured results when the distorting potential is varied?

1.4 Hypothesis

Using the same distorting potential, the OP and DWBA methods will yield similar results for elastic electron scattering from sodium and potassium atoms at high energies but the results near the ionization threshold will be different mainly due to exchange and convergence effects.

1.5 Objectives

1.5.1 General Objective

To calculate and compare OP and DWBA differential and integral cross section values for elastic scattering of electrons by sodium and potassium atoms at intermediate energies.

1.5.2 Specific Objectives

i. To formulate the T-matrix element for elastic scattering of electrons by alkali atoms in the OP and DWBA methods.

ii. To calculate DCS and ICS for elastic scattering of electrons by sodium and potassium using the OP and DWBA methods.

iii. To compare the DCS and ICS results obtained from the two methods with each other.

iv. To compare the calculated DCS and ICS results with available experimental data and other theoretical results.

1.6 Significance and Anticipated Output

It is anticipated that the energy region of convergence of the distorted wave series to the first order term, and the relative significance of the effect of exchange on the scattering electron and on the target atom, will be established for electron – atom elastic scattering.

1.7 Conceptual Framework

The study will apply two different perturbative methods to investigate electron scattering from alkali atoms. The same distorting potential, obtained from modelling the second order formal optical potential, will be used in both approaches.

1.8 Limitations of the Study

Complete evaluation of the non-local polarization potential in the distorting potential requires use of powerful computers which were not available to us. Also there are relatively few experimental data to compare with our calculated results.

CHAPTER 2

LITERATURE REVIEW

2.1 Electron – Sodium Elastic Scattering

Electron – sodium scattering has attracted a lot of interest over the years. Gehenn and Reichert (1972) measured relative electron – sodium elastic scattering DCS at angles 25° – 150° at energies ranging from 1 – 20 eV. Teubner *et al*. (1978) reported absolute elastic DCS at 54.4, 75, 100, and 150 eV over an angular range of $12^{\circ}-140^{\circ}$. Srivastava and Vuskovic (1980) measured absolute DCS at 10, 20, and 54.4 eV incident energies and at scattering angles ranging from $10^{\circ}-120^{\circ}$. The experimental results of Srivastava and Vuskovic (1980) and Teubner *et al*. (1978) do not agree with each other at the common energy of 54.4 eV. Marinkovic *et al*. (1992) measured DCS for electron – sodium scattering at 10, 20, and 54.4 eV over the angular range $6^{\circ}-150^{\circ}$. These results are in agreement with the experimental results of Srivastava and Vuskovic (1980) at 10 eV and with the results of Teubner *et al.* (1978) at 54.4 eV.

Teubner *et al.* (1978) carried out DCS calculations at 54.4 – 150 eV using a complex optical potential in which the polarization and absorption parts were evaluated using the closure approximation. The results were found to reproduce their measured DCS well. However, as Mitroy *et al.* (1987) have noted, the absorption potential used by Teubner *et al.* (1978) did not correspond to the physics of the electron-sodium system since in their approximation, they used a single closure energy (which unfortunately they did not specify) for both the 2p and 3s subshells, whose energies are 40.3 eV and 4.96 eV respectively. It is therefore

desirable to evaluate the polarization and absorption potential without such approximation as we have done in the present research. McCarthy *et al*. (1985) calculated elastic cross sections for electron scattering from sodium at 54.4 eV using the coupled-channels optical (CCO) method. Compared with the experimental data due to Teubner *et al.* (1978), the DCS were seriously overestimated at large scattering angles. They attributed this to the one-electron (Hartree-Fock) wavefunction used in their calculation.

Mitroy *et al*. (1987) carried out a comprehensive comparison between theoretical calculations and experimental data for electron-sodium scattering in the close-coupling (CC) approach at intermediate energies 10 – 217 eV. The CC differential cross section results were generally lower than the experimental results of Srivastava and Vuskovic (1980) at 10 and 20 eV but were in good qualitative agreement with the unormalized results of Gehenn and Reichert (1972). At 54.4 eV, the CC results were close to the data of Srivastava and Vuskovic (1980) at forward scattering angles ($\theta > 40^{\circ}$) but where generally higher at backward (i.e. large) scattering angles. Compared to the experimental data of Teubner *et al.* (1978) at 54.4, 100, and 150 eV, the CC results were close to the experimental DCS at small scattering angles but significantly higher at backward scattering angles. In an attempt to isolate the cause of the discrepancy between theory and experiment, Mitroy *et al*. (1987) performed sophisticated calculations using configuration interaction target wave functions but found that these calculations gave essentially the same results as CC calculations done using Hartree-Fock wave functions. Also observing that the experimental results did not agree with each other, they concluded that the discrepancy was due to large systematic errors in the experimental data. In the differential cross sections reported by Teubner *et al*. (1978), the systematic error is estimated at 15%.

Balashov *et al*. (1989) calculated differential cross sections of the elastic transition in sodium atom induced by intermediate-energy electrons using the distorted wave Born (DWBA) approximation with a phenomenological optical potential at 20, 54.4, 75, and 100 eV. The DWBA results compared well with the close-coupling calculation of Mitroy *et al*. (1987) at 20 eV for large scattering angles ($\theta > 80^{\circ}$) but not for lower angles. At 54.4 and 100 eV the DWBA results of Balashov *et al*. (1989) were generally lower than the CC results of Mitroy *et al*. (1987) at all scattering angles. As noted by Balashov *et al*. (1989) this was probably due to the fact that the CC calculation only included a few states which do not seem to account fully for the distortion effect, that is the polarization and excitation of the atom by the scattering electrons.

The DWBA results of Balashov *et al*. (1989) were close to the experimental absolute differential cross section results of Srivastava and Vuskovic (1980) at 20 eV and 54.4 eV for small scattering angles ($\theta \leq 40^{\circ}$). There was very good agreement at 54.4, 75, and 100 eV between the DWBA results of Balashov *et al*. (1989) and the experimental results of Teubner *et al.* (1978) as well as with the experimental results of Allen *et al*. (1987) at 54.4 eV. Overall the DWBA results of Balashov *et al*. (1989) are in good agreement with the experimental results. However, as indicated by Thirumalai and Truhlar (1982), the imaginary part of the optical potential used in their DWBA calculation is semi-empirical having a constant of proportionality that is adjusted such that the calculation reproduces the experimental absorption cross sections as well as possible. This limits the applicability of the optical potential used by Balashov *et al.* (1989) to atomic targets where such experimental data is available. Therefore in this research *ab-initio* polarization and absorption potentials have been used in order to avoid such limitations.

Bray *et al*. (1989) applied the distorted wave approximation to a two-channel close-coupling (CC2) as well as a DWBA calculation of DCS for electron-sodium scattering at the electron-impact energy of 54.4 eV. They also presented unitarised distorted wave Born (UDWB) and distorted wave second order Born approximation (DWSB) results which were found to be in very good agreement with the CC2 results. When compared with their DWBA results, they found that the CC2 method gave significantly lower DCS results at all scattering angles. As noted by Bray *et al*. (1989), this is due to the fact that their DWBA calculation utilized a real (static) potential which ignored the strong effect of dipole coupling to the 3p channel. Consequently in the present research a complex distorting potential has been used in the DWBA calculation.

Bray *et al*. (1991) applied the coupled-channels optical (CCO) method for electron-atom scattering to electron-sodium elastic scattering at 10, 20, 22.1, 40, 54.4, and 100 eV. The differential cross sections were found to be in good agreement with the unpublished experimental results of Lorentz and Miller, as reported by McCarthy and Weigold (2005). Madison *et al*. (1992) reported distorted wave second order Born approximation (DWSB) DCS calculations for elastic scattering of sodium by 10 – 150 eV electrons. They found that the DWSB results were typically in reasonably good agreement with the experimental results of Marinkovic *et al*. (1992), Lorentz and Miller (McCarthy and Weigold, 1995), and the results of Srivastava and Vuskovic (1980). In carrying out comparison with these experimental data Madison *et al.* (1992) integrated the experimental data over the angular range of the measurements and then normalized the data to their DWSB results. This procedure is questionable since it tends to give good agreement between the theory and the renormalized DCS data and may conceal genuine discrepancies between theory and experiment. Therefore in this work, no attempt has been made to renormalize existing

experimental data but rather they have been used as reported. Bray (1994) used the convergent close-coupling method to calculate DCS at 1 – 54.4 eV. The results gave the best agreement with experiment results (which they renormalized to their theory) over the entire energy range compared with all previous theoretical calculations.

2.2 Electron – Potassium Elastic Scattering

The study of electron – potassium elastic scattering has spanned many decades. McMillen (1934) measured relative DCS at 5 – 150 eV over the angular range $25^\circ - 160^\circ$. Buckman *et al*. (1979) reported absolute DCS for elastic electron – potassium scattering in the energy range 54.4 – 200 eV over the angular range $2^\circ - 145^\circ$. Vuskovic and Srivastava (1980) measured elastic DCS at 7, 20, 40, 60, and 100 eV incident energies in the scattering angular range of $5^\circ - 120^\circ$. Buckman *et al*. (1979) also carried out an optical potential calculation using the closure approximation which they compared with their experimental results. They found the OP calculation to be in excellent agreement with the experiment DCS at 200 eV. However at lower energies, the agreement became progressively worse as the OP calculation underestimated the DCS at large scattering angles. This indicates that the closure approximation is only valid at high energies.

McCarthy *et al*. (1985) used the coupled-channels optical (CCO) theory to calculate DCS for elastic electron potassium scattering at 54.4 eV. Compared to the experimental results of Buckman *et al.* (1979), the CCO results were in close agreement in the forward direction ($\theta \geq 30^\circ$) but were higher than the measured results at larger scattering angles. As in the case

of electron-sodium elastic scattering McCarthy *et al*. (1985) concluded that the one-electron (Hartree-Fock) model for potassium was inadequate for large-angle scattering.

Mitroy (1993) calculated intermediate energy elastic electron-potassium DCS using the unitarised distorted wave Born approximation (UDWBA) at 54.4 – 200 eV, and found that compared to the results of Buckman *et al*. (1979) and Vuskovic and Srivastava (1980), the experimental results were substantially smaller in magnitude than the UDWBA cross sections for large angle scattering at all impact energies considered. Mitroy (1993) also compared the UDWBA calculation with the unnormalised cross section data of McMillen (1934) by first normalising the experimental data to roughly match the UDWBA calculation at the smallest angle and found the agreement between the UDWBA results and the normalised results of McMillen (1934) to be uniformly good. However as we have noted earlier, there is need to compare theoretical results with absolute measurements in order to definitely validate a particular theoretical approach.

Bray *et al*. (1993) calculated electron-potassium DCS using the coupled-channels optical (CCO) method at 1 – 100 eV. They found the results to be in generally good agreement with available absolute experimental data. Madison *et al*. (1995) examined elastic scattering of electrons from potassium atom using potential scattering theory (optical potential, OP method) and perturbation theory (second order distorted wave Born approximation, DWSB) in the energy range 7 – 100 eV. They concluded that to use the OP approach both non-local effects of polarization and absorption must be properly modelled to get accurate elastic DCS. With this in mind, we have evaluated a non-local polarization potential for elastic electron-alkali atom elastic scattering which we have applied to obtain present DCS and ICS results.

CHAPTER 3

METHODOLOGY

In section 3.1 of this chapter we give the exact T-matrix element for electron-atom scattering as derived from the Lippmann-Schwinger equation and show how it is used to calculate the differential cross sections. In section 3.2 the first order distorted wave Born approximation and the optical potential T-matrix elements are derived by introduction of the distorting potential in the electron-atom total Hamiltonian. In section 3.3 the T-matrix elements for both the OP and DWBA methods are evaluated. In section 3.4 the complete distorting potential used in our calculations is presented and finally in section 3.5 the numerical procedures and computer program used are discussed.

3.1 Lippmann-Schwinger Equation

The electron-atom scattering problem is governed by the Schrödinger equation;

$$\left(E - H\right)\left|\Psi_i^{(\pm)}\right\rangle = 0 \tag{1}$$

where E is the total energy of the system , $\left|\Psi_i^{(\pm)}\right\rangle$ is the formal solution satisfying outgoing or incoming boundary conditions, and H is the total Hamiltonian of the system given by;

$$H = K + H_T + V \tag{2}$$

In equation (2), K is the kinetic energy operator of the projectile electron, H_T is the target Hamiltonian, and V is the electron-atom interaction potential. In atomic units these are given by;

$$K = -\frac{1}{2}\nabla^2 \tag{3}$$

$$H_T = \sum_{i=1}^{N}\left(-\frac{1}{2}\nabla_i{}^2 - \frac{Z}{r_i}\right) + \sum_{j=1}^{N-1}\sum_{i>j}^{N}\frac{1}{|\mathbf{r}_i - \mathbf{r}_j|} \tag{4}$$

$$V = -\frac{Z}{r} + \sum_{i=1}^{N}\frac{1}{|\mathbf{r}_i - \mathbf{r}|} \tag{5}$$

In the asymptotic region where the interaction potential can be neglected, the system is governed by the Schrödinger equation;

$$(E - K - H_T)|\Phi_i\rangle = 0 \tag{6}$$

The channel state $|\Phi_i\rangle$, which describes the electron-atom system in the asymptotic region, is related to the collision state $|\Psi_i^{(\pm)}\rangle$, which describes the system in the interaction region, by the Lippmann-Schwinger (LS) equation thus (McCarthy and Weigold, 2005; Gell-Mann and Goldberger, 1953);

$$|\Psi_i^{(\pm)}\rangle = |\Phi_i\rangle + \frac{1}{E - K - H_T + i\varepsilon}V|\Psi_i^{(\pm)}\rangle \tag{7}$$

where $\varepsilon \to 0^+$. The transition matrix T_{fi} defined by;

$$T_{fi} = \langle \Phi_f | V | \Psi_i^{(+)} \rangle \tag{8}$$

gives the amplitude of the probability that the electron-atom system initially in the collision state $|\Psi_i^{(+)}\rangle$ is found at a later time after the collision in the channel state $|\Phi_f\rangle$. The differential cross section which is given by;

$$\frac{d\sigma}{d\Omega} = (2\pi)^4 \frac{k_f}{k_i} |T_{fi}|^2 \tag{9}$$

is the number of scattered electrons entering unit solid angle per unit time per unit incident flux. In equation (9), $k_f (k_i)$ is the final (initial) momentum (in atomic units) of the scattering electron. Using the LS equation (7) in equation (8) yields the exact transition matrix (*T*-matrix) LS equation;

$$T_{fi} = \langle \Phi_f | V | \Phi_i \rangle + \sum_j \int d\mathbf{k}' \langle \Phi_f | V | \Phi_j \rangle \frac{1}{E - k'^2/2 - \omega_j + i\varepsilon} \langle \Phi_j | V | \Psi_i^{(+)} \rangle \tag{10}$$

where equation (10) involves summation over the complete set of target states $|\varphi_j\rangle$ and integration over the continuum states $|\mathbf{k}'\rangle$ of the projectile, and ω_j are the eigenvalues of the target states $|\varphi_j\rangle$. That is;

$$|\Phi_j\rangle = |\varphi_j \mathbf{k}'\rangle \tag{11}$$

and;

$$H_T |\varphi_j\rangle = \omega_j |\varphi_j\rangle \tag{12}$$

3.2 Distorted Wave Approximation and Optical Potential Method

In perturbative methods, the *T*-matrix given by equation (10), which involves the unknown collision state $|\Psi_i^{(+)}\rangle$, is determined iteratively. For faster convergence of the perturbation series a distorting potential *U* is first introduced in equation (2) thus;

$$H = (K + H_T + U) + (V - U) \tag{13}$$

Equations (1) and (6) then become;

$$\left(E-K-H_T-U\right)\left|\Psi_i^{(\pm)}\right\rangle=\left(V-U\right)\left|\Psi_i^{(\pm)}\right\rangle \tag{14}$$

and; $$\left(E-K-H_T-U\right)\left|\mathrm{X}_i^{(\pm)}\right\rangle=0 \tag{15}$$

respectively. Writing $\left|\mathrm{X}^{(\pm)}\right\rangle=\left|\varphi_i\chi_i^{(\pm)}\right\rangle$ explicitly, where $\left|\chi_i^{(\pm)}\right\rangle$ are the distorted waves describing the scattering electron which satisfy outgoing or incoming boundary conditions, equation (15) becomes separable thus;

$$\left(E-K-U\right)\left|\chi_i^{(\pm)}\right\rangle=0 \tag{16}$$

$$H_T\left|\varphi_i\right\rangle=\omega_i\left|\varphi_i\right\rangle \tag{17}$$

The LS equations corresponding to the forms of the Schrödinger equation given by equations (14) and (15) are;

$$\left|\Psi_i^{(\pm)}\right\rangle=\left|\mathrm{X}_i^{(\pm)}\right\rangle+\frac{1}{E-K-H_T-U+i\varepsilon}\left(V-U\right)\left|\Psi_i^{(\pm)}\right\rangle \tag{18}$$

$$\left|\mathrm{X}_i^{(\pm)}\right\rangle=\left|\Phi_i\right\rangle+\frac{1}{E-K-H_T+i\varepsilon}U\left|\mathrm{X}_i^{(\pm)}\right\rangle \tag{19}$$

Using equation (19) in equation (8) yields;

$$T_{fi}=\left\langle \mathrm{X}_f^{(-)}\middle|V\middle|\Psi_i^{(+)}\right\rangle-\left\langle \mathrm{X}_f^{(-)}\middle|U\frac{1}{E-K-H_T+i\varepsilon}V\middle|\Psi_i^{(+)}\right\rangle \tag{20}$$

And rearranging equation (7) thus;

$$\frac{1}{E-K-H_T+i\varepsilon}V\left|\Psi_i^{(\pm)}\right\rangle=-\left|\Phi_i\right\rangle+\left|\Psi_i^{(\pm)}\right\rangle$$

and substituting into equation (20) gives;

$$T_{fi} = \left\langle \mathrm{X}_f^{(-)} | V | \Psi_i^{(+)} \right\rangle + \left\langle \mathrm{X}_f^{(-)} | U | \Phi_i \right\rangle - \left\langle \mathrm{X}_f^{(-)} | U | \Psi_i^{(+)} \right\rangle$$

or

$$T_{fi} = \left\langle \mathrm{X}_f^{(-)} | U | \Phi_i \right\rangle + \left\langle \mathrm{X}_f^{(-)} | V - U | \Psi_i^{(+)} \right\rangle \tag{21}$$

Writing equation (21) explicitly in terms of the initial (final) target states $|\varphi_i\rangle$ ($|\varphi_f\rangle$) gives;

$$T_{fi} = \left\langle \chi_f^{(-)} \varphi_f | U | \varphi_i \beta \right\rangle + \left\langle \chi_f^{(-)} \varphi_f | V - U | \Psi_i^{(+)} \right\rangle \tag{22}$$

where $|\beta\rangle = |\mathbf{k}\rangle$ is the initial plane wave state of the projectile electron. Equation (22) is the exact T-matrix element for electron-atom scattering which however involves the unknown collision state $\left|\Psi_i^{(+)}\right\rangle$. The first order distorted wave Born approximation (DWBA) is obtained by truncating equation (18) thus;

$$\left|\Psi_i^{(\pm)}\right\rangle \approx \left|\mathrm{X}_i^{(\pm)}\right\rangle = \left|\chi_i^{(\pm)} \varphi_i\right\rangle \tag{23}$$

In writing equation (23), the second and higher orders in the exact T-matrix given in equation (22) are ignored leading to the following form of the T-matrix;

$$T_{fi}^{DWBA} = \left\langle \chi_f^{(-)} \varphi_f | U | \varphi_i \beta \right\rangle + \left\langle \chi_f^{(-)} \varphi_f | V - U | \varphi_i \chi_i^{(+)} \right\rangle \tag{24}$$

For elastic scattering, $|\varphi_f\rangle = |\varphi_i\rangle$ and the optical potential T- matrix element is obtained from the equation (22) by ignoring the second term in the equation to yield;

$$T_{fi}^{OP} = \left\langle \chi_f^{(-)} | U | \beta \right\rangle \tag{25}$$

The use of equation (25) instead of (22) for elastic scattering is justified when the distorting potential U very closely approximates the electron-atom interaction potential V. For elastic

scattering, the difference between the DWBA and OP methods is the second term in equation (24) which upon introduction of the antisymmetrization operator (as discussed in section 3.3 below) gives rise to an extra direct and exchange term in the DWBA transition matrix element.

3.3 Evaluation of the T-Matrix Element

In order to take into account the Pauli exclusion principle in electron-atom elastic scattering, the antisymmetrization operator A is introduced in the second term in equation (24) thus;

$$T_{fi}^{DWBA} = \left\langle \chi_f{}^{(-)} \varphi_f \left| U \right| \beta \varphi_i \right\rangle + \left\langle \chi_f{}^{(-)} \varphi_f \left| V - U \right| \mathrm{A} \chi_i{}^{(+)} \varphi_i \right\rangle \tag{26}$$

For elastic scattering, the T-matrix element then becomes;

$$T_{fi}^{DWBA} = \left\langle \chi_f{}^{(-)}(0) \middle| U(0) \middle| \beta(0) \right\rangle + \left\langle \chi_f{}^{(-)}(0) \middle| U_{st}(0) - U(0) \middle| \chi_i{}^{(+)}(0) \right\rangle$$

$$- \left\langle \chi_f{}^{(-)}(0) \varphi(1,2,\ldots,N) \middle| \left(-\frac{Z}{r} + \sum_{i=1}^{N} \frac{1}{|\mathbf{r}_i - \mathbf{r}|} \right) - U(0) \middle| \left(\sum_{i=1}^{N} \wp_{0i} \right) \chi_i{}^{(+)}(0) \varphi(1,2,\ldots,N) \right\rangle \tag{27}$$

To obtain equation (27) we have assumed that the target wavefunction $|\varphi\rangle$ is properly antisymmetrized. The antisymmetrization operator A then has the form (Madison and Bartschat, 1996);

$$\mathrm{A} = \frac{1}{N+1} \left(1 - \sum_{i=1}^{N} \wp_{0i} \right) \tag{28}$$

where $\wp_{0i}$ is the operator that exchanges the space and spin coordinates $\mathbf{r},\sigma$ of the projectile electron and the coordinates $\mathbf{r}_i,\sigma_i$ of the i^{th} target electron. Also in the second term of equation (28), U_{st} is the static potential given by;

$$U_{st} = \left\langle \varphi(1,2,...,N) \middle| V \middle| \varphi(1,2,...,N) \right\rangle \tag{29}$$

The T-matrix element T_{fi} in equation (27) may be written in terms of the direct and exchange matrix elements thus;

$$T_{fi}^{DWBA} = T_{fi}{}^{D} - T_{fi}{}^{E} \tag{30}$$

where;

$$T_{fi}{}^{D} = \left\langle \chi_f{}^{(-)}(0) \middle| U(0) \middle| \beta(0) \right\rangle + \left\langle \chi_f{}^{(-)}(0) \middle| U_{st}(0) - U(0) \middle| \chi_i{}^{(+)}(0) \right\rangle \tag{31}$$

and;

$$T_{fi}{}^{E} = \left\langle \chi_f{}^{(-)}(0)\varphi(1,2,...,N) \middle| \left(-\frac{Z}{r} + \sum_{i=1}^{N} \frac{1}{|\mathbf{r}_i - \mathbf{r}|} \right) - U(0) \middle| \left(\sum_{i=1}^{N} \wp_{0i} \right) \chi_i{}^{(+)}(0)\varphi(1,2,...,N) \right\rangle \tag{32}$$

3.3.1 The Direct Matrix Element

We write the distorting potential U as a complex optical potential U_{opt} thus;

$$U = U_{opt} = U_{st} + U_{ex} + U_{pol} + iU_{abs} \tag{33}$$

where U_{ex} is the exchange potential, U_{pol} is the polarization potential, and U_{abs} is the absorption potential. Then considering the first term $T_{fi}{}^{D1} = T_{fi}{}^{OP}$ in equation (31) we have

$$T_{fi}^{D1} = \left\langle \chi_f^{(-)}(0) \middle| U(0) \middle| \beta(0) \right\rangle \tag{34}$$

In coordinate representation;

$$\left\langle \mathbf{r} | \beta \right\rangle = \sqrt{\frac{2}{\pi}} \frac{1}{k_i r} \sum_{l_i m_i} i^{l} f_{l_i}(k_i, r) Y_{l_i m_i}(\hat{\mathbf{r}}) Y^*_{l_i m_i}(\hat{\mathbf{k}}_i) \tag{35}$$

$$\left\langle \mathbf{r} \middle| \chi_f^{(-)} \right\rangle = \sqrt{\frac{2}{\pi}} \frac{1}{r} \sum_{l_f m_f} i^{l_f} e^{-i\delta_{l_f}} u_{l_f}(k_f, r) Y_{l_f m_f}(\hat{\mathbf{r}}) Y^*_{l_f m_f}(\hat{\mathbf{k}}_f) \tag{36}$$

and;

$$\left\langle \chi_f^{(-)} \middle| \mathbf{r} \right\rangle = \sqrt{\frac{2}{\pi}} \frac{1}{r} \sum_{l_f m_f} i^{-l_f} e^{i\delta_{l_f}} u_{l_f}(k_f, r) Y^*_{l_f m_f}(\hat{\mathbf{r}}) Y_{l_f m_f}(\hat{\mathbf{k}}_f) \tag{37}$$

where f_l is the regular Ricatti-Bessel function and the radial distorted (partial) waves u_l satisfy the Schrödinger equation (McCarthy and Weigold, 2005);

$$\left[\frac{d^2}{dr^2} - \frac{l(l+1)}{r} + 2(E - U) \right] u_l = 0 \tag{38}$$

where $E = k^2/2$ is the energy of the incident electron. Equation (38) is solved subject to the boundary condition $\lim_{r\to\infty} u_l(r) = r\left[\cos\delta_l j_l(kr) - \sin\delta_l n_l(kr)\right]$, where j_l and n_l are the spherical Bessel and spherical Neumann functions respectively, and δ_l is the phase shift. Using equations (35) and (37) in equation (34), we obtain, since $k_f = k_i = k$ for elastic scattering;

$$T_{fi}^{D1} = \frac{2}{\pi} \frac{1}{k} \sum_{l_i m_i l_f m_f} i^{(l_i - l_f)} e^{i\delta_{l_f}} \int_0^\infty f_{l_i}(k, r) U(r) u_{l_f}(k, r)$$

$$\times Y_{l_f m_f}(\hat{\mathbf{k}}_f) Y^*_{l_i m_i}(\hat{\mathbf{k}}_i) \int d\hat{\mathbf{r}} Y^*_{l_f m_f}(\hat{\mathbf{r}}) Y_{l_i m_i}(\hat{\mathbf{r}}) \tag{39}$$

From the orthogonality property of spherical harmonics;

$$\int d\hat{\mathbf{r}} Y^*_{l_f m_f}(\hat{\mathbf{r}}) Y_{l_i m_i}(\hat{\mathbf{r}}) = \delta_{l_f l_i} \delta_{m_f m_i} \tag{40}$$

and the addition theorem;

$$\sum_{m=-l}^{l} Y^*_{lm}(\hat{\mathbf{k}}_i) Y_{lm}(\hat{\mathbf{k}}_f) = \frac{(2l+1)}{4\pi} P_l(\cos\theta) \tag{41}$$

where P_l is a Legendre polynomial and $\hat{\mathbf{k}}_f \cdot \hat{\mathbf{k}}_i = \cos\theta$.

Using equations (40) and (41), equation (39) becomes;

$$T_{fi}^{D1} = \frac{2}{\pi} \frac{1}{k} \sum_l \frac{(2l+1)}{4\pi} P_l(\cos\theta) e^{i\delta_l} \int_0^\infty dr f_l(k,r) U(r) u_l(k,r) \tag{42}$$

Finally using (Mertzbacher, 1970);

$$2\int_0^\infty f_l(k,r) U(r) u_l(k,r) = -\sin\delta_l \tag{43}$$

gives (Madison *et al*., 1995);

$$T_{fi}^{D1} = -\frac{1}{4\pi^2} \frac{1}{k} \sum_{l=0}^{\infty} (2l+1) e^{i\delta_l} \sin\delta_l P_l(\cos\theta) \tag{44}$$

Thus the direct T-matrix element T_{fi}^{D1} may be written in terms of the elastic scattering amplitude $f(\theta)$ thus;

$$T_{fi}^{D1} = -\frac{1}{(2\pi)^2} f(\theta) \tag{45}$$

where;

$$f(\theta)=\frac{1}{k}\sum_{l=0}^{\infty}(2l+1)e^{i\delta_l}\sin\delta_l P_l(\cos\theta) \tag{46}$$

We now consider the second term $T_{fi}{}^{D2}$ in equation (31);

$$T_{fi}{}^{D2}=\left\langle \chi_f{}^{(-)}(0)\middle|U_{st}(0)-U(0)\middle|\chi_i{}^{(+)}(0)\right\rangle \tag{47}$$

Now using;

$$\left\langle \mathbf{r}\middle|\chi_i{}^{(+)}\right\rangle=\sqrt{\frac{2}{\pi}}\frac{1}{r}\sum_{l_i m_i} i^{l_i}e^{i\delta_{l_i}}u_{l_i}(k_i,r)Y_{l_i m_i}(\hat{\mathbf{r}})Y^*{}_{l_i m_i}(\hat{\mathbf{k}}_i) \tag{48}$$

and equation (37) in equation (47) yields;

$$T_{fi}{}^{D2}=\frac{2}{\pi}\sum_{l_i m_i l_f m_f} i^{(l_i-l_f)}e^{i(\delta_{l_i}+\delta_{l_f})}\int_0^{\infty}dr u_{l_f}(k,r)\overline{U}(r)u_{l_i}(k,r)$$

$$\times Y_{l_f m_f}(\hat{\mathbf{k}}_f)Y^*{}_{l_i m_i}(\hat{\mathbf{k}}_i)\int d\hat{\mathbf{r}}Y^*{}_{l_f m_f}(\hat{\mathbf{r}})Y_{l_i m_i}(\hat{\mathbf{r}}) \tag{49}$$

where we have written the residual potential as $\overline{U}=U_{st}-U=-(U_{exch}+U_{pol}+iU_{abs})$

Again using equations (40) and (41) in (49) yields (Schiff, 1968);

$$T_{fi}{}^{D2}=\frac{1}{2\pi^2}\sum_{l=0}^{\infty}(2l+1)e^{i2\delta_l}\left\{\int_0^{\infty}dr u_l(k,r)\overline{U}(r)u_l(k,r)\right\}P_l(\cos\theta) \tag{50}$$

where the phase shifts δ_l correspond to scattering from the U potential.

3.3.2 The Exchange Matrix Element

We now consider the exchange matrix element $T_{fi}{}^{E}$ given in equation (32), which we write as

$$T_{fi}{}^{E} = T_{fi}{}^{E1} + T_{fi}{}^{E2} + T_{fi}{}^{E3} \tag{51}$$

where;

$$T_{fi}{}^{E1} = \left\langle \chi_f{}^{(-)}(0)\varphi(1,2,...,N) \middle| -\frac{Z}{r} \middle| \left(\sum_{i=1}^{N} \wp_{0i} \right) \chi_i{}^{(+)}(0)\varphi(1,2,...,N) \right\rangle \tag{52}$$

$$T_{fi}{}^{E2} = \left\langle \chi_f{}^{(-)}(0)\varphi(1,2,...,N) \middle| \sum_{i=1}^{N} \frac{1}{|\mathbf{r}_i - \mathbf{r}|} \middle| \left(\sum_{i=1}^{N} \wp_{0i} \right) \chi_i{}^{(+)}(0)\varphi(1,2,...,N) \right\rangle \tag{53}$$

$$T_{fi}{}^{E3} = \left\langle \chi_f{}^{(-)}(0)\varphi(1,2,...,N) \middle| U(0) \middle| \left(\sum_{i=1}^{N} \wp_{0i} \right) \chi_i{}^{(+)}(0)\varphi(1,2,...,N) \right\rangle \tag{54}$$

The target-atom wavefunction φ is assumed to be of the form of a determinantal wavefunction (Cowan, 1981);

$$\varphi = \frac{1}{\sqrt{N!}} \sum_{P} (-1)^{p} \phi_{\alpha_1}(1)\phi_{\alpha 2}(2)\cdots\phi_{\alpha_N}(N) \tag{55}$$

where the summation is over all the $N!$ permutations P of the quantum numbers $\alpha_i (i = 1,2,\cdots,N)$ of the single-electron target orbitals, p is the parity of the permutations ($+1$ for even permutations and -1 for odd permutations). The one-electron target orbitals ϕ_α are of the form;

$$\phi_\alpha = \frac{1}{r} P_{n_\alpha l_\alpha}(r) Y_{l_\alpha m_\alpha}(\hat{\mathbf{r}}) \langle \sigma | \mu_\alpha \rangle \tag{56}$$

where $\langle\sigma|\mu_\alpha\rangle$ is the spin state of the target electron. For target orbitals ϕ_α that are orthogonal to the distorted waves $\chi^{(\pm)}$, the first and third terms in equation (51) vanish (Itikawa, 1986). For the second term, we write since the Coulomb interaction is a symmetric operator;

$$T_{fi}^{E2} = N\left\langle \chi_f^{(-)}(0)\wp(1,2,...,N)\left|\frac{1}{|\mathbf{r}_1-\mathbf{r}|}\right|\left(\sum_{i=1}^{N}\wp_{0i}\right)\chi_i^{(+)}(0)\wp(1,2,...,N)\right\rangle \tag{57}$$

And using equation (55) in (57) yields;

$$T_{fi}^{E2} = \frac{1}{(N-1)!}\sum_{PP'}(-1)^{p+p'}\left\langle \chi_f^{(-)}(0)\phi_{\alpha_1}(1)\phi_{\alpha 2}(2)\cdots\left|\frac{1}{|\mathbf{r}_1-\mathbf{r}|}\right|\left(\sum_{i=1}^{N}\wp_{0i}\right)\chi_i^{(+)}(0)\phi_{\alpha_1'}(1)\phi_{\alpha' 2}(2)\cdots\right\rangle \tag{58}$$

Owing to the orthogonality of the target orbitals we require;

$$\alpha_n' = \alpha_n \qquad \text{for} \qquad n \geq 2 \tag{59}$$

and assuming the target orbitals ϕ_α are orthogonal to the distorted waves $\chi^{(\pm)}$, all matrix elements involving $\wp_{0i}$ with $i \neq 1$ vanish. For elastic scattering the condition given by equation (59) implies also that $\alpha_1' = \alpha_1$ and consequently $P = P'$, and $p = p'$. Therefore equation (58) reduces to;

$$T_{fi}^{E2} = \frac{1}{(N-1)!}\sum_{P=1}^{N!}\left\langle \chi_f^{(-)}(0)\phi_{\alpha_1}(1)\left|\frac{1}{|\mathbf{r}_1-\mathbf{r}|}\right|\chi_i^{(+)}(1)\phi_{\alpha_1}(0)\right\rangle \tag{60}$$

Since for a given set of orbital quantum numbers α_1 there are $(N-1)!$ permutations of the other $N-1$ sets of quantum numbers satisfying equation (59) and having the same value of the matrix element we have;

$$T_{fi}^{E2} = \sum_{\alpha}\left\langle \chi_f^{(-)}(0)\phi_{\alpha_1}(1)\left|\frac{1}{|\mathbf{r}_1-\mathbf{r}|}\right|\chi_i^{(+)}(1)\phi_{\alpha_1}(0)\right\rangle \tag{61}$$

where the summation is now over all the N occupied orbitals ϕ_α of the target atom. Using equation (61) in equation (51) yields;

$$T_{fi}^{E} \approx T_{fi}^{E2} = \sum_{\beta \in C} \left\langle \chi_f^{(-)}(0)\phi_\beta(1)\left|\frac{1}{|\mathbf{r}_1 - \mathbf{r}|}\right|\chi_i^{(+)}(1)\phi_\beta(0)\right\rangle + \left\langle \chi_f^{(-)}(0)\phi_\nu(1)\left|\frac{1}{|\mathbf{r}_1 - \mathbf{r}|}\right|\chi_i^{(+)}(1)\phi_\nu(0)\right\rangle \quad (62)$$

where the first term is the summation over the core orbitals of the alkali atom denoted by β, and ν denotes the quantum numbers of the valence orbital.

To evaluate the first and second terms in equation (62) we note that for the alkali atoms Na and K, the ionic cores have the configurations $1s^2 2s^2 2p^6\ ^1\mathbf{S}$ and $1s^2 2s^2 2p^6 3s^2 3p^6\ ^1\mathbf{S}$ respectively while the ground states have the configurations $1s^2 2s^2 2p^6 3s^1\ ^2\mathbf{S}$ and $1s^2 2s^2 2p^6 3s^2 3p^6 4s^1\ ^2\mathbf{S}$ respectively (Cowan, 1981; Bray *et al*., 1991). Thus for elastic scattering from these targets, the total spin of the $N+1$ projectile-target system is due to the projectile and valence electrons only and also the scattering electron alone makes a contribution to the total angular momentum of the system. Consequently, the first term in equation (62) yields exchange scattering amplitudes similar to inert atom targets while the second term gives rise to hydrogenic singlet and triplet scattering amplitudes (McCarthy and Weigold, 1995). Substituting equations (37), (48) and (56) in the first term in equation (62) we obtain;

$$\sum_\beta \left\langle \chi_f^{(-)}(0)\phi_\beta(1)\left|\frac{1}{|\mathbf{r}_1 - \mathbf{r}|}\right|\chi_i^{(+)}(1)\phi_\beta(0)\right\rangle = \frac{2}{\pi}\sum_{l_i m_i}\sum_{l_f m_f}\sum_{\lambda\mu}\sum_{\beta} i^{(l_i - l_f)} e^{i(\delta_{l_i}+\delta_{l_f})}(-1)^\mu Y^*_{l_i m_i}(\hat{\mathbf{k}}_i) Y_{l_f m_f}(\hat{\mathbf{k}}_f)$$

$$\times \int d\hat{\mathbf{r}} Y^*_{l_f m_f}(\hat{\mathbf{r}}) C^\lambda_{-\mu}(\hat{\mathbf{r}}) Y_{l_\beta m_\beta}(\hat{\mathbf{r}}) \int d\hat{\mathbf{r}}_1 Y^*_{l_\beta m_\beta}(\hat{\mathbf{r}}_1) C^\lambda_\mu(\hat{\mathbf{r}}_1) Y_{l_i m_i}(\hat{\mathbf{r}}_1)$$

$$\times F^\lambda_{n_\beta l_\beta n_\beta l_\beta l_i l_f} \delta_{m_s m_{s\beta}} \delta_{m_{s\beta} m_s} \quad (63)$$

where $m_s\left(m_{s_\beta}\right)$ is the projection of the spin of the projectile (atomic core) electron and $F^{\lambda}_{n_\beta l_\beta n_\beta l_\beta l_i l_f}$ is the Slater integral defined as;

$$F^{\lambda}_{n_\beta l_\beta n_\beta l_\beta l_i l_f} = \int dr_1 dr \frac{r_<^{\lambda}}{r_>^{\lambda+1}} P_{n_\beta l_\beta}(r_1) P_{n_\beta l_\beta}(r) u_{l_i}(k_i, r_1) u_{l_f}(k_f, r) \tag{64}$$

In writing equation (63) we have expanded the two potential Coulomb potential in terms of renormalized spherical harmonics $C^l_m(\hat{\mathbf{r}})$ thus;

$$\frac{1}{|\mathbf{r}_1 - \mathbf{r}|} = \sum_{\lambda\mu} \frac{r_<^{\lambda}}{r_>^{\lambda+1}} (-1)^{\mu} C^{\lambda}_{\mu}(\hat{\mathbf{r}}_1) C^{\lambda}_{-\mu}(\hat{\mathbf{r}}) \tag{65}$$

where;

$$C^l_m(\hat{\mathbf{r}}) = \left(\frac{4\pi}{2l+1}\right)^{1/2} Y_{lm}(\hat{\mathbf{r}}) \tag{66}$$

Applying the Wigner-Eckart theorem (McCarthy and Weigold, 2005; Cowan, 1981) to evaluate the angular integrals in equation (63) gives;

$$\int d\hat{\mathbf{r}} Y^*_{l_f m_f}(\hat{\mathbf{r}}) C^{\lambda}_{-\mu}(\hat{\mathbf{r}}) Y_{l_\beta m_\beta}(\hat{\mathbf{r}}) = (-1)^{-m_f} \left[l_f, l_\beta\right]^{1/2} \begin{pmatrix} l_f & \lambda & l_\beta \\ 0 & 0 & 0 \end{pmatrix} \begin{pmatrix} l_f & \lambda & l_\beta \\ -m_f & -\mu & m_\beta \end{pmatrix} \tag{67a}$$

and;

$$\int d\hat{\mathbf{r}} Y^*_{l_\beta m_\beta}(\hat{\mathbf{r}}_1) C^{\lambda}_{\mu}(\hat{\mathbf{r}}_1) Y_{l_i m_i}(\hat{\mathbf{r}}_1) = (-1)^{-m_\beta} \left[l_\beta, l_i\right]^{1/2} \begin{pmatrix} l_\beta & \lambda & l_i \\ 0 & 0 & 0 \end{pmatrix} \begin{pmatrix} l_\beta & \lambda & l_i \\ -m_\beta & \mu & m_i \end{pmatrix} \tag{67b}$$

where the quantity in brackets is the Wigner 3-j symbol and $\left[l\right]^{1/2} \equiv (2l+1)^{1/2}$. From the properties of the 3-j symbol we have;

$$\begin{pmatrix} l_f & \lambda & l_\beta \\ -m_f & -\mu & m_\beta \end{pmatrix} = (-1)^{l_f+\lambda+l_\beta} \begin{pmatrix} l_f & \lambda & l_\beta \\ m_f & \mu & -m_\beta \end{pmatrix} = \begin{pmatrix} l_\beta & \lambda & l_f \\ -m_\beta & \mu & m_f \end{pmatrix} \tag{68}$$

Using equations (67) and (68) in (63) we obtain;

$$\sum_\beta \left\langle \chi_f^{(-)}(0)\phi_\beta(1) \left| \frac{1}{|\mathbf{r}_1 - \mathbf{r}|} \right| \chi_i^{(+)}(1)\phi_\beta(0) \right\rangle = \frac{2}{\pi} \sum_{l_i m_i} \sum_{l_f m_f} \sum_{\lambda\mu} \sum_\beta i^{(l_i - l_f)} e^{i(\delta_{l_i} + \delta_{l_f})} Y^*_{l_i m_i}(\hat{\mathbf{k}}_i) Y_{l_f m_f}(\hat{\mathbf{k}}_f)$$

$$\times (-1)^{-(m_f + m_\beta - \mu)} [l_f, l_i]^{1/2} [l_\beta] \begin{pmatrix} l_f & \lambda & l_\beta \\ 0 & 0 & 0 \end{pmatrix} \begin{pmatrix} l_\beta & \lambda & l_i \\ 0 & 0 & 0 \end{pmatrix} \begin{pmatrix} l_\beta & \lambda & l_f \\ -m_\beta & \mu & m_f \end{pmatrix} \begin{pmatrix} l_\beta & \lambda & l_i \\ -m_\beta & \mu & m_i \end{pmatrix}$$

$$\times F^\lambda_{n_\beta l_\beta n_\beta l_\beta l_i l_f} \delta_{m_s m_{s_\beta}} \delta_{m_{s_\beta} m_s} \tag{69}$$

From the properties of the 3-j symbol we have $-m_\beta + \mu + m_f = 0$ and consequently $m_\beta + m_f - \mu = m_\beta + m_f - (m_\beta - m_f) = 2m_f$. Then summing over the magnetic quantum numbers m_β and over μ in equation (69) we get;

$$\sum_{m_\beta \mu} \begin{pmatrix} l_\beta & \lambda & l_f \\ -m_\beta & \mu & m_f \end{pmatrix} \begin{pmatrix} l_\beta & \lambda & l_i \\ -m_\beta & \mu & m_i \end{pmatrix} = \delta_{l_f l_i} \delta_{m_f m_i} \delta(l_\beta \lambda l_f) \tag{70}$$

where $\delta(l_\beta \lambda l_f)$ denotes the triangle relations, that is $|l_f - l_\beta| \le \lambda \le l_f + l_\beta$ and that the sum $l_\beta + \lambda + l_f$ is an integral. Substituting equation (70) in (69) yields;

$$\sum_\beta \left\langle \chi_f^{(-)}(0)\phi_\beta(1) \left| \frac{1}{|\mathbf{r}_1 - \mathbf{r}|} \right| \chi_i^{(+)}(1)\phi_\beta(0) \right\rangle = \frac{2}{\pi} \sum_{l_i m_i} \sum_{n_\beta l_\beta} e^{i2\delta_{l_i}} Y^*_{l_i m_i}(\hat{\mathbf{k}}_i) Y_{l_i m_i}(\hat{\mathbf{k}}_f)$$

$$\times \sum_{\lambda = |l_i - l_\beta|}^{l_i + l_\beta} [l_\beta][l_i] \begin{pmatrix} l_i & \lambda & l_\beta \\ 0 & 0 & 0 \end{pmatrix} \begin{pmatrix} l_\beta & \lambda & l_i \\ 0 & 0 & 0 \end{pmatrix} F^\lambda_{n_\beta l_\beta n_\beta l_\beta l_i l_i} \tag{71}$$

Finally using the addition theorem of spherical harmonics equation (41) we have (Bray *et al.*, 1989);

$$\sum_{\beta}\left\langle \chi_f^{(-)}(0)\phi_\beta(1)\left|\frac{1}{|\mathbf{r}_1-\mathbf{r}|}\right|\chi_i^{(+)}(1)\phi_\beta(0)\right\rangle=\frac{1}{2\pi^2}\sum_{l=0}^{\infty}\sum_{n_\beta l_\beta}\sum_{\lambda=|l-l_\beta|}^{l+l_\beta}e^{i2\delta_l}[l_\beta][l]^2\begin{pmatrix} l & \lambda & l_\beta \\ 0 & 0 & 0\end{pmatrix}^2 F^{\lambda}_{n_\beta l_\beta n_\beta l_\beta l l}\ P_l(\cos\theta) \tag{72}$$

To evaluate the second term in equation (62), we make use of equations (37), (48), and (56) again to obtain;

$$\left\langle \chi_f^{(-)}(0)\phi_\upsilon(1)\left|\frac{1}{|\mathbf{r}_1-\mathbf{r}|}\right|\chi_i^{(+)}(1)\phi_\upsilon(0)\right\rangle=\frac{2}{\pi}\sum_{l_i m_i l_f m_f}\sum_{\lambda\mu}\sum_{\beta} i^{(l_i-l_f)}e^{i(\delta_{l_i}+\delta_{l_f})}(-1)^{\mu}Y^*_{l_i m_i}(\hat{\mathbf{k}}_i)Y_{l_f m_f}(\hat{\mathbf{k}}_f)$$

$$\times\int d\hat{\mathbf{r}}Y^*_{l_f m_f}(\hat{\mathbf{r}})C^{\lambda}_{-\mu}(\hat{\mathbf{r}})Y_{l_\upsilon m_\upsilon}(\hat{\mathbf{r}})\int d\hat{\mathbf{r}}_1 Y^*_{l_\upsilon m_\upsilon}(\hat{\mathbf{r}}_1)C^{\lambda}_{\mu}(\hat{\mathbf{r}}_1)Y_{l_i m_i}(\hat{\mathbf{r}}_1)$$

$$\times F^{\lambda}_{n_\upsilon l_\upsilon n_\upsilon l_\upsilon l_i l_f}\left\langle s_\upsilon s m_{s_\upsilon} m_s \middle| s s_\upsilon m_s m_{s_\upsilon}\right\rangle \tag{73}$$

where $s(s_\upsilon)$ is the spin of the projectile (valence) electron and $m_s(m_{s_\upsilon})$ is the corresponding projection. Now writing;

$$\sum_{\mu}(-1)^{\mu}\int d\hat{\mathbf{r}}Y^*_{l_f m_f}(\hat{\mathbf{r}})C^{\lambda}_{-\mu}(\hat{\mathbf{r}})Y_{l_\upsilon m_\upsilon}(\hat{\mathbf{r}})\int d\hat{\mathbf{r}}_1 Y^*_{l_\upsilon m_\upsilon}(\hat{\mathbf{r}}_1)C^{\lambda}_{\mu}(\hat{\mathbf{r}}_1)Y_{l_i m_i}(\hat{\mathbf{r}}_1)=\left\langle l_f l_\upsilon m_f m_\upsilon\middle|\mathbf{C}^{\lambda}\cdot\mathbf{C}^{\lambda}\middle|l_\upsilon l_i m_\upsilon m_i\right\rangle \tag{74}$$

where the scalar product of the spherical tensor operator $\mathbf{C}^{\lambda}$ is defined as (McCarthy and Weigold, 2005);

$$\mathbf{C}^{\lambda}\cdot\mathbf{C}^{\lambda}=\sum_{\mu}(-1)^{\mu}C^{\lambda}_{\mu}(\hat{\mathbf{r}}_1)C^{\lambda}_{-\mu}(\hat{\mathbf{r}}) \tag{75}$$

and then using the representation (closure) theorem twice in equation (74), we have;

$$\left\langle l_f l_\upsilon m_f m_\upsilon\middle|\mathbf{C}^{\lambda}\cdot\mathbf{C}^{\lambda}\middle|l_i l_\upsilon m_i m_\upsilon\right\rangle=\sum_{J'M'}\sum_{JM}\left\langle l_f l_\upsilon m_f m_\upsilon\middle|J'M'\right\rangle\left\langle J'M'\middle|\mathbf{C}^{\lambda}\cdot\mathbf{C}^{\lambda}\middle|JM\right\rangle\left\langle JM\middle|l_\upsilon l_i m_\upsilon m_i\right\rangle$$

$$= \sum_{J'M'} \sum_{JM} C^{J'M'}_{l_f l_\upsilon m_f m_\upsilon} C^{JM}_{l_\upsilon l_i m_\upsilon m_i} \left\langle J'M' \middle| \mathbf{C}^\lambda \cdot \mathbf{C}^\lambda \middle| JM \right\rangle \tag{76}$$

In equation (76), $C^{j_3 m_3}_{j_1 j_2 m_1 m_2}$ is a Clebsch – Gordan coefficient and J is the total angular momentum of the projectile - target system and M is the corresponding projection. Using the identity (McCarthy and Weigold, 2005);

$$\left\langle (l_f l_\upsilon) J'M' \middle| \mathbf{C}^\lambda \cdot \mathbf{C}^\lambda \middle| (l_\upsilon l_i) JM \right\rangle = \delta_{J'J} \delta_{M'M} (-1)^{l_f + l_\upsilon + J} \left[l_f, l_i \right]^{1/2} \left[l_\upsilon \right] \begin{pmatrix} l_f & \lambda & l_\upsilon \\ 0 & 0 & 0 \end{pmatrix} \begin{pmatrix} l_\upsilon & \lambda & l_i \\ 0 & 0 & 0 \end{pmatrix} \begin{Bmatrix} l_f & l_\upsilon & J \\ l_i & l_\upsilon & \lambda \end{Bmatrix} \tag{77}$$

in equation (73) yields (McCarthy *et al*., 1983);

$$\left\langle \chi_f^{(-)}(0) \phi_\upsilon(1) \left| \frac{1}{|\mathbf{r}_1 - \mathbf{r}|} \right| \chi_i^{(+)}(1) \phi_\upsilon(0) \right\rangle = -\frac{2}{\pi} \sum_{l_i m_i} \sum_{l_f m_f} \sum_{\lambda} \sum_{S} \sum_{JM} (-1)^S (2S+1)\ i^{(l_i - l_f)} e^{i(\delta_{l_i} + \delta_{l_f})}$$

$$\times Y^*_{l_i m_i}(\hat{\mathbf{k}}_i) Y_{l_f m_f}(\hat{\mathbf{k}}_f) (-1)^{l_f + l_\upsilon + J} \left[l_f, l_i \right]^{1/2} \left[l_\upsilon \right] \begin{pmatrix} l_f & \lambda & l_\upsilon \\ 0 & 0 & 0 \end{pmatrix} \begin{pmatrix} l_\upsilon & \lambda & l_i \\ 0 & 0 & 0 \end{pmatrix} \begin{Bmatrix} l_f & l_\upsilon & J \\ l_i & l_\upsilon & \lambda \end{Bmatrix} C^{JM}_{l_f l_\upsilon m_f m_\upsilon} C^{JM}_{l_\upsilon l_i m_\upsilon m_i} F^\lambda_{n_\upsilon l_\upsilon n_\upsilon l_\upsilon l_i l_f} \tag{78}$$

where the quantity in curly brackets $\{\ \}$ is the Wigner 6-j symbol which is related to the Racah coefficient (Cowan, 1981) by;

$$W(j_1 j_2 l_2 l_1; j_3 l_3) = (-1)^{j_1 + j_2 + l_1 + l_2} \begin{Bmatrix} j_1 & j_2 & j_3 \\ l_1 & l_2 & l_3 \end{Bmatrix} \tag{79}$$

In equation (78) the summation over the total spin S of the projectile-target system is obtained from equation (73) as follows;

$$\left\langle s_\upsilon s m_{s_\upsilon} m_s \middle| s s_\upsilon m_s m_{s_\upsilon} \right\rangle = \sum_{SM_S} \left\langle s_\upsilon s m_{s_\upsilon} m_s \middle| SM_S \right\rangle \left\langle SM_S \middle| s s_\upsilon m_s m_{s_\upsilon} \right\rangle$$

$$= \sum_{SM_S} (-1)^{s + s_\upsilon - S} \left\langle s s_\upsilon m_s m_{s_\upsilon} \middle| SM_S \right\rangle \left\langle SM_S \middle| s s_\upsilon m_s m_{s_\upsilon} \right\rangle$$

$$= -\sum_{SM_S} (-1)^S \left| C^{SM_S}_{ss_\upsilon m_s m_{s_\upsilon}} \right|^2 = -\sum_{S} (-1)^S (2S+1) \tag{80}$$

since $s = s_\upsilon = 1/2$. In equation (78) since $l_\upsilon = 0$ and $m_\upsilon = 0$ for the valence electron in an alkali atom, we have (Cowan, 1981);

$$\begin{Bmatrix} l_f & l_\upsilon & J \\ l_i & l_\upsilon & \lambda \end{Bmatrix} = \delta_{l_f \lambda} \delta_{l_i J} \frac{(-1)^{l_f + J}}{[l_f, J]^{1/2}} \tag{81}$$

Making the above substitutions, equation (78) becomes;

$$\left\langle \chi_f{}^{(-)}(0)\phi_\upsilon(1) \left| \frac{1}{|\mathbf{r}_1 - \mathbf{r}|} \right| \chi_i{}^{(+)}(1)\phi_\upsilon(0) \right\rangle = -\frac{2}{\pi} \sum_{l_i m_i} \sum_{S} (-1)^S (2S+1) e^{i2\delta_l} [l_i]$$

$$\times Y^*{}_{l_i m_i}(\hat{\mathbf{k}}_i) Y_{l_i m_i}(\hat{\mathbf{k}}_f) \begin{pmatrix} l_i & l_i & 0 \\ 0 & 0 & 0 \end{pmatrix} \begin{pmatrix} 0 & l_i & l_i \\ 0 & 0 & 0 \end{pmatrix} C^{l_i m_i}_{l_i 0 m_i 0} C^{l_i m_i}_{0 l_i 0 m_i} F^{\lambda}_{nsnsl_i l_i} \tag{82}$$

The Clebsch-Gordan coefficient is written in terms of the 3-j symbol as;

$$C^{jm}_{j_1 j_2 m_1 m_2} = (-1)^{j_1 - j_2 + m} [j]^{1/2} \begin{pmatrix} j_1 & j_2 & j \\ m_1 & m_2 & -m \end{pmatrix} \tag{83}$$

Consequently (Cowan, 1981);

$$C^{l_i m_i}_{l_i 0 m_i 0} = (-1)^{l_i + m_i} [l_i]^{1/2} \begin{pmatrix} l_i & 0 & l_i \\ m_i & 0 & -m_i \end{pmatrix} = 1 \tag{84}$$

Using the addition theorem (equation 41) in (82) we obtain for the valence orbital;

$$\left\langle \chi_f{}^{(-)}(0)\phi_\upsilon(1) \left| \frac{1}{|\mathbf{r}_1 - \mathbf{r}|} \right| \chi_i{}^{(+)}(1)\phi_\upsilon(0) \right\rangle = -\frac{1}{2\pi^2} \sum_{l=0}^{\infty} \sum_{S=0}^{S=1} (-1)^S (2S+1) e^{i2\delta_l} [l]^2 \begin{pmatrix} l & l & 0 \\ 0 & 0 & 0 \end{pmatrix}^2 F^{\lambda}_{nsnsll} \; P_l(\cos\theta) \tag{85}$$

The DWBA transition matrix element, given in equation (30), therefore has the computational form of a sum of direct and exchange T-matrix elements given in equations (44), (50), (72) and (85). For the OP method, the T-matrix element is just the direct term given in equation (44).

3.4 The Distorting Potential

In evaluating the direct and exchange terms in the T-matrix element given in equations (45), (50), (72), and (85), the radial solutions u_l which satisfy the Schrodinger equation (38) need to be evaluated, where the distorting (optical) potential is given by equation (33). In this work, we have used the static potential U_{st} , which is defined in equation (29), and given in terms of the ground state radial wavefunctions $P_{n_a l_a}$ of the target atom by;

$$U_{st}(r) = \langle 0|V|0\rangle = -\frac{Z}{r} + \sum_{n_a l_a} 2(2l_a+1)\int_0^\infty dr' \frac{{P_{n_a l_a}}^2(r')}{r_>} \tag{86}$$

and the Furness-McCarthy exchange potential U_{ex} of the form (Furness and McCarthy, 1973);

$$U_{ex}(r,E) = \frac{1}{2}\left\{\left(E - U_{st}(r)\right) - \left[\left(E - U_{st}(r)\right)^2 + 4\pi\rho(r) - (-1)^S 2R_j^2\right]^{\frac{1}{2}}\right\} \tag{87}$$

where E is the impact energy of the incident electron, $\rho(r)$ is the electron-charge density of core electrons of the target atom, R_j is given in terms of the radial wavefunction $P_{n_j l_j}$ of the valence electron as $R_j = P_{n_j l_j}/r$, and S is the total spin of the electron-alkali atom system

Note that $S = 0$ corresponds to a singlet state, while $S = 1$ is for a triplet state.

The ab-initio non-local complex polarization plus absorption potentials are given respectively by (Bartschat *et al*., 1988);

$$U_{pol}(r)u_l + iU_{abs}(r)u_l = -2\sum_{n\neq 0} V_{on}(r)\int_0^{\infty} dr' G_0^{(+)}(\bar{k};r,r')V_{no}(r')u_l(k,r') \tag{88}$$

In equation (88), the summation implies a sum over all the discrete intermediate states of the target atom and an integral over the continuum states of the atom while the complex free particle Green's function $G_o^{(+)}(\bar{k},r,r')$ is given in terms of the regular and irregular Ricatti-Bessel functions f_l and g_l by;

$$G_0^{(+)}(\bar{k};r,r') = \frac{1}{\bar{k}} f_l(\bar{k}r_<)\left[g_l(\bar{k}r_>) + if_l(\bar{k}r_>)\right] \tag{89}$$

Further $\bar{k} = \left[k^2 - 2\Delta\right]^{\frac{1}{2}}$, where Δ is the energy gap between the ground and nth excited (intermediate) state, and $V_{on}(r)$ is the direct matrix element defined by;

$$V_{on}(r) = \langle 0|V|n\rangle \tag{90}$$

The interaction potential *V* is;

$$V = -\frac{Z}{r} + \sum_{i=1}^{N}\frac{1}{|\mathbf{r}_i - \mathbf{r}|} \tag{91}$$

and for single determinant atomic wavefunctions the direct matrix element reduces to the matrix element of *V* between the initial $|\alpha\rangle$ and $|\beta\rangle$ final states of the active target electron thus;

$$V_{on}(r) = \left\langle \alpha\left|\frac{1}{|\mathbf{r} - \mathbf{r}'|}\right|\beta\right\rangle \tag{92}$$

Then coupling the angular momenta of the active target electron and that of the scattering electron we write;

$$|\alpha\rangle = |n_\alpha l_\alpha m_\alpha l_i m_i\rangle \tag{93a}$$

$$|\beta\rangle = |n_\beta l_\beta m_\beta l_f m_f\rangle \tag{93b}$$

And using the expansion;

$$\frac{1}{|\mathbf{r}-\mathbf{r}'|} = \sum_{\lambda\mu} \frac{r_<^\lambda}{r_>^{\lambda+1}} (-1)^\mu C_\mu^\lambda(\hat{\mathbf{r}}) C_{-\mu}^\lambda(\hat{\mathbf{r}}') \tag{94}$$

equation (92) becomes;

$$V_{on}(r) = \int_0^\infty dr' \frac{r_<^\lambda}{r_>^{\lambda+1}} P_{n_\alpha l_\alpha}(r') P_{n_\beta l_\beta}(r')$$

$$\times \sum_{\lambda\mu} (-1)^\mu \int d\hat{\mathbf{r}} Y^*{}_{l_f m_f}(\hat{\mathbf{r}}) C_{-\mu}^\lambda(\hat{\mathbf{r}}) Y_{l_i m_i}(\hat{\mathbf{r}}) \int d\hat{\mathbf{r}}' Y^*{}_{l_\beta m_\beta}(\hat{\mathbf{r}}') C_\mu^\lambda(\hat{\mathbf{r}}') Y_{l_\alpha m_\alpha}(\hat{\mathbf{r}}') \tag{95}$$

The summation in equation (95) may be written as;

$$\sum_{\lambda\mu} (-1)^\mu \int d\hat{\mathbf{r}} Y^*{}_{l_f m_f}(\hat{\mathbf{r}}) C_{-\mu}^\lambda(\hat{\mathbf{r}}) Y_{l_i m_i}(\hat{\mathbf{r}}) \int d\hat{\mathbf{r}}' Y^*{}_{l_\beta m_\beta}(\hat{\mathbf{r}}') C_\mu^\lambda(\hat{\mathbf{r}}') Y_{l_\alpha m_\alpha}(\hat{\mathbf{r}}') = \sum_\lambda \left\langle l_f l_\beta m_f m_\beta \left| \mathbf{C}^\lambda \cdot \mathbf{C}^\lambda \right| l_i l_\alpha m_i m_\alpha \right\rangle$$

$$= \sum_{J'M'} \sum_{JM} C^{J'M'}_{l_f l_\beta m_f m_\beta} C^{JM}_{l_i l_\alpha m_i m_\alpha} \delta_{J'J} \delta_{M'M} (-1)^{l_i + l_\beta + J} [J]^{1/2} \begin{Bmatrix} l_f & l_\beta & J \\ l_\alpha & l_i & \lambda \end{Bmatrix}$$

$$\times (-1)^{l_f} [l_f, l_i]^{1/2} (-1)^{l_\beta} [l_\beta, l_\alpha]^{1/2} \begin{pmatrix} l_f & \lambda & l_i \\ 0 & 0 & 0 \end{pmatrix} \begin{pmatrix} l_\beta & \lambda & l_\alpha \\ 0 & 0 & 0 \end{pmatrix} \tag{96}$$

where $\mathbf{C}^\lambda$ is the spherical tensor operator. Since $l_\alpha = 0, m_\alpha = 0$ for the valence electron in alkali atoms, we have;

$$\begin{Bmatrix} l_f & l_\beta & J \\ l_\alpha & l_i & \lambda \end{Bmatrix} = \delta\left(l_f l_\beta J\right)\delta_{l_\beta \lambda}\delta_{l_i J}\frac{(-1)^{l_f + l_\beta + J}}{\left[l_\beta, J\right]^{1/2}} \tag{97}$$

Equation (96) then becomes;

$$\sum_\lambda \left\langle l_f l_\beta m_f m_\beta \middle| \mathbf{C}^\lambda \cdot \mathbf{C}^\lambda \middle| l_i l_\alpha m_i m_\alpha \right\rangle = \sum_{JM} C^{JM}_{l_f l_\beta m_f m_\beta} C^{l_i m_i}_{l_i 0 m_i 0}\delta_{J l_i}\delta_{M m_i}(-1)^{l_i + l_\beta}$$
$$\times \left[l_f, l_i\right]^{1/2}\begin{pmatrix} l_f & l_\beta & l_i \\ 0 & 0 & 0 \end{pmatrix}\begin{pmatrix} l_\beta & l_\beta & 0 \\ 0 & 0 & 0 \end{pmatrix}\delta\left(l_f l_\beta J\right)\delta_{l_\beta \lambda}\delta_{l_i J} \tag{98}$$

Writing; $$G^\lambda_{n_\alpha l_\alpha n_\beta l_\beta}(r) = \int_0^\infty dr' \frac{r_<^\lambda}{r_>^{\lambda+1}} P_{n_\alpha l\alpha}(r') P_{n_\beta l\beta}(r') \tag{99}$$

and using equations (98) and (99) in (95) we obtain;

$$V_{on}(r) = G^{l_\beta}_{n_\alpha l_\alpha n_\beta l_\beta}(r)\sum_{l_i m_i} C^{l_i m_i}_{l_f l_\beta m_f m_\beta}(-1)^{l_i + l_\beta}\left[l_f, l_i\right]^{1/2}\begin{pmatrix} l_f & l_\beta & l_i \\ 0 & 0 & 0 \end{pmatrix}\begin{pmatrix} l_\beta & l_\beta & 0 \\ 0 & 0 & 0 \end{pmatrix}\delta\left(l_f l_\beta l_i\right) \tag{100}$$

Finally applying the orthogonality property of Clebsch-Gordan coefficients we get;

$$V_{on}(r)V_{n0}(r') = G^{l_\beta}_{n_\alpha l_\alpha n_\beta l_\beta}(r) G^{l_\beta}_{n_\alpha l_\alpha n_\beta l_\beta}(r')\frac{1}{2l_f + 1}\sum_{l_f = |l_\beta - l_i|}^{l_\beta + l_i}\left[l_f, l_i\right]\begin{pmatrix} l_f & l_\beta & l_i \\ 0 & 0 & 0 \end{pmatrix}^2\begin{pmatrix} l_\beta & l_\beta & 0 \\ 0 & 0 & 0 \end{pmatrix}^2 \tag{101}$$

Equation (88) therefore becomes;

$$U_{pol}(r)u_l + iU_{abs}(r)u_l = -\frac{2}{2l_f + 1}\sum_{l_f = |l_\beta - l_i|}^{l_\beta + l_i}\left[l_f, l_i\right]\begin{pmatrix} l_f & l_\beta & l_i \\ 0 & 0 & 0 \end{pmatrix}^2\begin{pmatrix} l_\beta & l_\beta & 0 \\ 0 & 0 & 0 \end{pmatrix}^2$$
$$\times \sum_{n_\beta l_\beta} G^{l_\beta}_{n_\alpha l_\alpha n_\beta l_\beta}(r)\int_0^\infty dr' G_0^{(+)}\left(\bar{k}; r, r'\right) G^{l_\beta}_{n_\alpha l_\alpha n_\beta l_\beta}(r') u_l(k, r') \tag{102}$$

In evaluating the non-local polarization potential in equation (102) which involves discrete excited states of the atoms, the 3p, 3d, 4p, and 4s excited states (Ryzhikh and Mitroy, 1997)

were used for sodium atom, while for the potassium atom 4p, 5p, 3d, and 5s excited states (Mitroy, 1993) were used. The complete evaluation of equation (102) involving all the discrete and continuum target states would require use of a supercomputer (Chen *et al*., 2008). Because of the slow convergence of the series in (102) for the imaginary part, we replaced the non-local absorption potential with the widely used local absorption potential of Staszewska *et al*. (1984) having the form;

$$U_{abs} = -\frac{1}{2} T_{loc}(r,E)\rho(r)\bar{\sigma}_b \tag{103}$$

where $T_{loc}(r,E) = \left(2\left(E - V_{se}\right)\right)^{\frac{1}{2}}$ is the local kinetic energy of the incident electron, $\rho(r) = \sum_{n_a l_a} 2\left(2l_a + 1\right) P_{n_a l_a} \Big/ \left(4\pi r^2\right)$ is the electron charge density of the target atom and $\bar{\sigma}_b$ is the average binary collision cross section given by;

$$\bar{\sigma}_b = \frac{32\pi^2 N_k}{15k^2} H(x)\left(f_1 + f_2\right) \tag{104}$$

In equation (104);

$$N_k = 3 \Big/ \left(4\pi {k_F}^3\right) \tag{105}$$

$$k_F = \left(3\pi^2 \rho\right)^{\frac{1}{3}} \tag{106}$$

$$f_1 = \frac{5{k_F}^3}{\left(\alpha - {k_F}^2\right)} - \frac{{k_F}^3\left(5\left(k^2 - \alpha\right) + 2{k_F}^2\right)}{\left(k^2 - \alpha\right)^2} \tag{107}$$

$$f_2 = \frac{2\left(2\alpha - k^2\right)^{\frac{5}{2}}}{\left(k^2 - \alpha\right)^2} H(y) \tag{108}$$

and;

$$\alpha = \left({k_F}^2 + 2\Delta\right) \tag{109}$$

In these equations k_F is the Fermi momentum and Δ is the average excitation energy of the target atom while in equations (104) and (108), *H* is the Heaviside unit step function with $x = k^2 - \left(2\alpha - k_F{}^2\right)$ and $y = 2\alpha - k^2$ respectively. The Roothaan-Hartree-Fock ground state wavefunctions for sodium and potassium as tabulated by Bunge *et al.* (1993) were used in evaluation of the distorting potential and the T-matrix elements.

3.5 Integral and Total Cross Sections

When the differential cross sections given by equation (9) are integrated over all scattering angles, the integral cross section (ICS) at a particular electron-impact energy is obtained thus (McCarthy and Weigold, 2005);

$$\sigma_I = \int_0^{\pi}\int_0^{2\pi} d\phi d\theta \sin\theta \left(\frac{d\sigma}{d\Omega}\right) \tag{110}$$

Related to the integral cross section is the momentum transfer cross section given by;

$$\sigma_M = \int_0^{\pi}\int_0^{2\pi} d\phi d\theta \sin\theta \left(1-\cos\theta\right)\left(\frac{d\sigma}{d\Omega}\right) \tag{111}$$

The total cross section is given using the optical theorem by;

$$\sigma_T = -\left(\frac{2}{k}\right)\left(2\pi\right)^3 \mathrm{Im} T_{oo} \tag{112}$$

where k is the momentum of the elastically-scattered electron, and T_{oo} is the forward-scattering T-matrix element obtained by setting $\theta = 0$. For a real distorting potential, equations (110) and (112) yield the same result, that is $\sigma_T = \sigma_I$. For a complex distorting

potential, equation (112) yields the total (elastic plus inelastic) cross section which differs from the value obtained from equation (110) by the absorption potential σ_{abs}, that is $\sigma_T = \sigma_I + \sigma_{abs}$.

3.6 Numerical Procedures

In this study, differential, integral, and total cross sections for electron-sodium and electron-potassium elastic scattering at intermediate energies have been calculated using program OPDWBA written in the C programming language (Deitel and Deitel, 2004). To solve the radial equation (38), Numerov's method was used for low orbital angular momentum quantum numbers $l \le 3$ and the corresponding phase shifts were extracted from the boundary condition using the relation (Madison and Bartschat, 1996);

$$\tan\delta_l = \left[ks_l'(ka) - \gamma_l s_l(ka) \big/ kc_l'(ka) - \gamma_l c_l(ka) \right] \tag{113}$$

In this expression $s_l = \rho j_l(\rho)$, $c_l = \rho \eta_l(\rho)$, $\gamma_l = u_l^{-1}(d\,u_l/dr)$ is the logarithmic derivative of the numerical solution at the matching point $r = a$ (chosen to ensure that the optical potential is negligible at that point), while s_l' and c_l' are the derivatives of s_l and c_l with respect to $\rho = kr$. For higher l values, extraction of the phase shift using equation (113) from the unormalized radial wavefunction is prone to errors (Shertzer and Temkin, 2006). Therefore the integral equation (Mertzbacher, 1970) corresponding to the radial equation (38) given by;

$$\tilde{u}_l(r) = rj_l(kr) + kr\int_0^\infty dr' j_l(kr_<) n_l(kr_>) \tilde{U}(r') \tilde{u}_l(r') r' \tag{114}$$

where $\tilde{U} = 2U$ and $\tilde{u}_l(r) = u_l/\cos\delta_l$, has been solved iteratively. The phase shift is then obtained from the K-matrix element;

$$\tan\delta_l = -k\int_0^\infty dr' j_l(kr')\tilde{U}(r')\,\tilde{u}_l(r')r' \tag{115}$$

The various integrals have been evaluated using the five-point quadrature rule (Fischer *et al.*, 1997);

$$\int_{x_j}^{x_{j+2}} y(x)dx = \frac{h}{90}\left\{34\left(y_{j+2}+y_j\right)-\left(y_{j+3}+y_{j-1}\right)+114y_{j+1}\right\} \tag{116}$$

At the ends of the integration range where use of equation (116) is not possible, the less accurate three-point Simpson's rule (Fischer *et al.*, 1997) was used;

$$\int_{x_j}^{x_{j+2}} y(x)dx = \frac{h}{3}\left[y_j+4y_{j+1}+y_{j+2}\right] \tag{117}$$

The functions of the program are described in the appendix.

CHAPTER 4

RESULTS AND DISCUSSION

4.1 Static Potential as the Distorting Potential

Figures 4.1 – 4.10 give the differential cross sections (DCS) for electron-sodium atom and electron-potassium atom elastic scattering at 10 – 100 eV and 7 – 200 eV respectively, using the static potential (given in equation 86) for both the OP and DWBA methods at scattering angles $0 \leq \theta \leq 180^{\circ}$. These results are denoted by OP_S and DWBA_S respectively.

4.1.1 Sodium

At 10eV electron-impact energy the present DWBA_S differential cross sections in figure 4.1 are in good agreement with the experimental results of Srivastava and Vuskovic (1980) and Marinkovic *et al.* (1992) at intermediate scattering angles but not at small angles. This indicates the need to include a polarization potential in the DWBA_S calculation to account for virtual excitation of the target atom since this potential is known to influence small angle scattering significantly. The present OP_S results are not in good accord with the DWBA_S results and the experimental results. This is because exchange effects, which are important at low electron-impact energies, have been included in the DWBA_S calculation through the exchange T-matrix element (give in equations 62, 72, and 85) but not in the OP_S calculation (equation 34 or 44). Also from figure 4.1, it is seen that the static potential, which is the only interaction considered in the OP_S calculation, does not adequately describe the electron-sodium elastic scattering process at energies near the ionization threshold. The 3CCO calculation (Bray *et al*., 1991) underestimates the differential cross sections compared to the experimental results at all scattering angles. The 3CCO calculation takes into account

polarization and absorption effects by coupling of the inelastic 3^2P and 3^2D channels to the elastic 3^2S channel and through use of a complex non-local optical potential to incorporate the remaining channels. The disagreement between the 3CCO results and experiment indicates that absorption effects, which account for real excitation and ionization and which tend to lower the calculated DCS, may have been overestimated in the calculation.

At 20eV (figure 4.2) the present DWBA_S differential cross section results are close to the measured results of Srivastava and Vuskovic (1980) at intermediate scattering angles but not at small angles, and are much higher than the measured results of Marinkovic *et al.* (1992) at intermediate and large scattering angles. The OP_S results are not in agreement with the DWBA_S results at small and intermediate scattering angles. This indicates that the exchange T-matrix used in the DWBA_S calculation has a significant effect on the scattering at this electron-impact energy since a low-energy electron has a greater likelihood of undergoing exchange with a target electron compared to a fast electron. The 3CCO calculation, which includes absorption effects, is in good agreement with the measured results of Srivastava and Vuskovic (1980) and Marinkovic *et al.* (1992) at small scattering angles but not at intermediate scattering angles. At 40eV (figure 4.3) the present DWBA_S and OP_S differential cross sections are in very close agreement with each other. This means that the exchange T-matrix does not have a very significant effect on the scattering at this electron-impact energy. Agreement between both the DWBA_S and OP_S calculations and the measured results is quite close at intermediate angles but not at small angles mainly due to absence of the polarization potential in both calculations. The 3CCO calculation tends to underestimate the DCS at scattering angles $\theta \geq 20^\circ$ due to inclusion of absorption effects

which generally tend to lower DCS values at intermediate to large scattering angles due to removal of electrons from the elastic channel.

At 54.4eV (figure 4.4) the present DWBA_S and OP_S differential cross sections results are virtually indistinguishable implying that the exchange T-matrix has almost no effect on the scattering at this electron-impact energy. Compared to the measured results of Teubner *et al.* (1978), Srivastava and Vuskovic (1980), and of Marinkovic *et al.* (1992), the present calculated results underestimate the differential cross sections at scattering angles $\theta < 10^{\circ}$ and overestimate the DCS at intermediate to large angles. This shows that both polarization and absorption effects are equally important at this electron-impact energy. The 3CCO calculation is in close agreement with measured results at small scattering angles only. The experimental results of Srivastava and Vuskovic (1980) are higher than the other experimental DCS at intermediate to large scattering angles. At 100 eV (Figure 4.5) the DWBA_S and OP_S calculations yield the same results at all scattering angles apart from the values near the differential cross sections minimum. Compared to the measured results of Teubner *et al.* (1978), the present results are overestimated at scattering angles $\theta > 20^{\circ}$ showing the need to include absorption effects, to lower the DCS at intermediate to large scattering angles. The present results are in good agreement with the 3CCO results of Bray *et al.* (1991). This is unexpected since the 3CCO calculation already includes absorption effects and is perhaps an indication that the absorption effects included in the 3CCO results are not completely adequate in the description of elastic scattering at this energy.

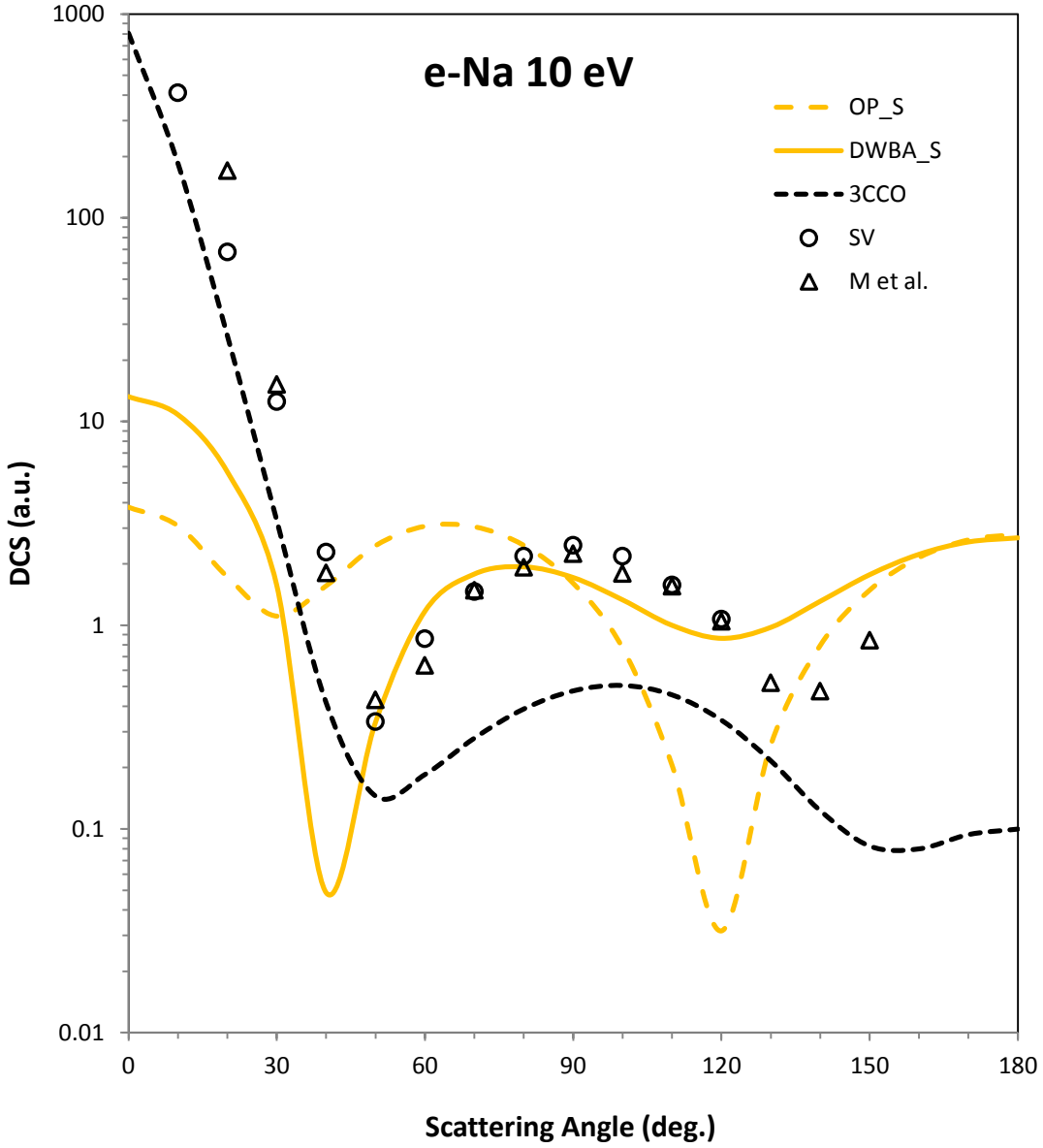

Figure 4.1: Differential cross sections for elastic scattering of electrons by sodium atom at 10eV impact energy. Experimental data: SV, Srivastava and Vuskovic (1980), M *et al.*, Marinkovic *et al.* (1992). Calculations: OP_S, present optical potential method with static potential, DWBA_S, present first order distorted wave Born approximation with static potential, 3CCO, 3-state coupled channels optical Method (Bray *et al.*, 1991).

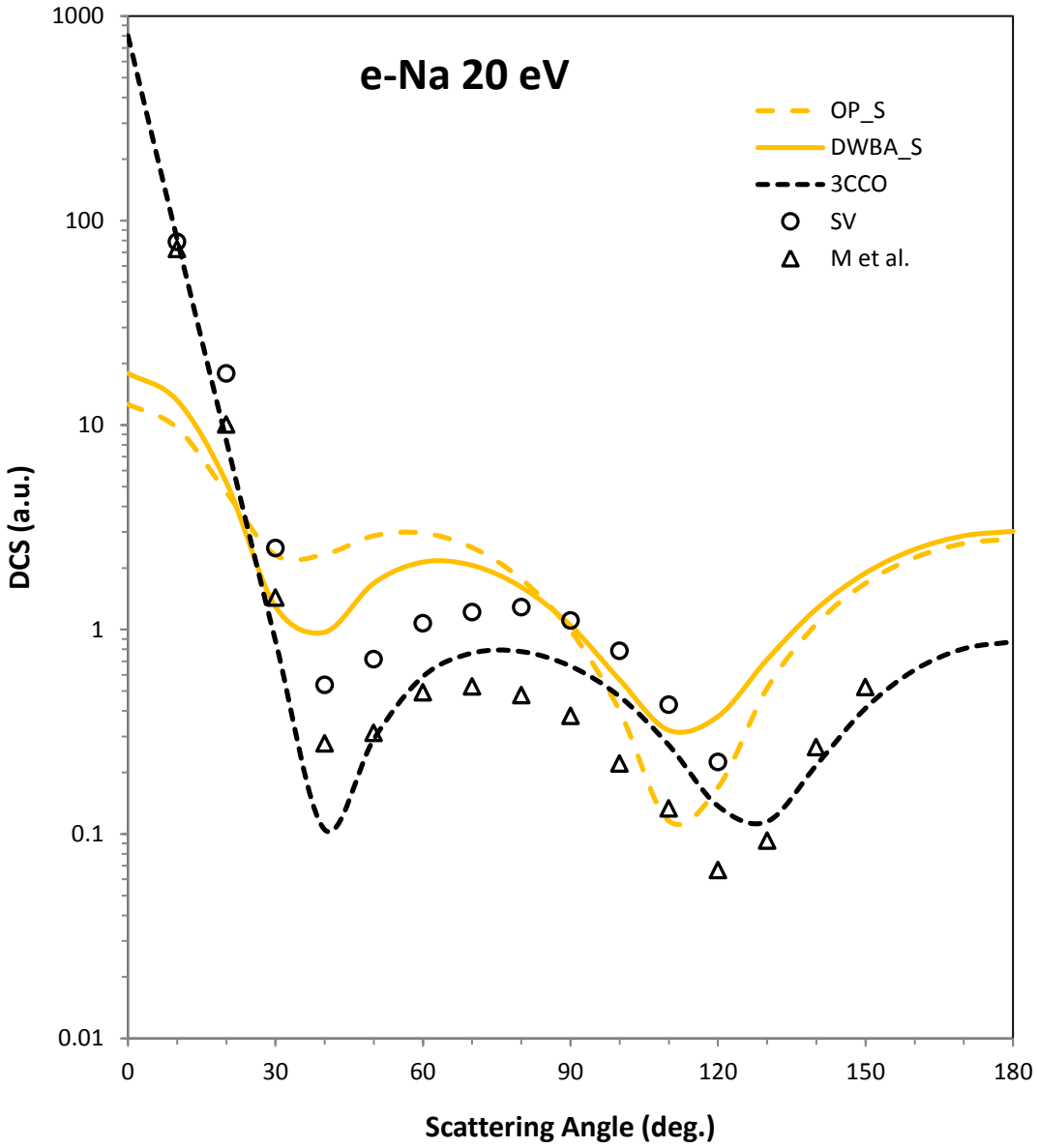

Figure 4.2: Differential cross sections for elastic scattering of electrons by sodium atom at 20eV impact energy. Experimental data: SV, Srivastava and Vuskovic (1980), M *et al.*, Marinkovic *et al.* (1992). Calculations: OP_S, present optical potential method with static potential, DWBA_S, present first order distorted wave Born approximation with static potential, 3CCO, 3-state coupled channels optical Method (Bray *et al.*, 1991).

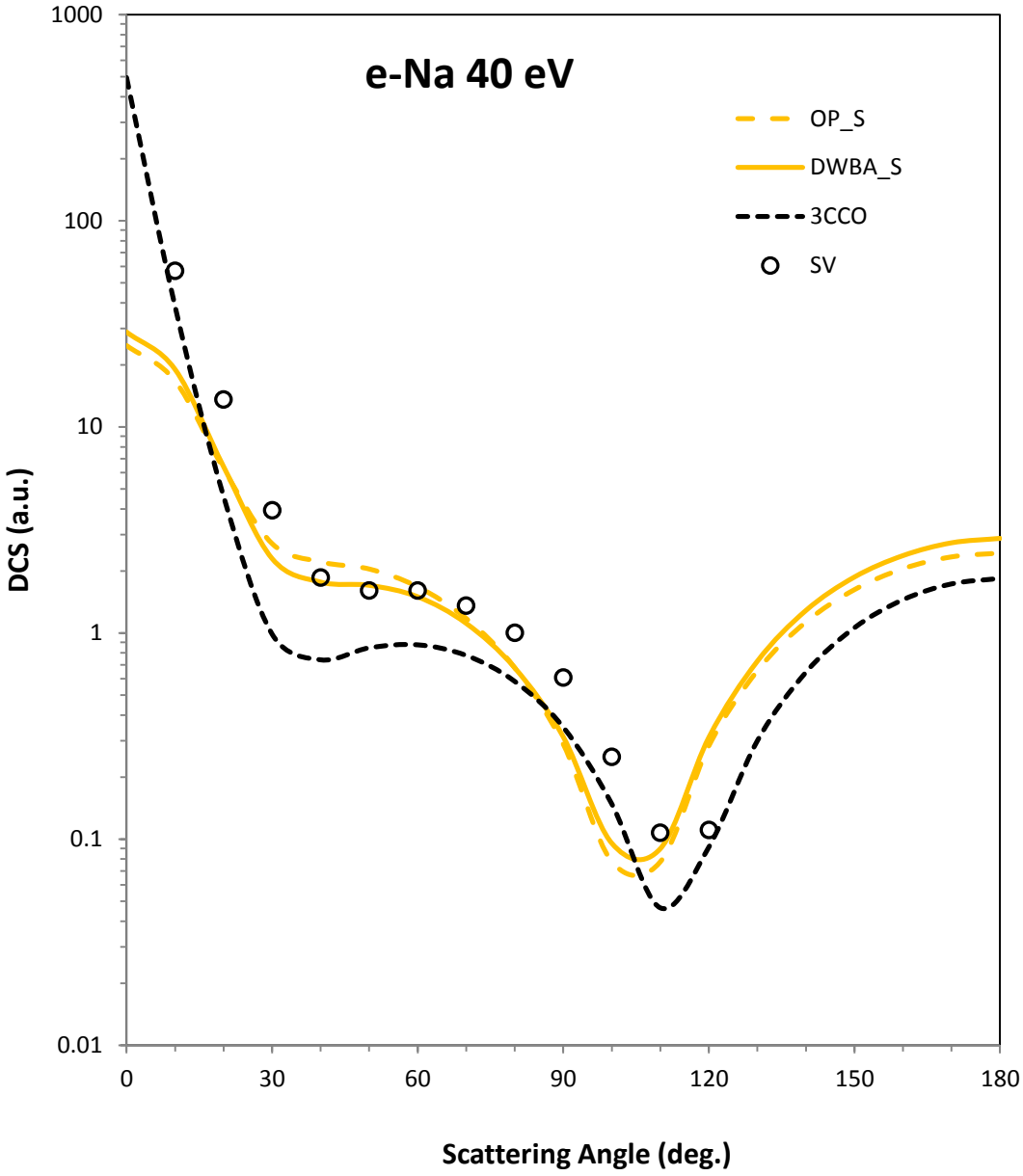

Figure 4.3: Differential cross sections for elastic scattering of electrons by sodium atom at 40eV impact energy. Experimental data: SV, Srivastava and Vuskovic (1980). Calculations: OP_S, present optical potential method with static potential, DWBA, present first order distorted wave Born approximation with static potential, 3CCO, 3-state coupled channels optical Method (Bray *et al*., 1991).

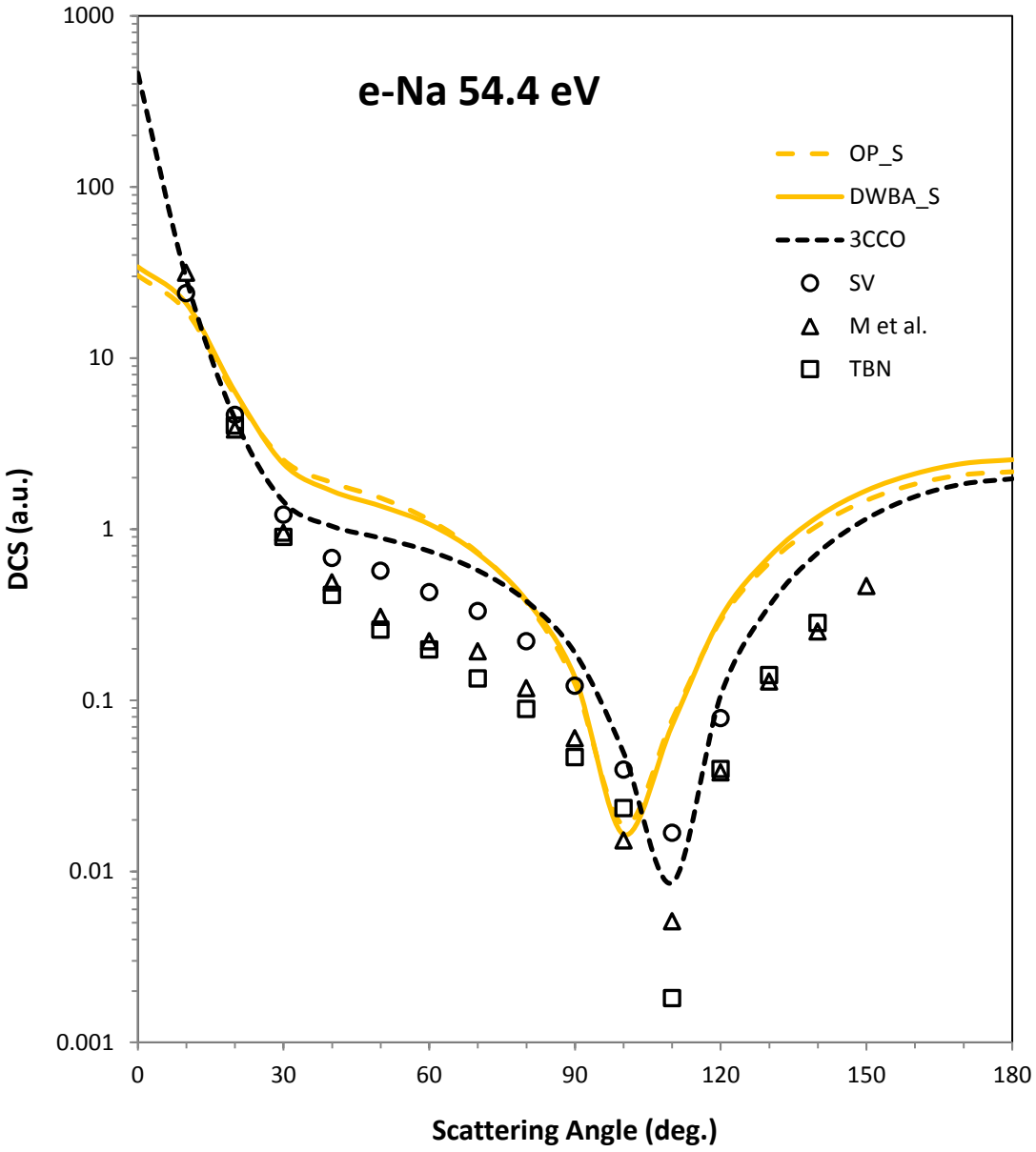

Figure 4.4: Differential cross sections for elastic scattering of electrons by sodium atom at 54.4eV impact energy. Experimental data: TBN, Teubner *et al*., (1978), SV, Srivastava and Vuskovic (1980), M *et al.*, Marinkovic *et al.* (1992). Calculations: OP_S, present optical potential method with static potential, DWBA_S, present first order distorted wave Born approximation with static potential, 3CCO, 3-state coupled channels optical Method (Bray *et al*., 1991).

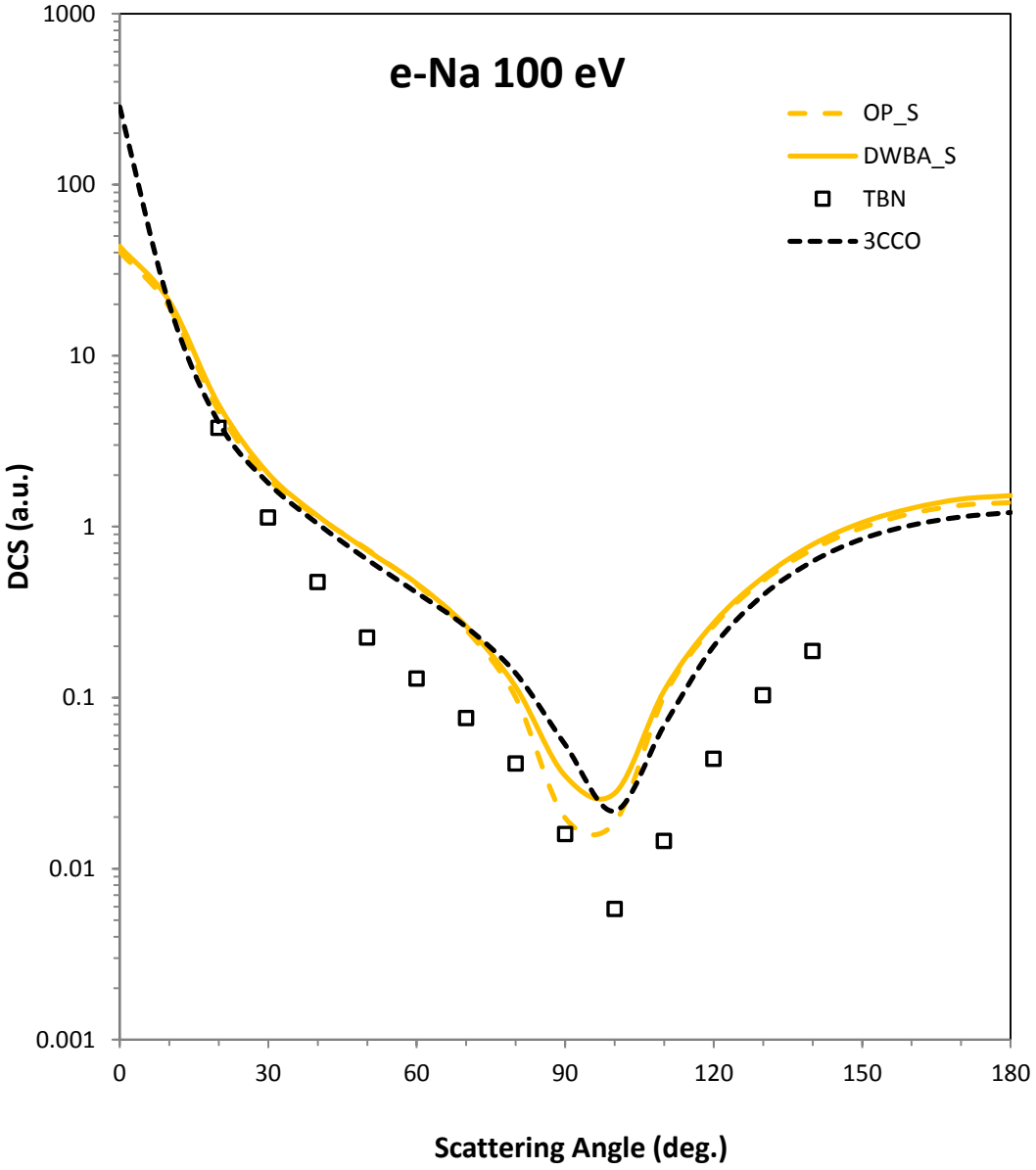

Figure 4.5: Differential cross sections for elastic scattering of electrons by sodium atom at 100eV impact energy. Experimental data: TBN, Teubner *et al*., (1978). Calculations: OP_S, present optical potential method with static potential, DWBA_S, present first order distorted wave Born approximation with static potential, 3CCO, 3-state coupled channels optical Method (Bray *et al*., 1991).

4.1.2 Potassium

For electron-potassium elastic scattering at 7eV, the present differential cross section results (figure 4.6) obtained using the DWBA_S and OP_S methods are in close agreement at all scattering angles apart from near the two DCS minima. This indicates that inclusion of the exchange T-matrix element in the DWBA_S calculation has only a small effect on the results. This implies that the effect of exchange on the heavier potassium atom is small compared to sodium. The present DCS do not agree well with the experimental results of Vuskovic and Srivastava (1980) since polarization and absorption effects have been omitted. The second order distorted-wave Born approximation (DWSB) of Madison *et al*. (1995), which involves a sum over all bound atomic states and integration over the continuum states of the valence electron to second order in perturbation theory, is in very good agreement with the measured results of Vuskovic and Srivastava (1980) for scattering angles $\theta \leq 60^{\circ}$. This is because polarization effects are taken into account in the DWSB calculation. The long-range polarization potential influences small-angle scattering since this is the potential felt by electrons moving far from the atom and which are scattered least. The discrepancy at larger scattering angles is not expected since the calculation by Madison *et al*. (1995) already includes absorption effects.

At 40eV (figure 4.7) electron-impact energy our DWBA_S and OP_S calculations yield nearly identical results indicating that the effect of the exchange T-matrix element is insignificant for electron-potassium elastic scattering at this electron-impact energy. There is good agreement with the measured differential cross sections results of Vuskovic and Srivastava (1980) and with the DWSB calculation of Madison *et al*. (1995) apart from small scattering angles due to the neglect of polarization effects. At 60eV (figure 4.8) the present

DWBA_S and OP_S calculations are very close at all scattering angles. The present DCS are in good agreement with the experimental results of Vuskovic and Srivastava at scattering angles $\theta \leq 60^{\circ}$ but are significantly higher at larger angles due to omission of absorption effects. The close agreement between the present DCS results and the DWSB results of Madison *et al*. (1995) at $\theta \geq 10^{\circ}$ is not expected since the DWSB calculation included absorption effects and should be in closer agreement with experiment than the present results. At 100eV (figure 4.9) the DWSB calculation of Madison *et al*. (1995) is in close agreement with both our DWBA_S and OP_S differential cross sections but not at small scattering angles because the present calculations do not include a polarization potential. Also since the present results do not include an absorption potential, the DWSB calculation is expected to give lower DCS at intermediate and large scattering angles compared to the present calculations but this is not the case especially at $30^{\circ} \leq \theta \leq 70^{\circ}$. Agreement between our DWBA_S and OP_S calculations and the absolute experimental results of Buckman *et al*. (1979) and Vuskovic and Srivastava (1980) is qualitative (i.e. there is good shape agreement). It is expected that inclusion of a polarization potential as well as an absorption potential in the DWBA_S and OP_S calculations will significantly improve agreement with experiment by raising the DCS at small scattering angles and lowering the DCS at large angles.

At 200eV (figure 4.10) the experimental DCS of Buckman *et al*. (1979) are in agreement with the present DWBA_S and OP_S calculations at small scattering angles but are lower than the present DCS at intermediate and large angles. This is due to absence of an absorption potential in the OP_S and DWBA_S calculation. Also since the DWBA_S and OP_S calculations are in agreement with each other, the scattering at this energy is clearly dominated by the direct (static) and absorption potentials.

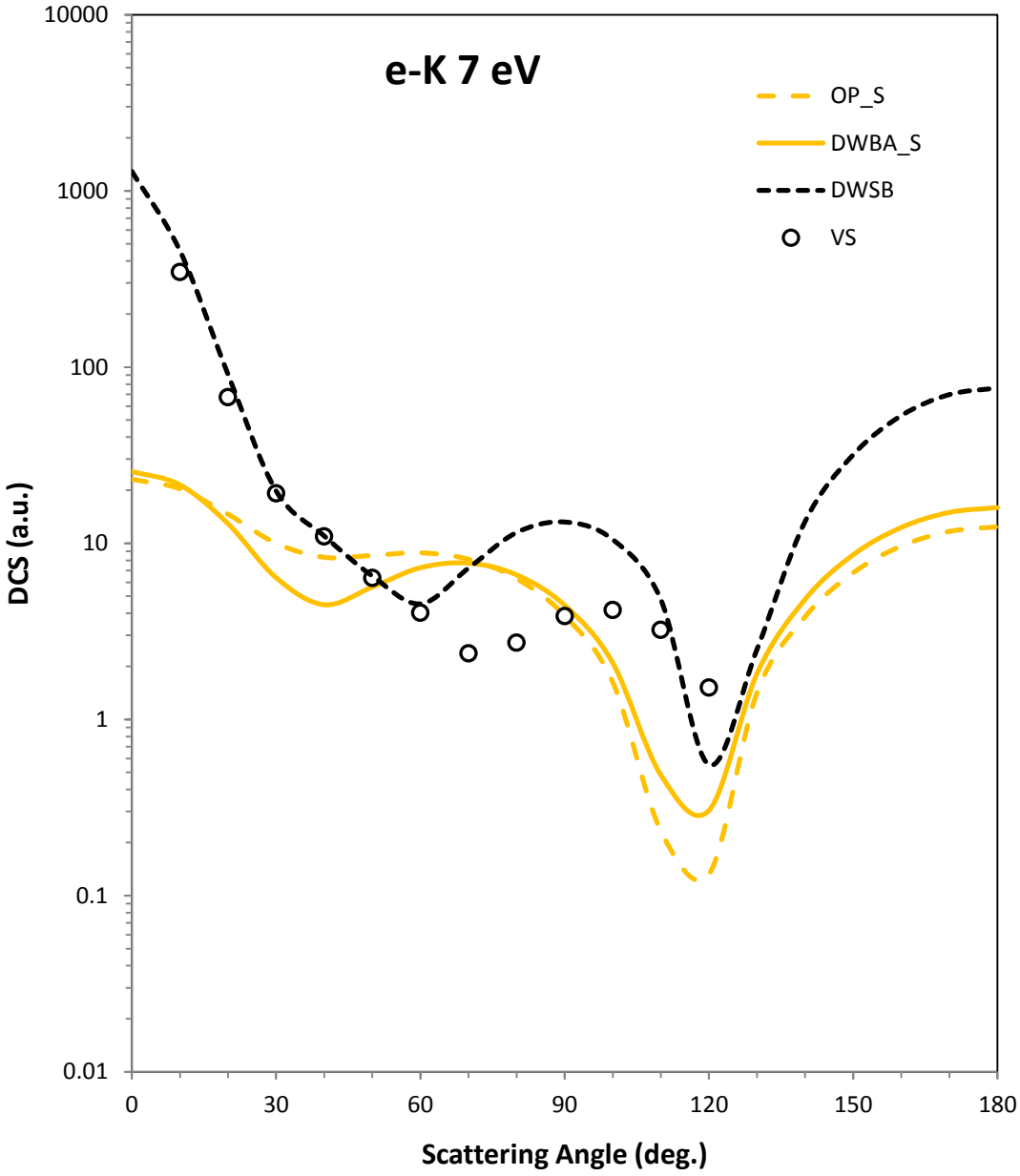

Figure 4.6: Differential cross sections for elastic scattering of electrons by potassium atom at 7eV impact energy. Experimental data: VS, Vuskovic and Srivastava (1980). Calculations: OP_S, present optical potential method with static potential, DWBA_S, present first order distorted wave Born approximation with static potential, DWSB, second order distorted wave Born approximation (Madison *et al.*, 1995).

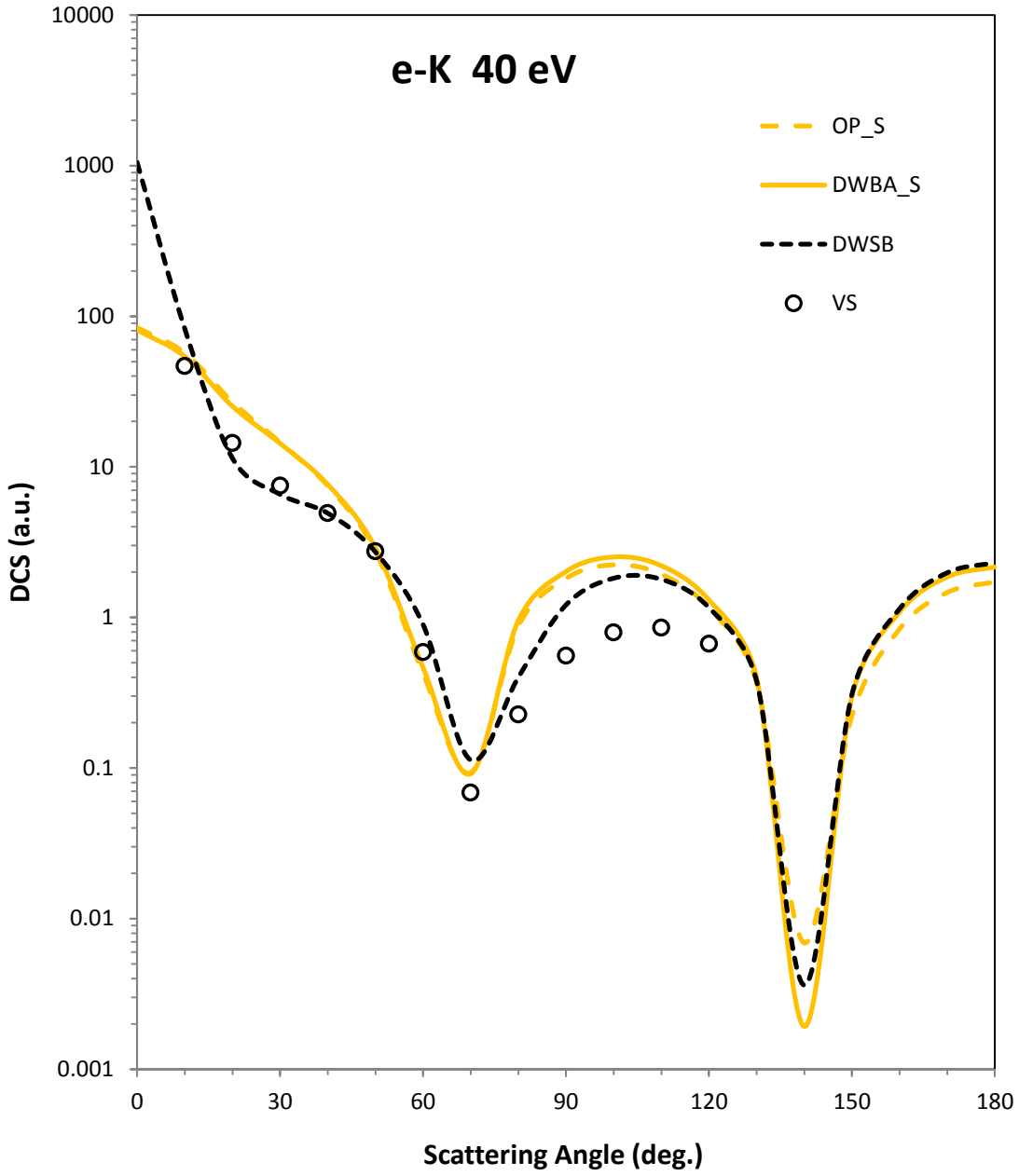

Figure 4.7: Differential cross sections for elastic scattering of electrons by potassium atom at 40eV impact energy. Experimental data: VS, Vuskovic and Srivastava (1980). Calculations: OP_S, present optical potential method with static potential, DWBA_S, present first order distorted wave Born approximation with static potential, DWSB, second order distorted wave Born approximation (Madison *et al*., 1995).

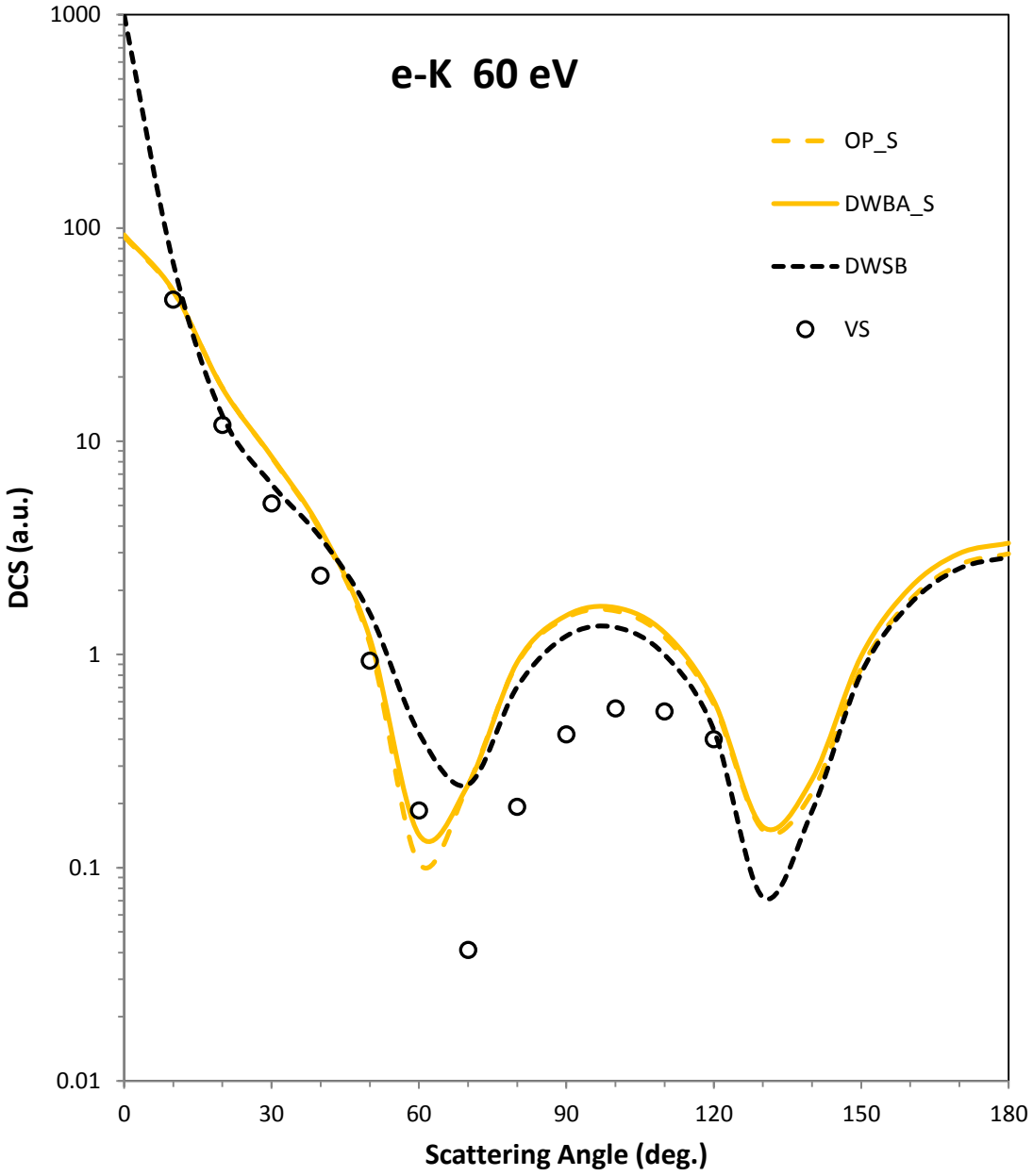

Figure 4.8: Differential cross sections for elastic scattering of electrons by potassium atom at 60eV impact energy. Experimental data: VS, Vuskovic and Srivastava (1980). Calculations: OP_S, present optical potential method with static potential, DWBA_S, present first order distorted wave Born approximation with static potential, DWSB, second order distorted wave Born approximation (Madison *et al*., 1995).

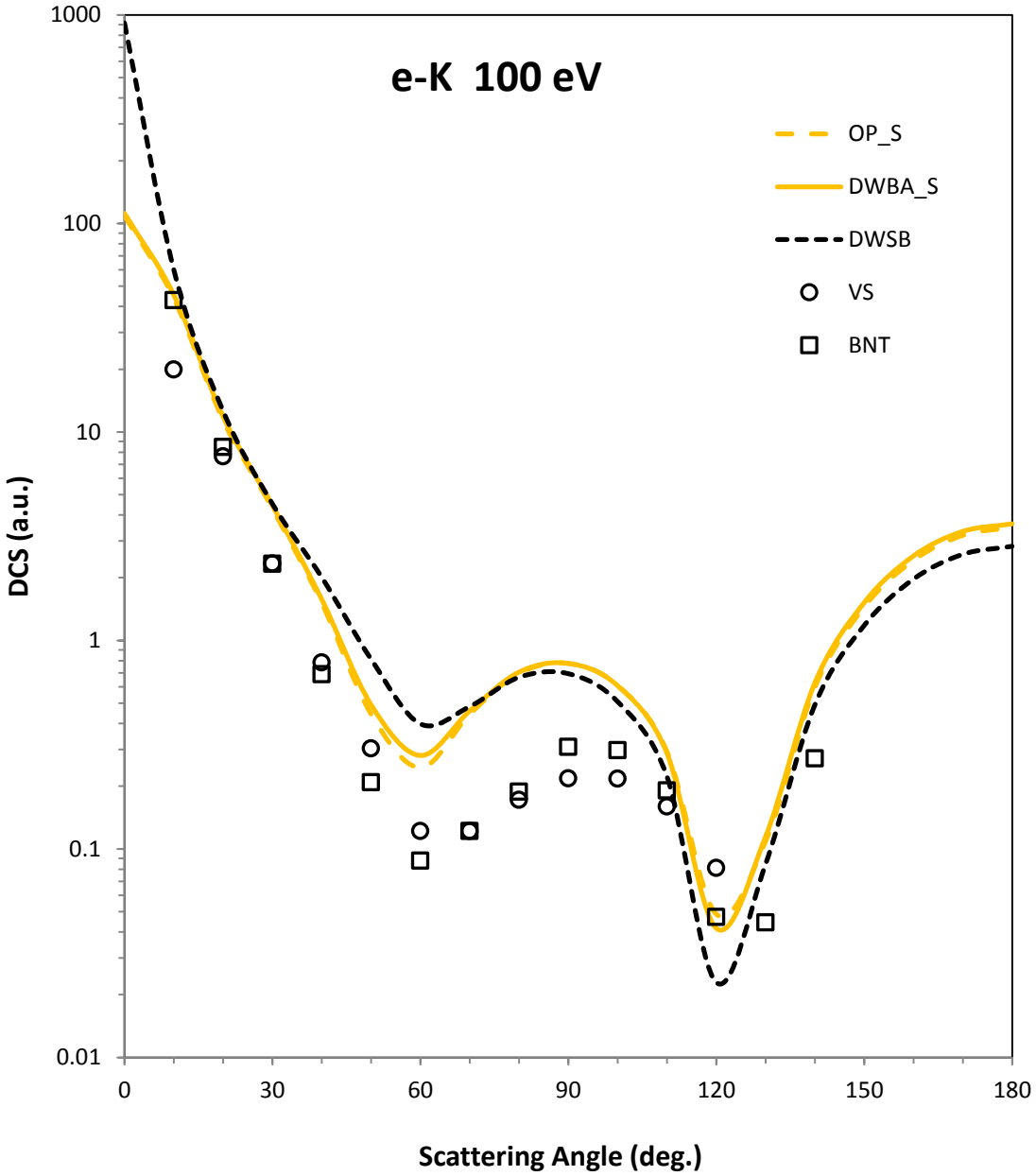

Figure 4.9: Differential cross sections for elastic scattering of electrons by potassium atom at 100eV impact energy. Experimental data: BNT, Buckman *et al*., (1979), VS, Vuskovic and Srivastava (1980). Calculations: OP_S, present optical potential method with static potential, DWBA_S, present first order distorted wave Born approximation with static potential, DWSB, second order distorted wave Born approximation (Madison *et al*., 1995).

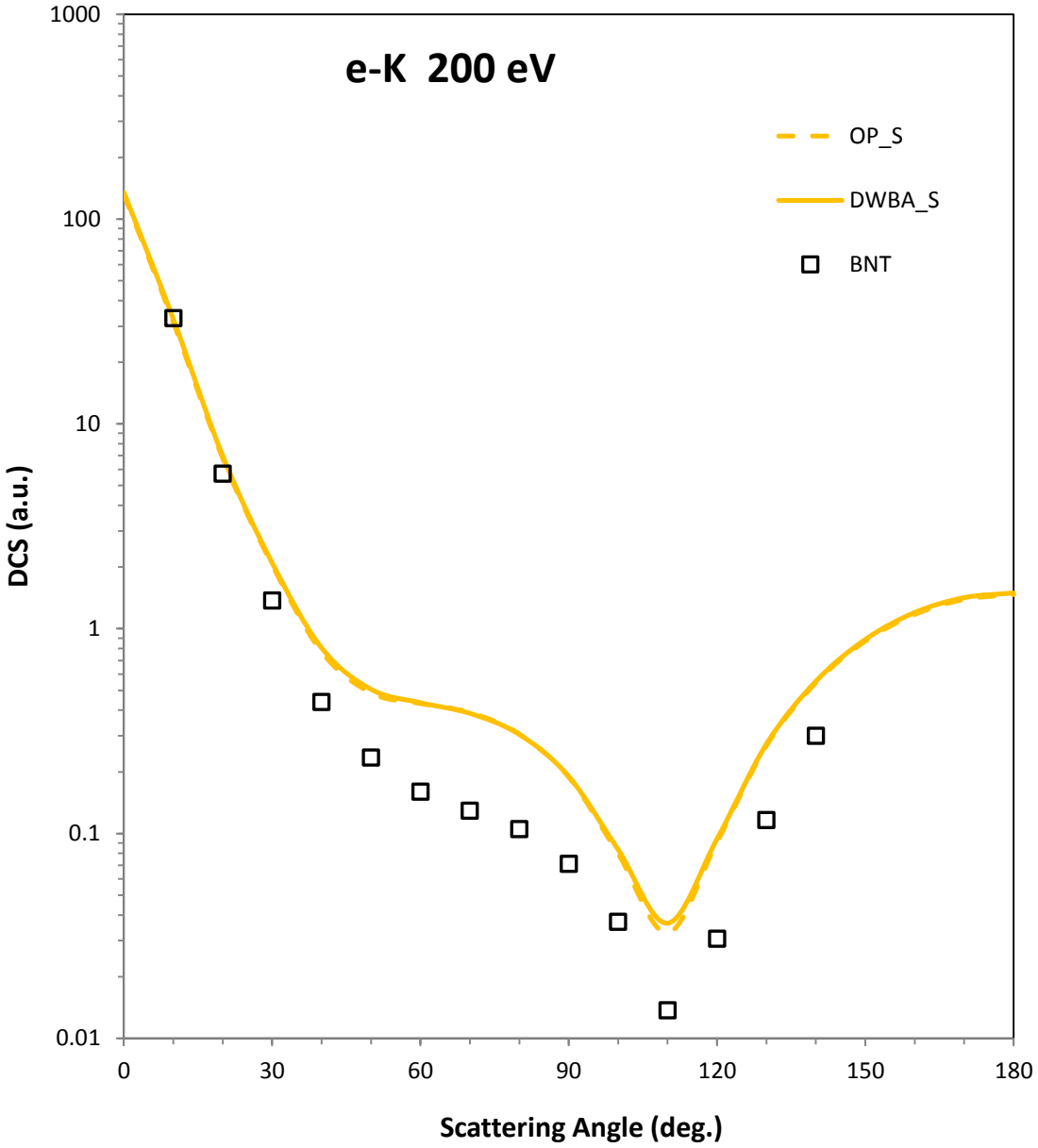

Figure 4.10: Differential cross sections for elastic scattering of electrons by potassium atom at 200eV impact energy. Experimental data: BNT, Buckman *et al*., (1979). Calculations: OP_S, present optical potential method with static potential, DWBA_S, present first order distorted wave Born approximation with static potential.

4.2 Static-Exchange Potential as the Distorting Potential

Figures 4.11 – 4.20 give the differential cross sections for electron-sodium atom and electron-potassium atom elastic scattering at 10 – 100 eV and 7 – 200 eV respectively, using the static-exchange potential for both the OP and DWBA methods at scattering angles $0 \leq \theta \leq 180^{\circ}$. These results are denoted by OP_SE and DWBA_SE respectively. For comparison, the OP_S, and DWBA_S results are also shown.

4.2.1 Sodium

From figure 4.11, it is evident that at 10 eV inclusion of the exchange potential (given in equation 87) in the OP_SE calculation has a dramatic effect on the DCS results and leads to much improved qualitative agreement with the experimental results of Srivastava and Vuskovic (1980) and of Marinkovic *et al.* (1992). This indicates that the effect of exchange on the scattering electron is significant at this electron-impact energy. Although the agreement between the present OP_SE and DWBA_SE results improves after inclusion of the exchange potential, the remaining difference between the two methods in figure 4.11 confirms that the effect of exchange on the sodium atom, as accounted for by the exchange T-matrix element, is equally important otherwise the two methods would give identical results. At 20 eV (Figure 4.12), the OP_SE and DWBA_SE results are similar. This is also the case at 40, 54.4, and 100 eV (Figures 4.13, 4.14, and 4.15). This trend indicates that exchange effects decrease in importance as the electron-impact energy increases. The close agreement between both the present OP_SE and DWBA_SE results at 20 eV and the experimental results of Srivastava and Vuskovic (1980) at intermediate and large scattering angles is not expected since the present results have not included absorption effects which are expected to lower the DCS values. Also at 40 eV, the present DCS results are already lower than the experimental

values. It is therefore highly likely that these experimental results have a systematic error since inclusion of the absorption potential is expected to lower the DCS at all energies above the first excitation threshold, including 20 eV and 40 eV (McEachran and Stauffer, 2009). The absorption potential is therefore expected to lead to disagreement with these measured results. Sources of statistical errors in the experimental data of Srivastava and Vuskovic (1980) include errors in the normalization procedure and errors in the measurement of the elastic to inelastic intensity ratios needed to place the differential cross section on an absolute scale. At 54.4 eV and 100 eV, the present OP_SE and DWBA_SE differential cross section results are higher than the measured results of Teubner *et al.* (1978), Srivastava and Vuskovic (1980) and Marinkovic *et al.* (1992), which is as expected since the OP_SE and DWBA_SE results have not included absorption effects. However at 54.4 eV the large difference between the experimental results of Srivastava and Vuskovic (1980), on the one hand, and the results of Teubner *et al.* (1978) and Marinkovic *et al.* (1992) on the other hand, casts further doubt on the accuracy of the experimental data and indicates presence of systematic errors in the measurement of differential cross sections specifically in the range $30^\circ \le \theta \le 120^\circ$.

4.2.2 Potassium

Figure 4.16 shows that the effect of the exchange T-matrix element in electron-potassium elastic scattering is significant at 7 eV since the OP_SE and DWBA_SE values are quite different even after inclusion of the exchange potential. However as the electron-impact energy increases, the effect becomes less important and the two methods yield similar DCS values as shown in figures 4.17-20. As expected, the OP_SE and DWBA_SE results obtained using a static-exchange potential are generally higher than the experimental results of Vuskovic and Srivastava (1980) at 7 – 100 eV, and the experimental data of Buckman *et al.*

(1979) at 100 eV and 200 eV, since absorption effects have been neglected. At 100 eV, it is noteworthy that the experimental results are in good agreement with each other.

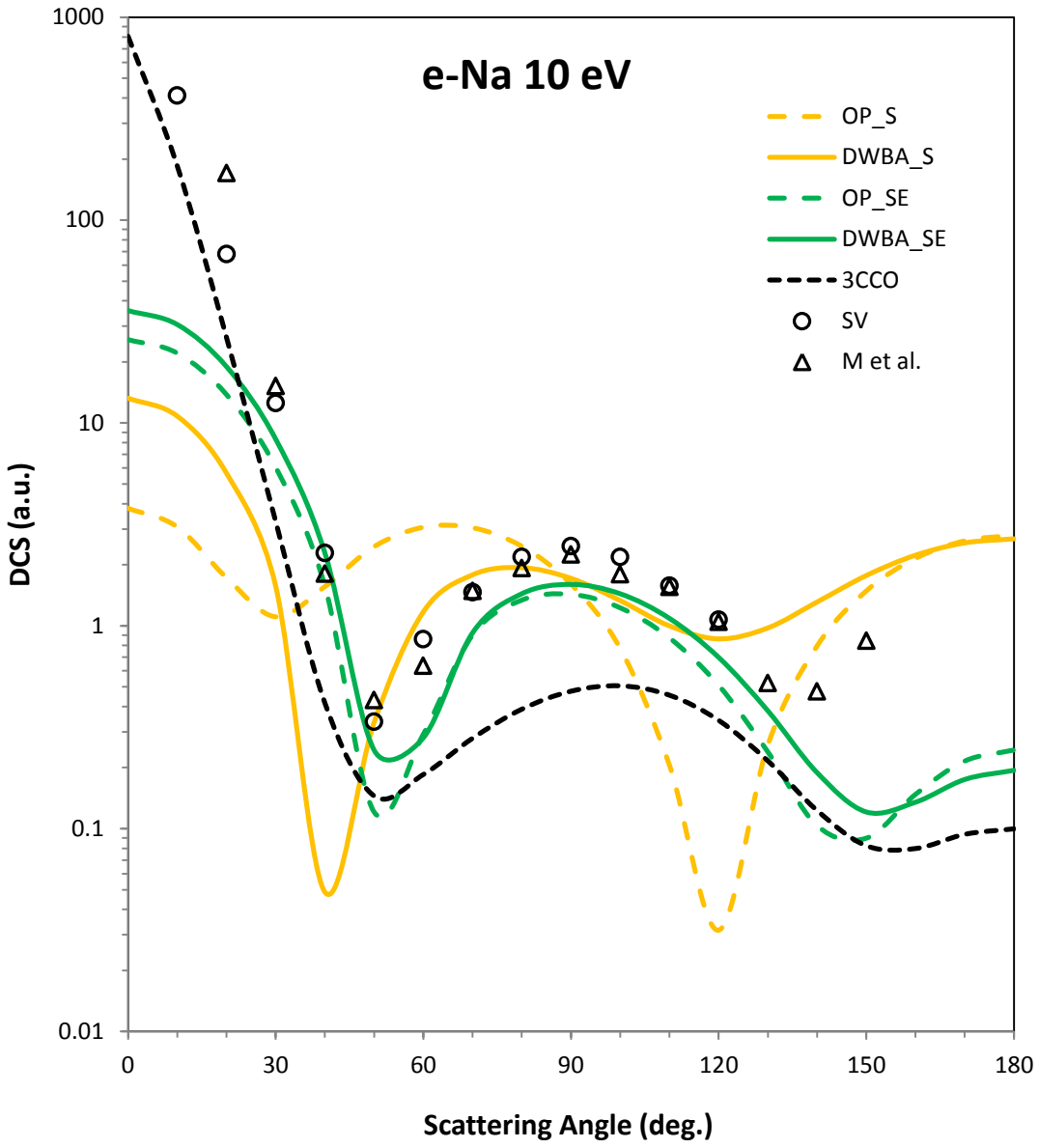

Figure 4.11: Differential cross sections for elastic scattering of electrons by sodium atom at 10eV impact energy. Experimental data: SV, Srivastava and Vuskovic (1980), M *et al.*, Marinkovic *et al.* (1992). Calculations: OP_SE, present optical potential method with the static-exchange potential, DWBA_SE, present first order distorted wave Born approximation with the static-exchange potential, 3CCO, 3-state coupled channels optical Method (Bray *et al.*, 1991).

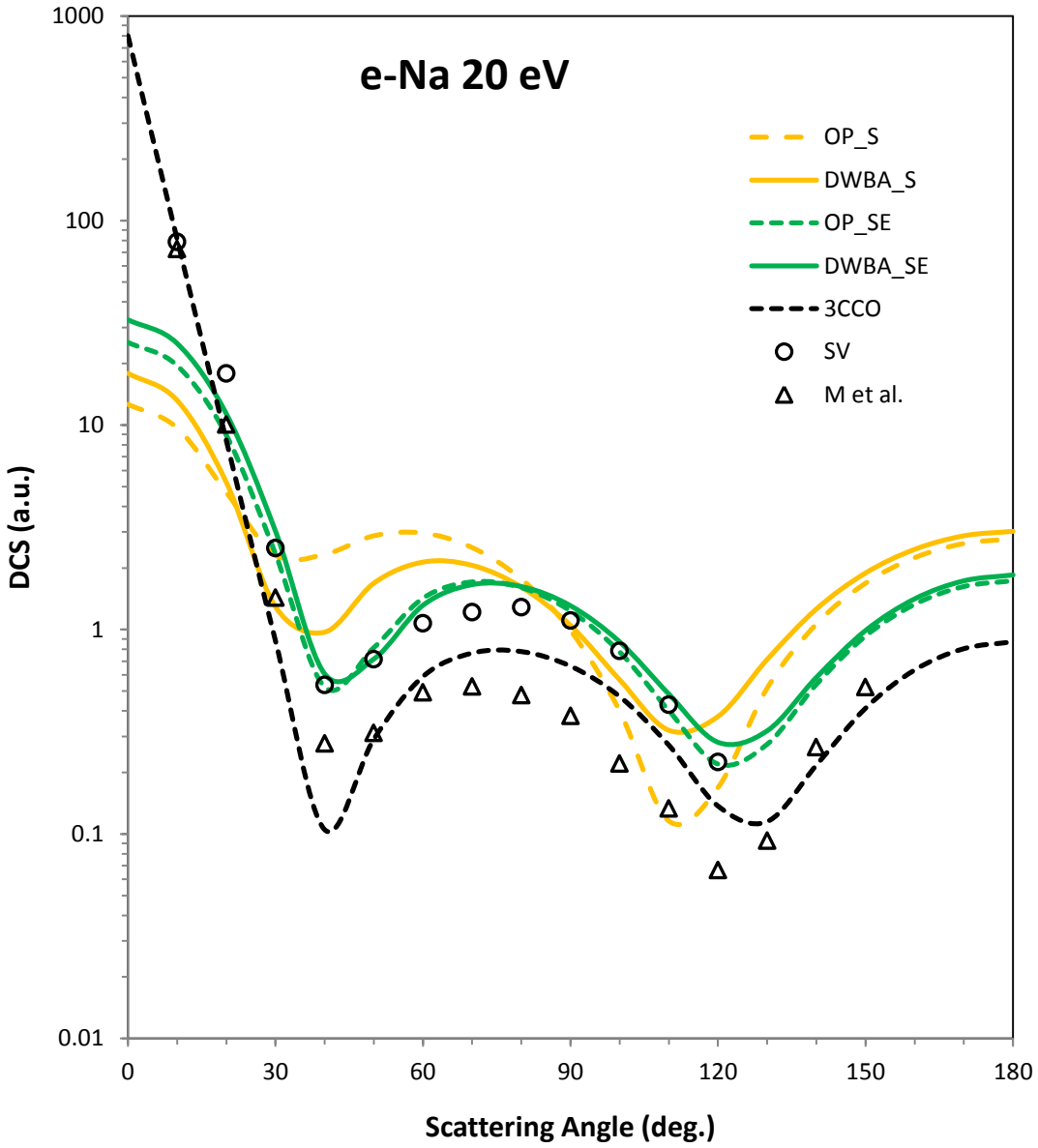

Figure 4.12: Differential cross sections for elastic scattering of electrons by sodium atom at 20eV impact energy. Experimental data: SV, Srivastava and Vuskovic (1980), M *et al.*, Marinkovic *et al.* (1992). Calculations: OP_SE, present optical potential method with the static-exchange potential, DWBA_SE, present first order distorted wave Born approximation with the static-exchange potential, 3CCO, 3-state coupled channels optical Method (Bray *et al.*, 1991).

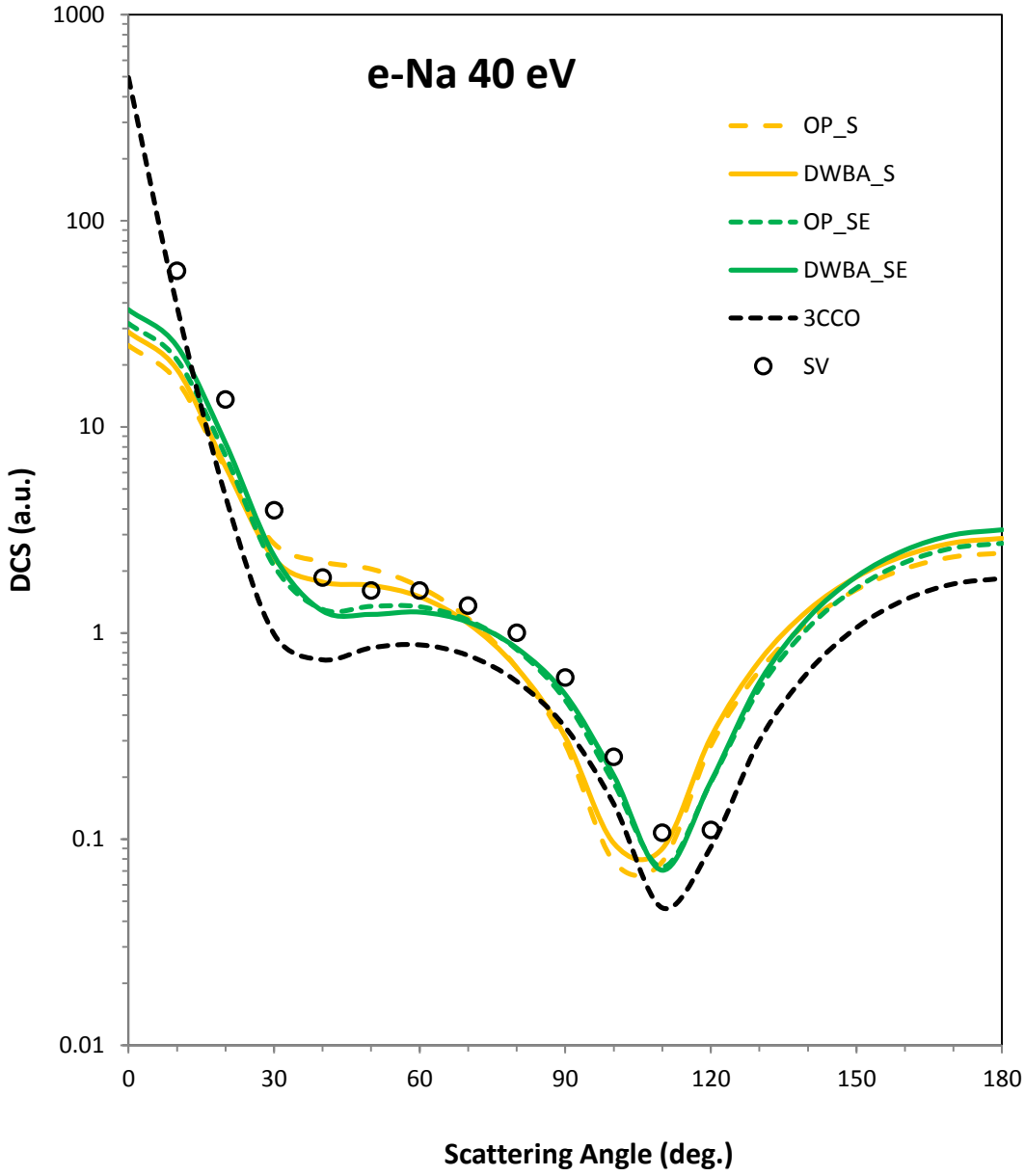

Figure 4.13: Differential cross sections for elastic scattering of electrons by sodium atom at 40eV impact energy. Experimental data: SV, Srivastava and Vuskovic (1980). Calculations: OP_SE, present optical potential method with the static-exchange potential, DWBA_SE, present first order distorted wave Born approximation with the static-exchange potential, 3CCO, 3-state coupled channels optical Method (Bray *et al*., 1991).

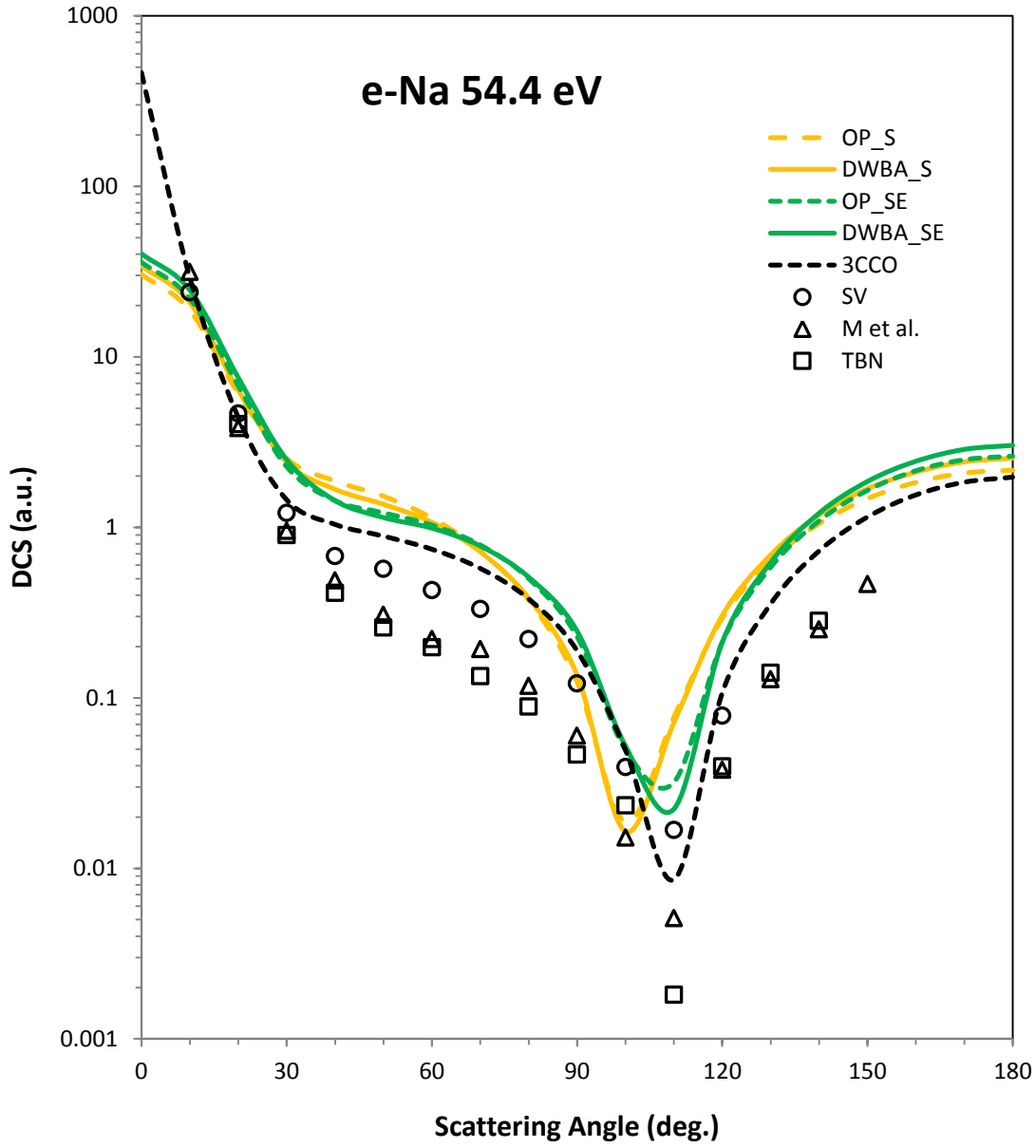

Figure 4.14: Differential cross sections for elastic scattering of electrons by sodium atom at 54.4eV impact energy. Experimental data: TBN, Teubner *et al*., (1978), SV, Srivastava and Vuskovic (1980), M *et al.*, Marinkovic *et al.* (1992). Calculations: OP_SE, present optical potential method with the static-exchange potential, DWBA_SE, present first order distorted wave Born approximation with the static-exchange potential, 3CCO, 3-state coupled channels optical Method (Bray *et al*., 1991).

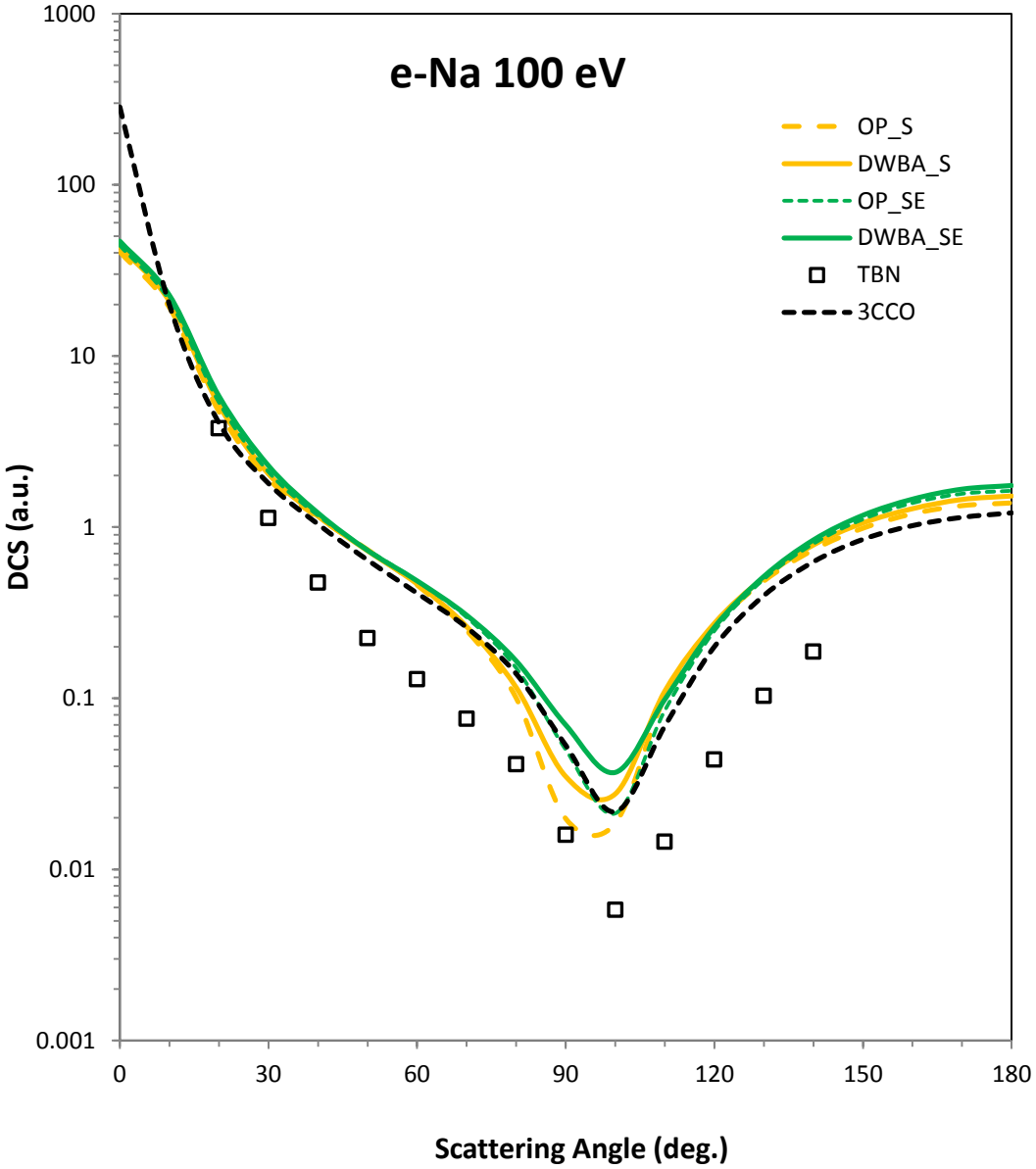

Figure 4.15: Differential cross sections for elastic scattering of electrons by sodium atom at 100eV impact energy. Experimental data: TBN, Teubner *et al*., (1978). Calculations: OP_SE, present optical potential method with the static-exchange potential, DWBA_SE, present first order distorted wave Born approximation with the static-exchange potential, 3CCO, 3-state coupled channels optical Method (Bray *et al*., 1991).

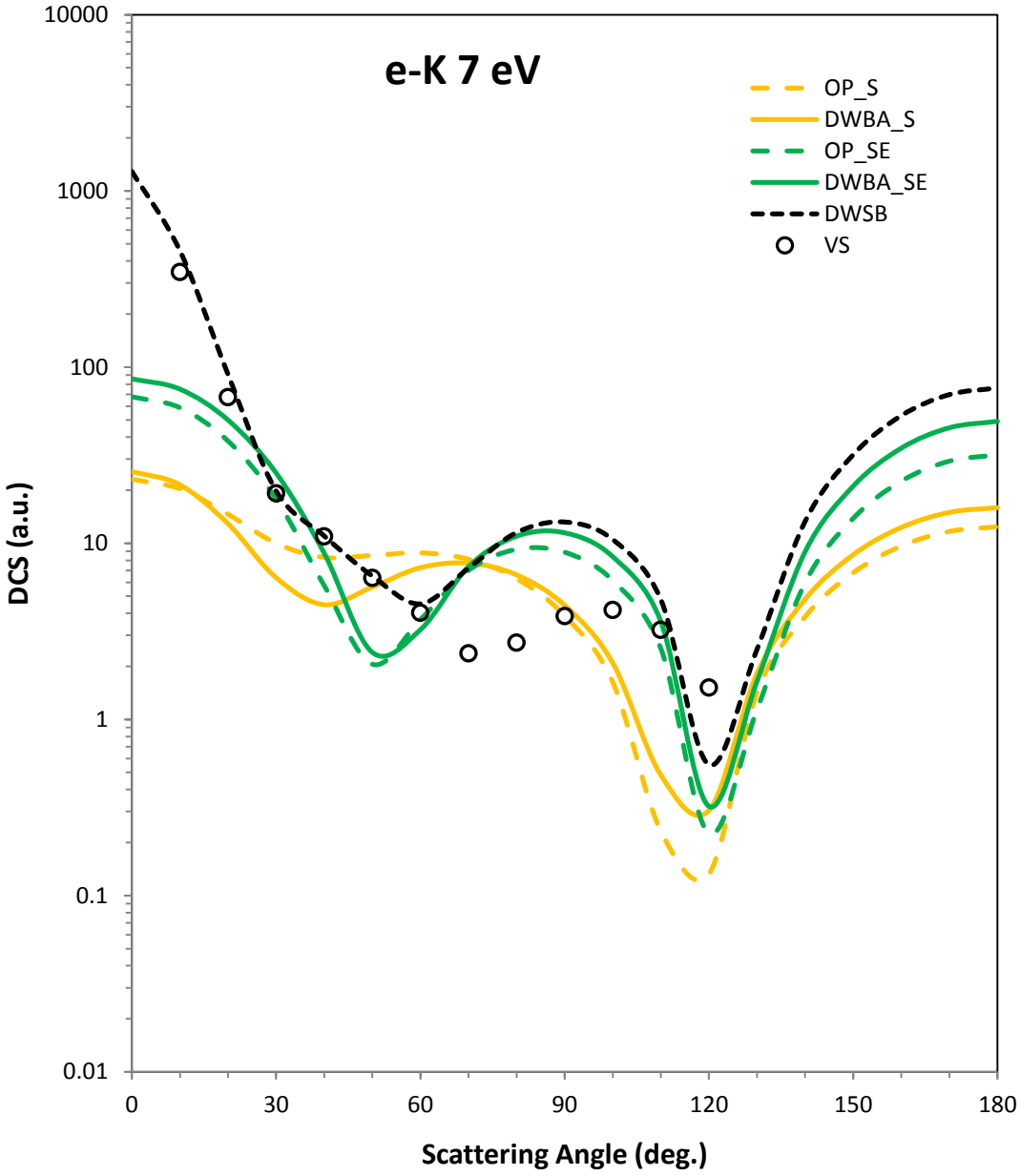

Figure 4.16: Differential cross sections for elastic scattering of electrons by potassium atom at 7eV impact energy. Experimental data: VS, Vuskovic and Srivastava (1980). Calculations: OP_SE, present optical potential method with the static-exchange potential, DWBA_SE, present first order distorted wave Born approximation with the static-exchange potential, DWSB, second order distorted wave Born approximation (Madison *et al.*, 1995).

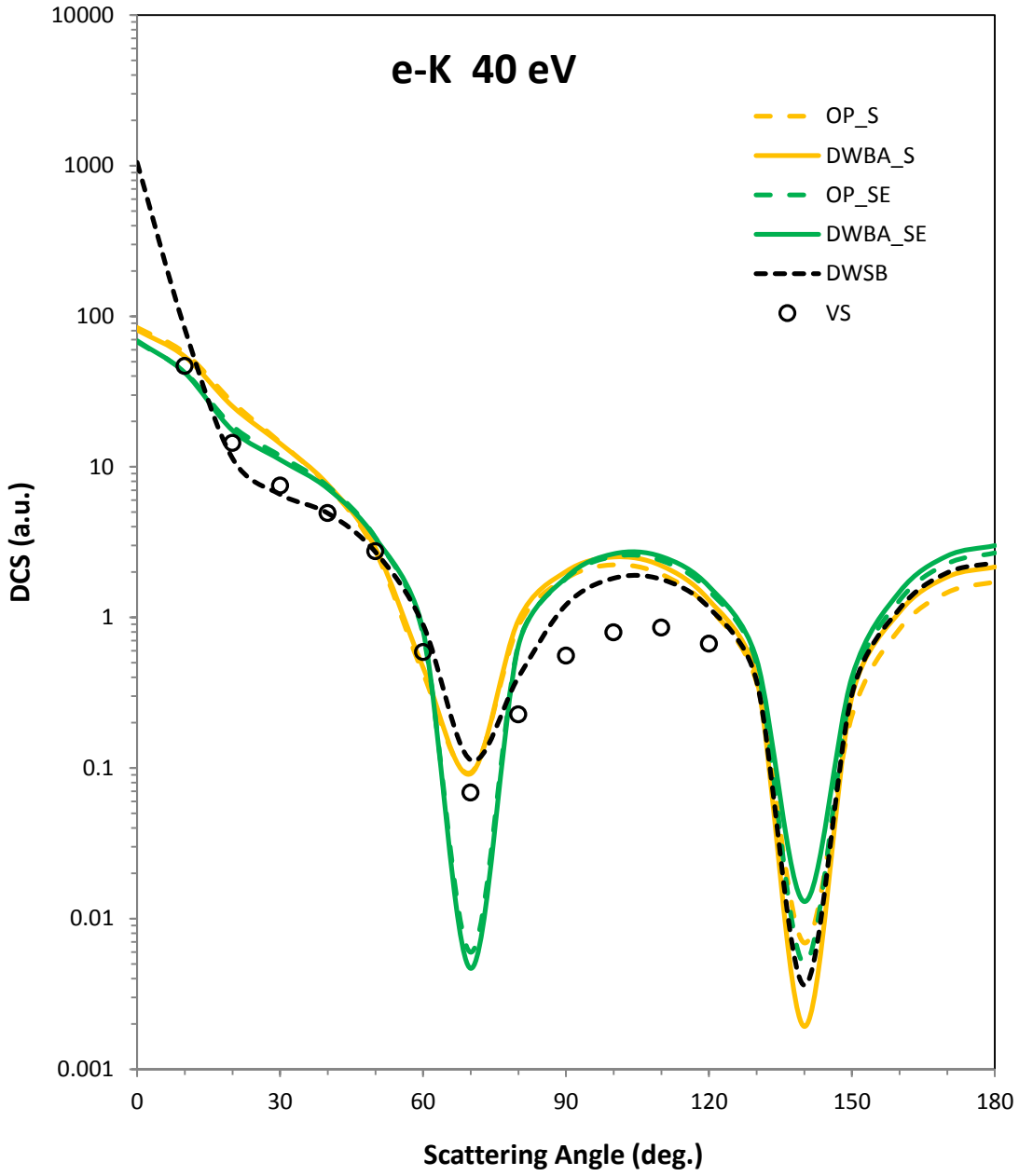

Figure 4.17: Differential cross sections for elastic scattering of electrons by potassium atom at 40eV impact energy. Experimental data: VS, Vuskovic and Srivastava (1980). Calculations: OP_SE, present optical potential method with the static-exchange potential, DWBA_SE, present first order distorted wave Born approximation with the static-exchange potential, DWSB, second order distorted wave Born approximation (Madison *et al*., 1995).

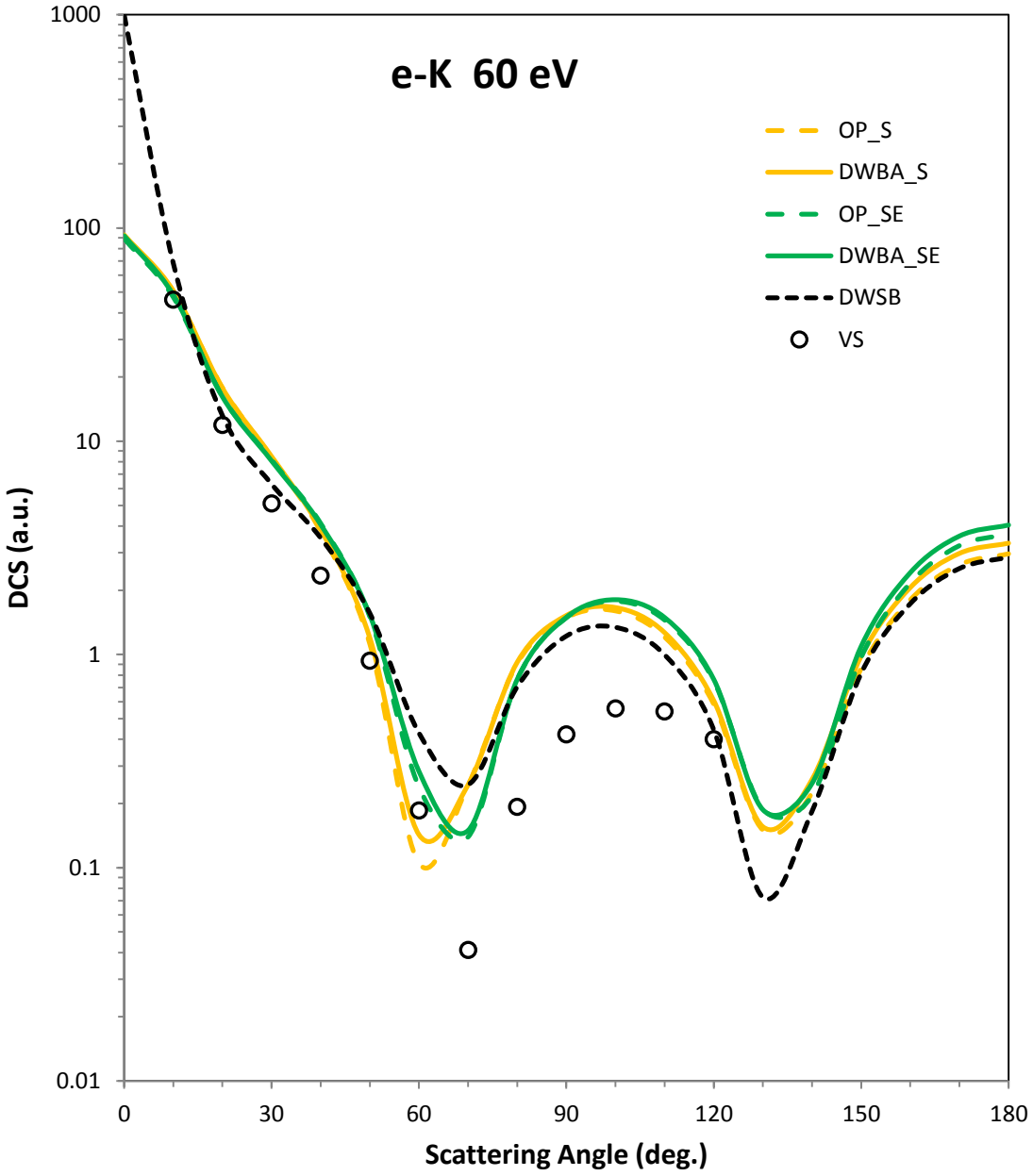

Figure 4.18: Differential cross sections for elastic scattering of electrons by potassium atom at 60eV impact energy. Experimental data: VS, Vuskovic and Srivastava (1980). Calculations: OP_SE, present optical potential method with the static-exchange potential, DWBA_SE, present first order distorted wave Born approximation with the static-exchange potential, DWSB, second order distorted wave Born approximation (Madison *et al*., 1995).

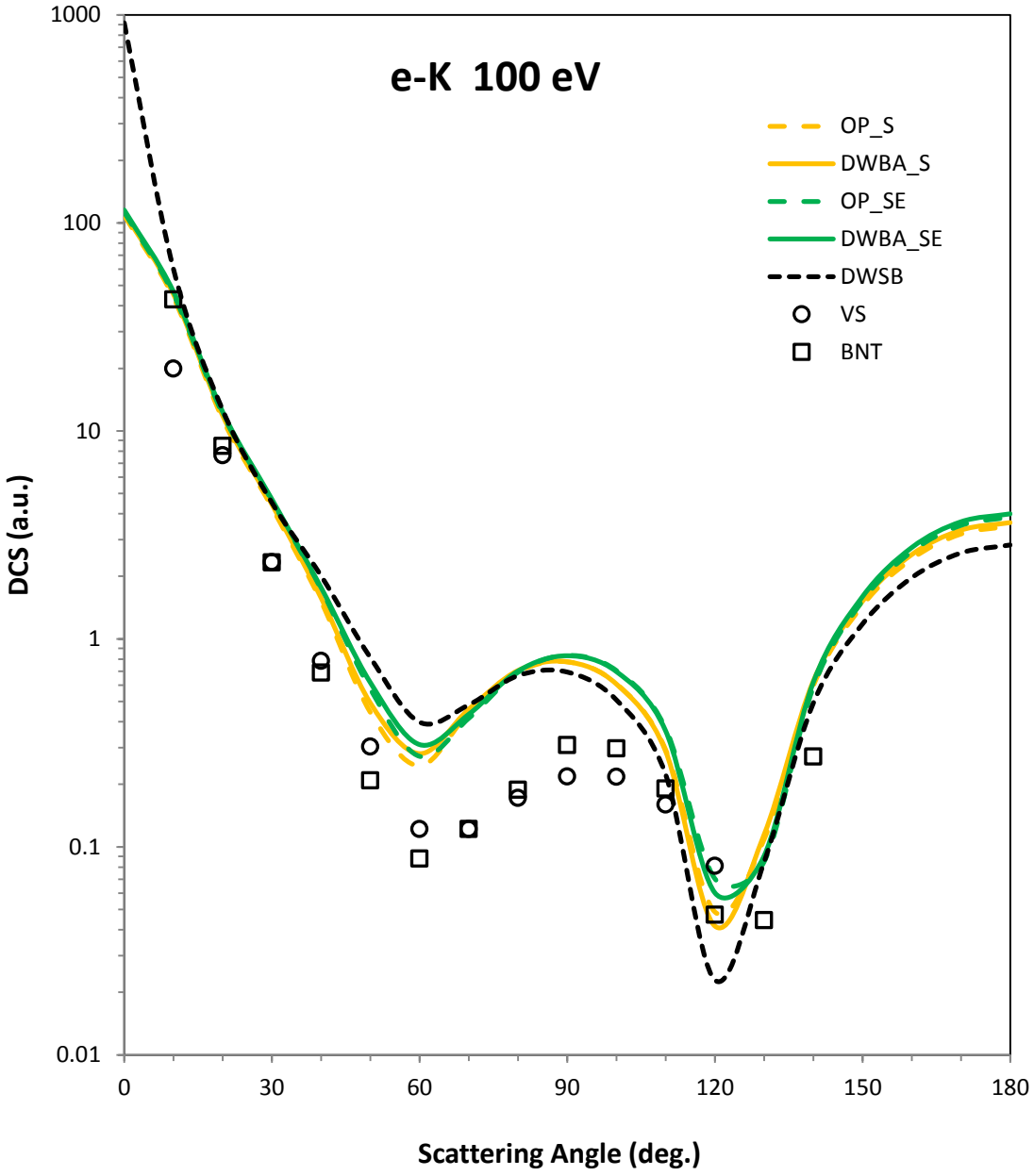

Figure 4.19: Differential cross sections for elastic scattering of electrons by potassium atom at 100eV impact energy. Experimental data: BNT, Buckman *et al*., (1979), VS, Vuskovic and Srivastava (1980). Calculations: OP_SE, present optical potential method with the static-exchange potential, DWBA_SE, present first order distorted wave Born approximation with the static-exchange potential, DWSB, second order distorted wave Born approximation (Madison *et al*., 1995).

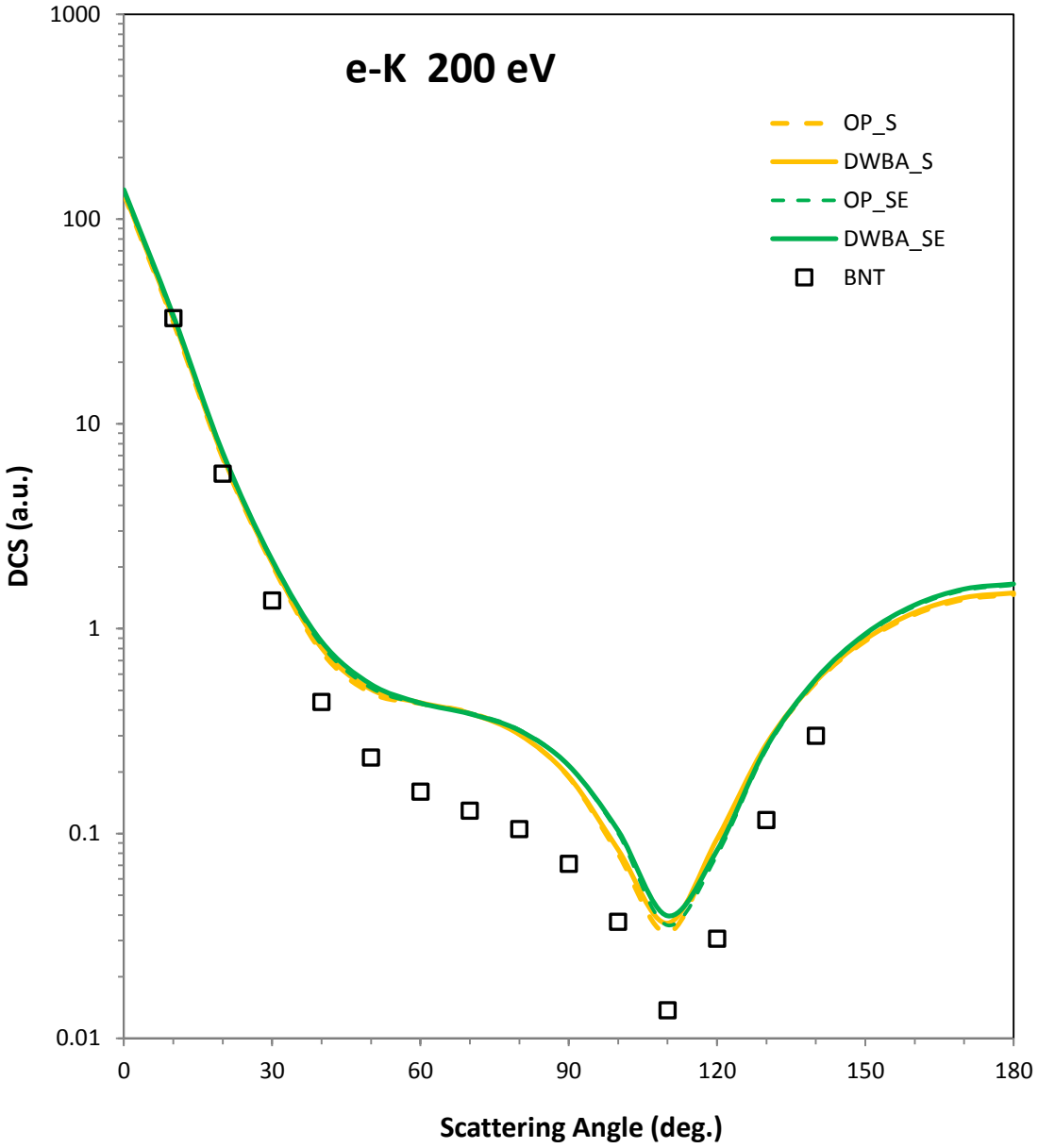

Figure 4.20: Differential cross sections for elastic scattering of electrons by potassium atom at 200eV impact energy. Experimental data: BNT, Buckman *et al*., (1979). Calculations: OP_SE, present optical potential method with the static-exchange potential, DWBA_SE, present first order distorted wave Born approximation with the static-exchange potential.

4.3 Static-Exchange-Polarization and Static-Exchange-Polarization-Absorption Potentials as the Distorting Potentials

Figures 4.21 – 4.25, and figures 4.27 – 4.31 show the OP and DWBA differential cross sections for electron-sodium atom and electron-potassium atom elastic scattering at 10 – 100 eV and 7 – 200 eV respectively, which are calculated using the static-exchange-polarization potential. These are denoted by OP_SEP and DWBA_SEP respectively. The DCS obtained using the static-exchange-polarization-absorption potential, for both the DWBA and OP methods are also shown and are labelled as OP_SEPA and DWBA_SEPA respectively. Figure 4.26 and figure 4.32 give the corresponding integral cross sections (ICS) for sodium atom and potassium atom respectively. Figure 4.33 and figure 4.34 give the total (elastic + inelastic) cross sections (TCS) for sodium atom and potassium atom respectively. The ICS are shown in tables 4.1 and 4.2. The final DCS obtained with the static-exchange-polarization-absorption potential, are shown in tables 4.3 and 4.4 for sodium atom, and tables 4.6 and 4.7 for potassium atom. These TCS are given in table 4.5 and table 4.8.

4.3.1 Sodium

From figure 4.21 it can be seen that inclusion of the non-local polarization potential (which is the real part of equation (102) in the OP_SEP results at 10 eV has the very large effect of increasing the small-angle electron-sodium atom differential cross sections. The effect of the polarization potential in the DWBA_SEP results is similar. The OP_SEP and DWBA_SEP differential cross sections obtained using a local static-exchange plus non-local polarization potential are in close agreement with each other but the OP_SEP results tend to be lower than the DWBA_SEP results at small scattering angles and near the DCS minima. The difference is caused by the additional direct and exchange terms (equations 50, 62, 72, and 85) in the

DWBA _SEP calculation. Inclusion of the polarization potential has the effect of improving agreement between both the OP_SEP and DWBA_SEP results and the experimental results of Marinkovic *et al.* (1992) and Srivastava and Vuskovic (1980) at small and intermediate scattering angles. The OP_SEP and DWBA_SEP differential cross sections are significantly higher than the 3CCO calculations of Bray *et al.* (1991) at most scattering angles. Inclusion of the absorption potential in both the OP_SEP and DWBA_SEP calculations is expected to improve agreement with the 3CCO results which have taken into account loss of flux into inelastic channels leading to lowering of the differential cross sections. At 10 eV, the OP_SEPA and DWBA_SEPA calculations obtained using the static-exchange-polarization-absorption potential (where the absorption potential is given by equations 103 – 109) yield very close differential cross sections apart from at large scattering angles. This slight difference is probably due to the extra direct term in the DWBA_SEPA T-matrix element (equation 50). It can also be seen that inclusion of the absorption potential of Staszewska *et al.* (1984) leads to less qualitative agreement between the present OP_SEPA and DWBA_SEPA results and the 3CCO results (Bray *et al.,* 1991) and the experimental results of Marinkovic *et al.* (1992) and Srivastava and Vuskovic (1980). This shows that the choice of the average excitation energy, which influences the absorption potential rather strongly, should be determined using an *ab initio* calculation instead of using the average of the first excitation energy and the ionization potential energy of the atom as is usually done.

At 20 eV (figure 4.22), both the OP_SEP and DWBA_SEP differential cross sections results obtained using a static-exchange-polarization potential are in very good agreement with the experimental results of Srivastava and Vuskovic (1980) although these present results have not yet included an absorption potential. The 3CCO results which have included absorption effects are much lower than the present results suggesting that absorption effects are

significant. This is supported by the much lower DCS results of Marinkovic *et al.* (1992) especially at intermediate and large scattering angles. It can be seen that at 20 eV the OP_SEPA and DWBA_SEPA calculations are in close agreement with each other and that inclusion of the absorption potential brings about closer agreement between the OP_SEPA and DWBA_SEPA results and the 3CCO results. At small scattering angles the OP_SEPA and DWBA_SEPA results are in very good agreement with the results of Srivastava and Vuskovic (1980) but are lower at larger scattering angles. This implies that the absorption potential used in the present calculations overestimates the effect of inelastic processes. However comparison with the experimental DCS of Marinkovic *et al.* (1992) indicates that absorption effects are quite significant at this electron impact energy. At 40 eV the OP_SEP and DWBA_SEP results are slightly lower than the experimental results of Srivastava and Vuskovic (1980) at most scattering angles but are higher than the 3CCO results. As expected, inclusion of absorption potential in the OP_SEPA and DWBA_SEPA calculations brings about better agreement between the present calculations and the 3CCO results.

In figure 4.24 it is seen that at 54.4 eV, the effect of the polarization potential is to increase the small-angle scattering for both the OP_SEP and DWBA_SEP differential cross sections. The OP_SEP, DWBA_SEP, and the 3CCO calculations of Bray *et al*. (1991) are generally higher than the measured results of Teubner *et al.* (1978), Srivastava and Vuskovic (1980), and Marinkovic *et al.* (1992) at intermediate to large scattering angles. Inclusion of an absorption potential in the OP_SEPA and DWBA_SEPA calculations brings about closer agreement between the present results and the 3CCO results as well as with the experimental DCS of Srivastava and Vuskovic (1980). The OP_SEPA and DWBA_SEPA results are however significantly larger than the experimental results of Teubner *et al.* (1979) and Marinkovic *et al.* (1992) especially at intermediate to large scattering angles. This implies

that all the inelastic processes are not fully accounted for in the potential of Staszewska *et al.* (1984) at this electron-impact energy for electron-sodium elastic scattering. At 100 eV (figure 4.25), the OP_SEP and DWBA_SEP differential cross sections are close to the 3CCO calculations indicating that absorption effects are not significant at this energy. However the considerably lower experimental results of Teubner *et al.* (1978) indicate that absorption effects are in fact quite important at this electron-impact energy which is confirmed by the better agreement between the present results and the experimental results when the absorption potential is included. The remaining discrepancy may probably be resolved by fully accounting for all the various inelastic channels open at this relatively high energy. It is also likely that the experimental data of Teubner *et al*. (1978), which is reported to have a systematic error of 15%, is not properly normalized. The effect of the polarization potential is also significant at this energy and brings about better agreement between both the present results and the 3CCO results.

In figure 4.26, the OP_SEP calculation the integral cross sections are in good agreement with the B-DWBA, CCC, 3CCO, and CC4 calculations at all electron impact energies considered. This indicates that the polarization potential used in the present calculation is quite accurate since this potential affects small-angle scattering significantly. The OP_SEP integral cross sections are however significantly lower than the experimental ICS of Srivastava and Vuskovic (1980) at 10, 20, and 40 eV. The DWBA_SEP method yields higher ICS results at all the electron-impact energies shown due to the additional direct and exchange terms in the T-matrix element. It is also evident that the effect of the absorption potential on the integral cross sections is to slightly increase the cross sections for both the OP_SEPA and DWBA_SEPA calculations at all electron impact energies considered.

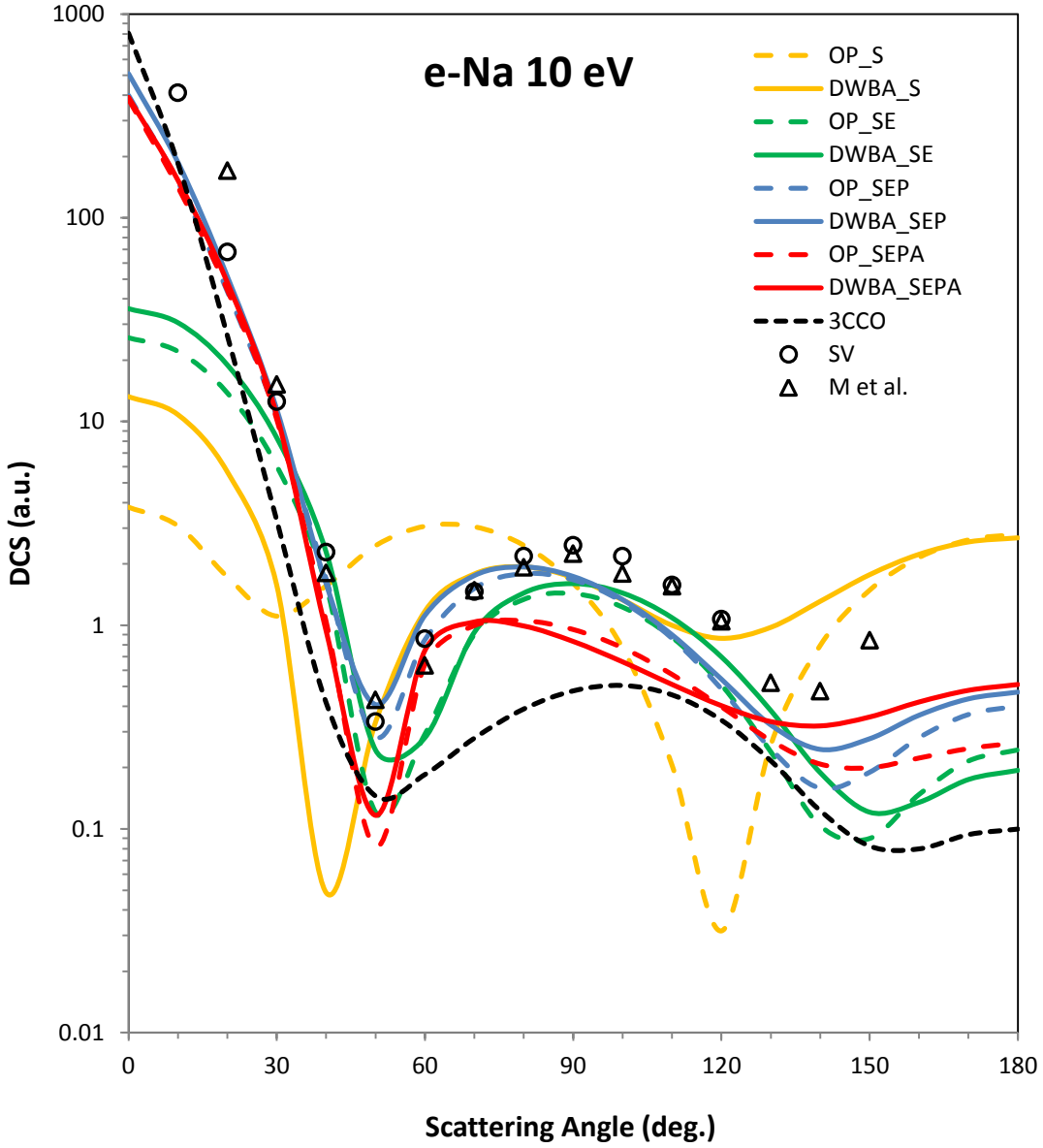

Figure 4.21: Differential cross sections for elastic scattering of electrons by sodium atom at 10eV impact energy. Experimental data: SV, Srivastava and Vuskovic (1980), M *et al.*, Marinkovic *et al.* (1992). Calculations: OP_SEP, present optical potential method with static-exchange-polarization potential, DWBA_SEP, present first order distorted wave Born approximation with static-exchange-polarization potential, OP_SEPA, present optical potential method with static-exchange-polarization-absorption potential, DWBA_SEPA present first order distorted wave Born approximation with static-exchange-polarization-absorption potential, 3CCO, 3-state coupled channels optical Method (Bray *et al*., 1991).

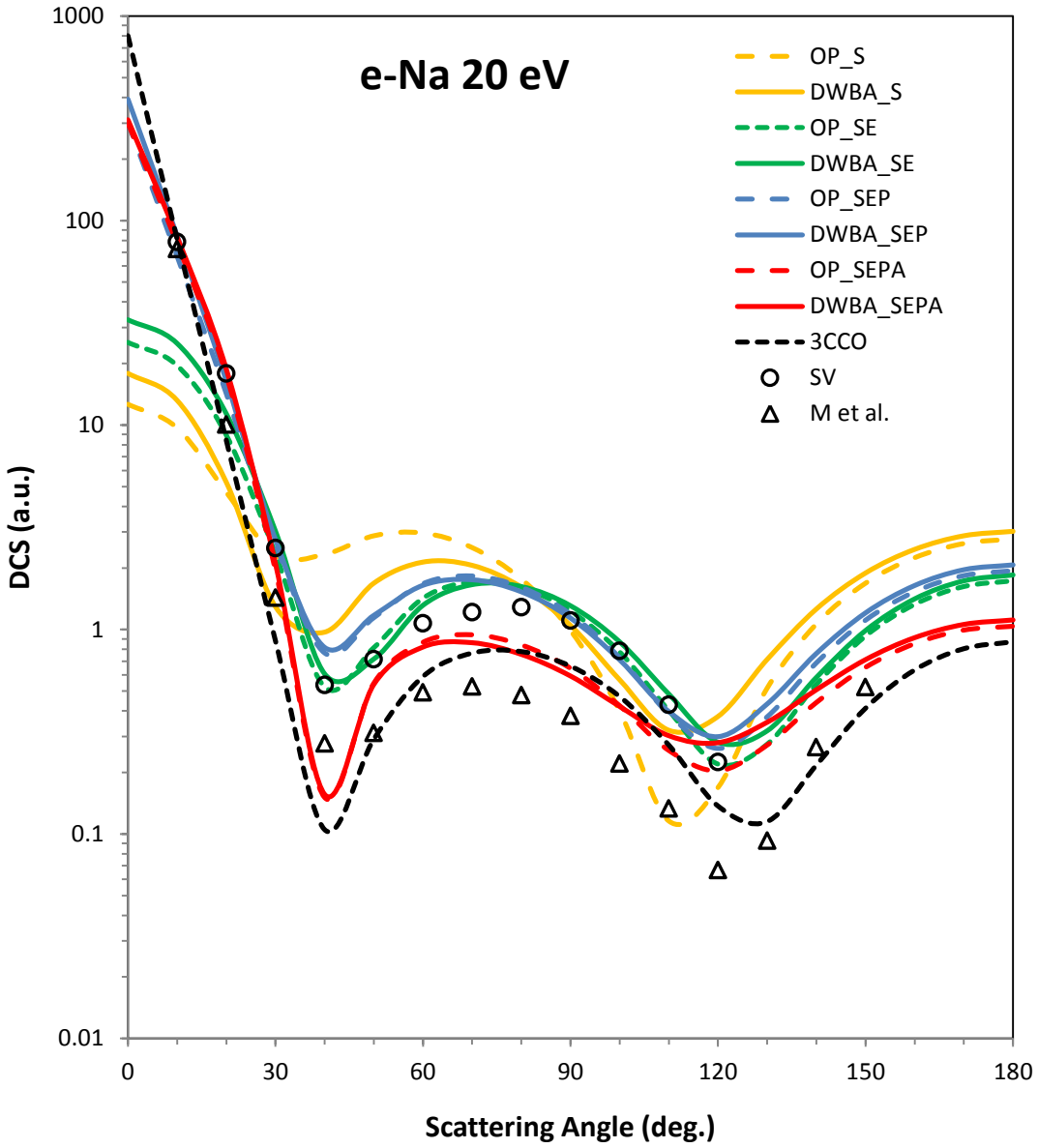

Figure 4.22: Differential cross sections for elastic scattering of electrons by sodium atom at 20eV impact energy. Experimental data: SV, Srivastava and Vuskovic (1980), M *et al.*, Marinkovic *et al.* (1992). Calculations: OP_SEP, present optical potential method with static-exchange-polarization potential, DWBA_SEP, present first order distorted wave Born approximation with static-exchange-polarization potential, OP_SEPA, present optical potential method with static-exchange-polarization-absorption potential, DWBA_SEPA present first order distorted wave Born approximation with static-exchange-polarization-absorption potential, 3CCO, 3-state coupled channels optical Method (Bray *et al*., 1991).

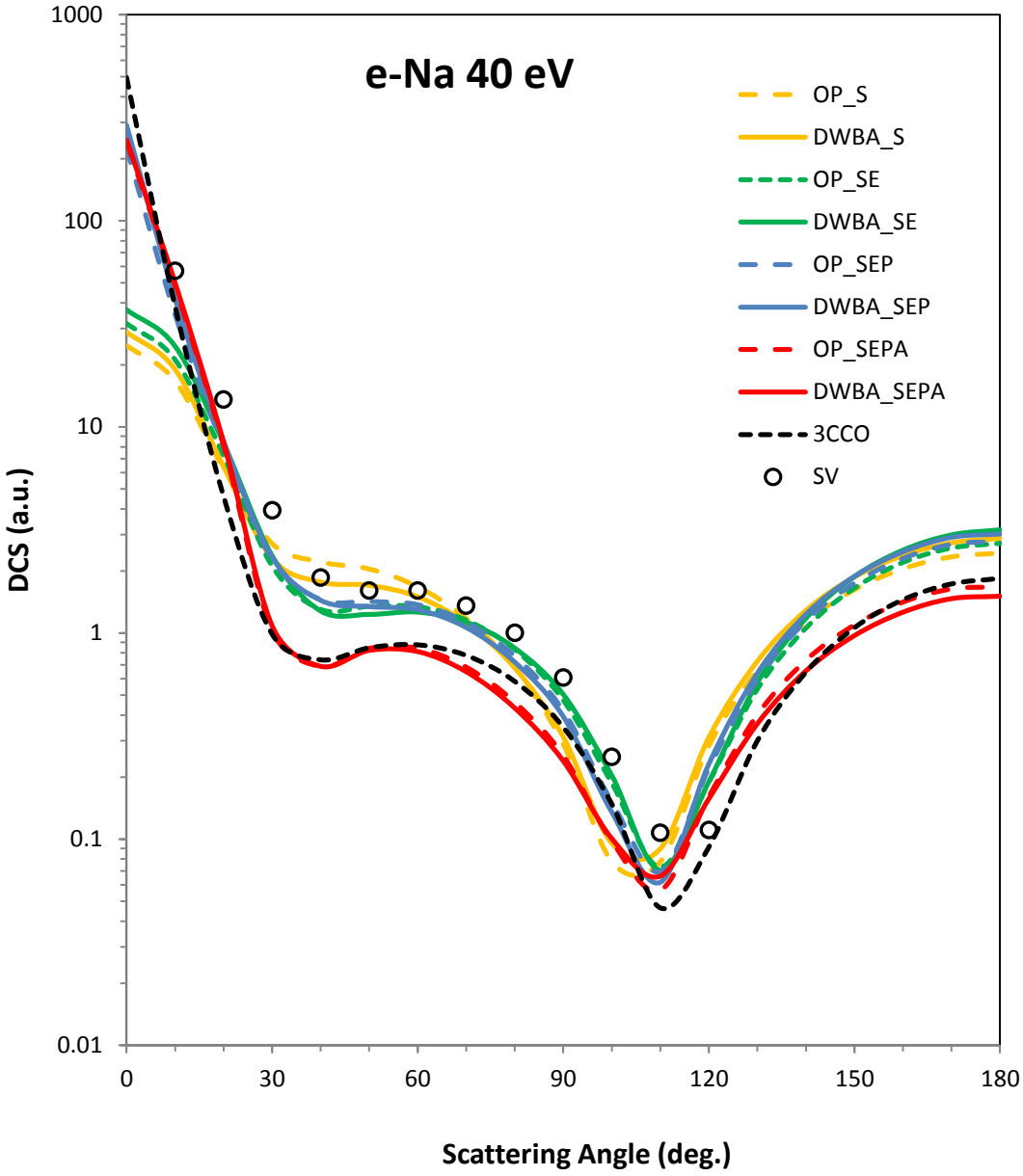

Figure 4.23: Differential cross sections for elastic scattering of electrons by sodium atom at 40eV impact energy. Experimental data: SV, Srivastava and Vuskovic (1980). Calculations: OP_SEP, present optical potential method with static-exchange-polarization potential, DWBA_SEP, present first order distorted wave Born approximation with static-exchange-polarization potential, OP_SEPA, present optical potential method with static-exchange-polarization-absorption potential, DWBA_SEPA present first order distorted wave Born approximation with static-exchange-polarization-absorption potential, 3CCO, 3-state coupled channels optical Method (Bray *et al*., 1991).

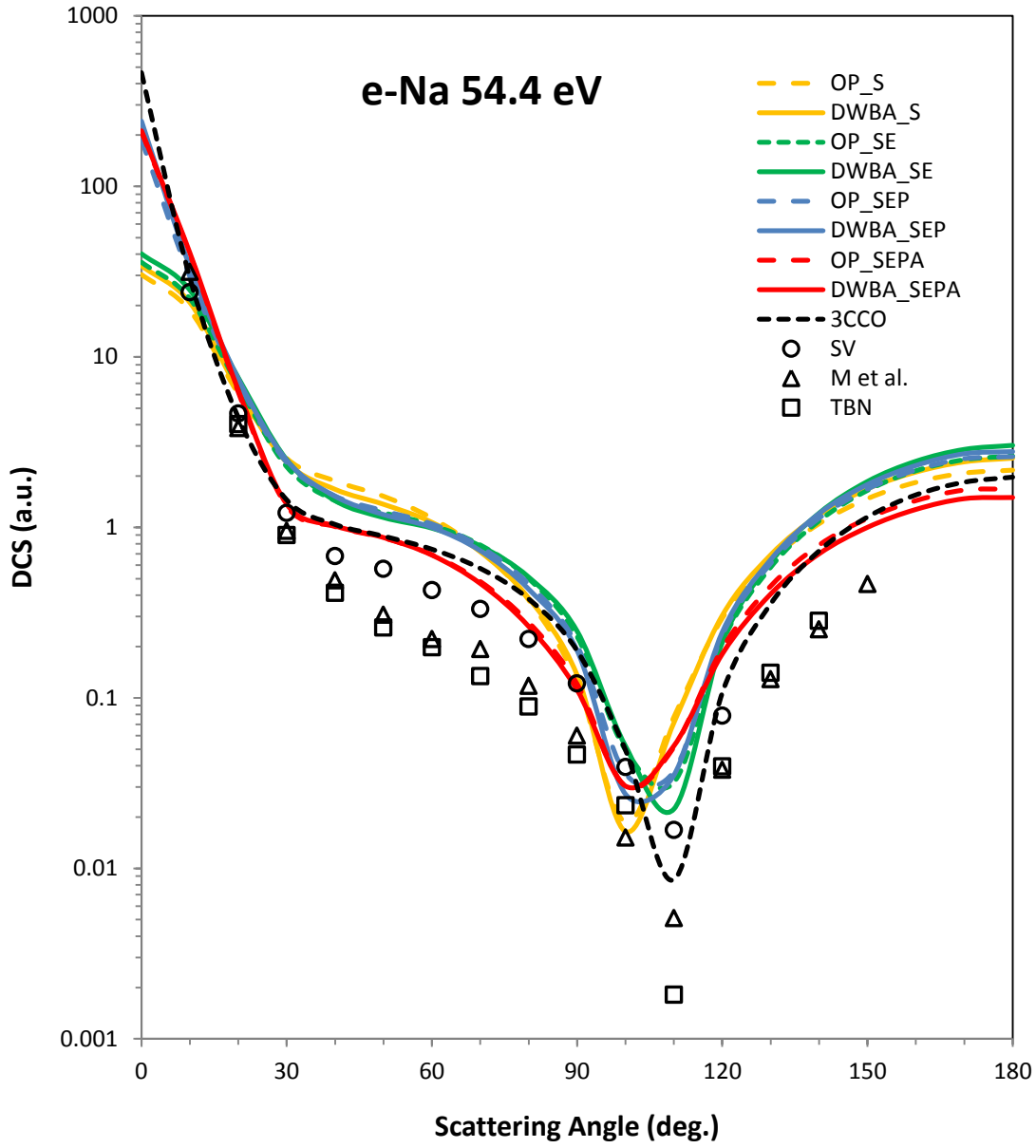

Figure 4.24: Differential cross sections for elastic scattering of electrons by sodium atom at 54.4eV impact energy. Experimental data: TBN, Teubner *et al*., (1978), SV, Srivastava and Vuskovic (1980), M *et al.*, Marinkovic *et al.* (1992). Calculations: OP_SEP, present optical potential method with static-exchange-polarization potential, DWBA_SEP, present first order distorted wave Born approximation with static-exchange-polarization potential, OP_SEPA, present optical potential method with static-exchange-polarization-absorption potential, DWBA_SEPA present first order distorted wave Born approximation with static-exchange-polarization-absorption potential, 3CCO, 3-state coupled channels optical Method (Bray *et al*., 1991).

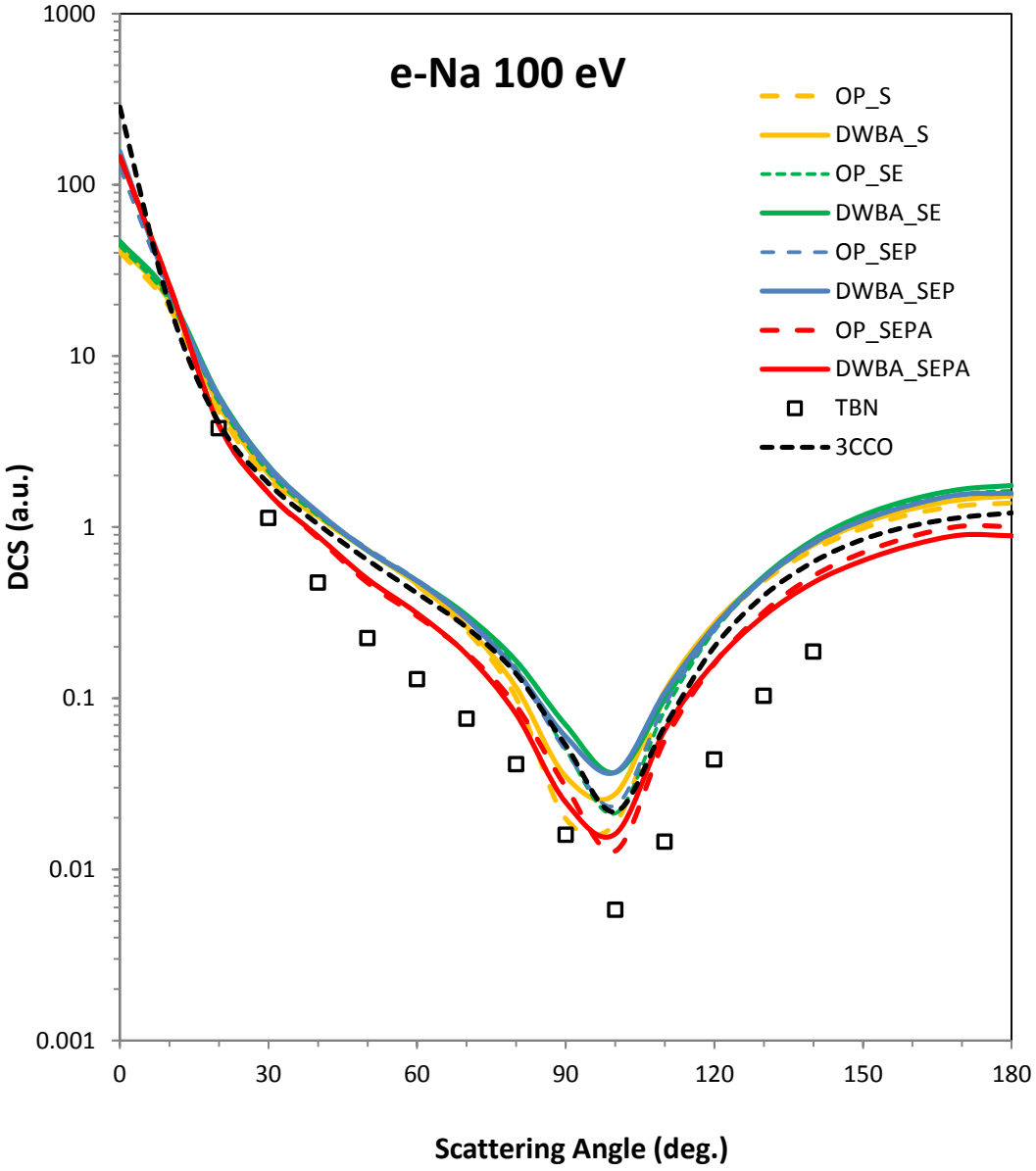

Figure 4.25: Differential cross sections for elastic scattering of electrons by sodium atom at 100eV impact energy. Experimental data: TBN, Teubner *et al*., (1978). Calculations: OP_SEP, present optical potential method with static-exchange-polarization potential, DWBA_SEP, present first order distorted wave Born approximation with static-exchange-polarization potential, OP_SEPA, present optical potential method with static-exchange-polarization-absorption potential, DWBA_SEPA present first order distorted wave Born approximation with static-exchange-polarization-absorption potential,3CCO, 3-state coupled channels optical Method (Bray *et al*., 1991).

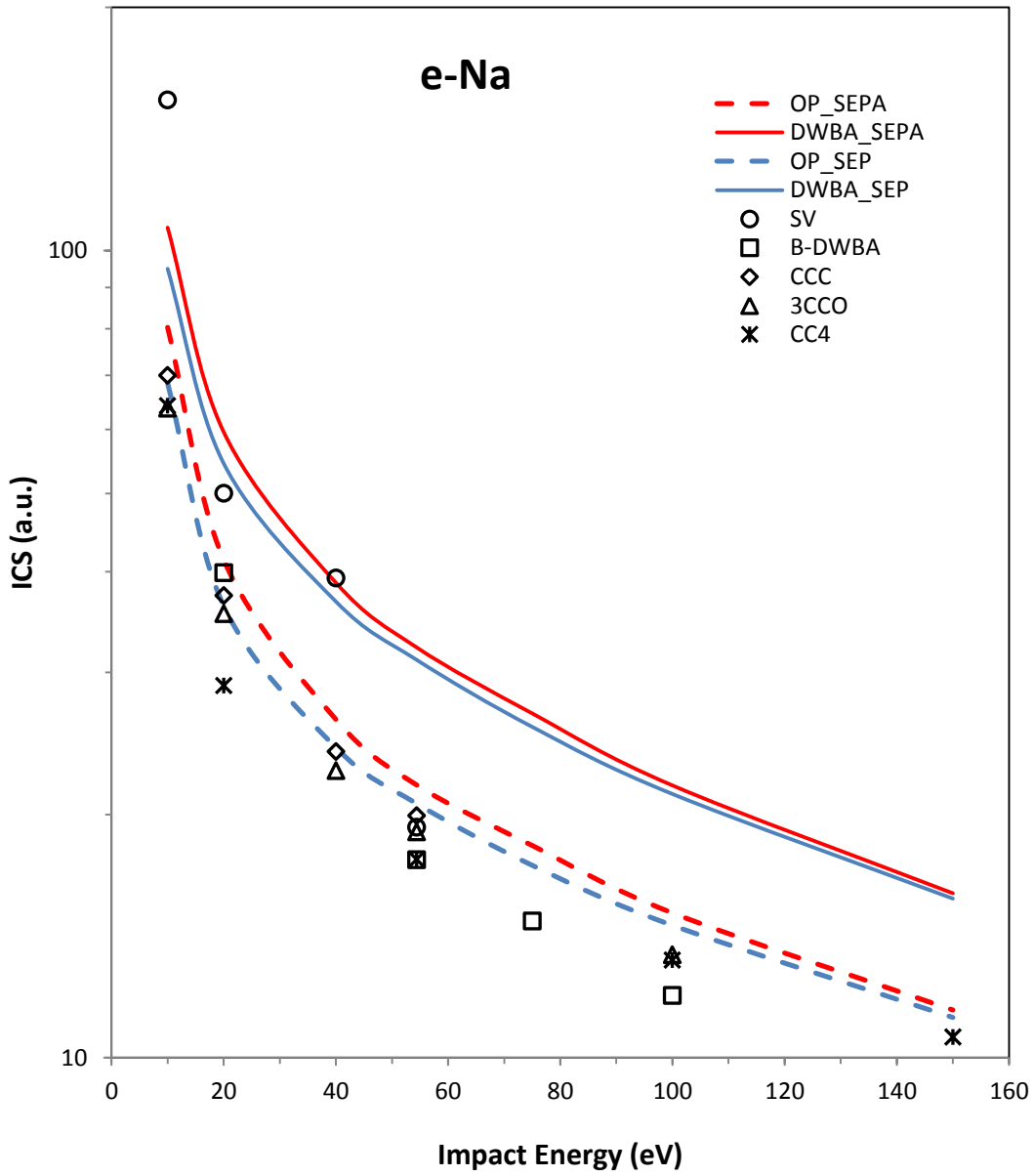

Figure 4.26: Integral cross sections for elastic scattering of electrons by sodium atom at 10 - 150 eV electron impact energies. Experimental data: SV, Srivastava and Vuskovic, (1980). Calculations: OP_SEPA, present optical potential method with static-exchange-polarization-absorption potential, DWBA_SEPA, present first order distorted wave Born approximation with static-exchange-polarization-absorption potential, OP_SEP, present optical potential method with static-exchange-polarization potential, DWBA_SEP, present first order distorted wave Born approximation with static-exchange-polarization potential, B-DWBA, distorted wave Born approximation (Balashov *et al*., 1989), 3CCO, 3-state coupled channels optical method (Bray *et al*., 1991), CCC, convergent close-coupling method (Bray 1994), CC4, 4-state close-coupling approximation (Mitroy *et al*., 1987).

Table 4.1: OP and DWBA integral cross sections for elastic scattering of electrons by sodium atom using static-exchange-polarization potential. SV, Srivastava and Vuskovic, (1980). B-DWBA, distorted wave Born approximation (Balashov *et al*., 1989), CCC, convergent close-coupling method (Bray 1994).

	Integral Cross Sections (a.u.)						
eV	OP_SEPA	DWBA_SEPA	OP_SEP	DWBA_SEP	SV	BDWBA	CCC
10	80.29	106.73	68.47	94.90	153.57		70.02
20	41.38	59.55	36.28	54.45	50	39.87	37.36
40	26.242	38.75	24.21	36.72	39.28		23.92
100	15.10	21.73	14.58	21.21		11.93	
150	11.45	15.97	11.21	15.73			

4.3.2 Potassium

From figure 4.27, it can be seen that at 7 eV for electron-potassium elastic scattering the OP_SEP and DWBA_SEP calculations give very similar results. Thus as the distorting potential becomes more complete or more accurate the effect of the additional direct and exchange terms in the DWBA_SEP transition matrix element (Equation 24) decreases in significance. There is also a marked improvement in the DWBA_SEP and OP_SEP differential cross sections obtained using a local static-exchange plus non-local polarization potential at small scattering angles compared with the experimental results of Vuskovic and Srivastava (1980) as well as with the DWSB method of Madison *et al*. (1995). It is therefore evident that the non-local polarization potential used in the present calculations adequately describes small-angle electron-potassium elastic scattering at this low energy slightly above the ionization threshold (4.33 eV) of potassium atom. However at intermediate to large scattering angles, the present OP_SEP and DWBA_SEP results are only in qualitative agreement with the DWSB calculation while agreement with the experimental results is far

from satisfactory. This is due to lack of an absorption potential in the OP_SEP and DWBA_SEP calculations. From figure 4.27 it is also clear that for electron-potassium elastic scattering at 7 eV, the OP_SEPA and DWBA_SEPA differential cross sections are very close as expected since the potential is now more complete and has incorporated the important features of the scattering process namely direct (static), exchange, polarization, and absorption processes. The agreement between the OP_SEPA and DWBA_SEPA results, on the one hand, and the DWSB calculation of Madison *et al.* (1995) and the measured results of Vuskovic and Srivastava (1980) on the other hand, is good only at small scattering angles and is semi-qualitative at large scattering angles. There appears to be a need to carry out more DCS measurements in order to draw a definite conclusion.

At 40 eV (figure 4.28) the OP_SEP and DWBA_SEP results are very similar showing that the effect of the additional T-matrix element terms in the DWBA_SEP method decreases with increase in electron-impact energy and that the distorting potential is more complete. There is good qualitative agreement between the OP_SEP and DWBA_SEP results and the experimental results of Vuskovic and Srivastava (1980) as well as with the DWSB differential cross sections of Madison *et al.* (1992). Use of the absorption potential in the OP_SEPA and DWBA_SEPA calculation brings about even better agreement. At 60 eV (figure 4.29), the OP_SEP and DWBA_SEP results are in close agreement with the DWSB but all these results are in disagreement with the experimental results of Vuskovic and Srivastava (1980). The very good quantitative agreement between the present OP_SEPA and DWBA_SEPA results (which include the absorption potential) and the DCS of Vuskovic and Srivastava (1980) confirms the significance of absorption effects. At 100 eV (figure 4.30), the OP_SEP and DWBA_SEP calculations are in close agreement with the DWSB

calculation. The experimental results of Buckman *et al*. (1979) and of Vuskovic and Srivastava (1980) are much lower than the OP_SEP and DWBA_SEP results. However, inclusion of the absorption potential in the OP_SEPA and DWBA_SEPA calculations brings about very good agreement with the experimental results. At 200 eV (Figure 4.31), the OP_SEP and DWBA_SEP results are much higher than the experimental results of Buckman *et al*. (1979) at intermediate and large scattering angles. This difference indicates that absorption effects are significant at this relatively high energy. From the OP_SEPA and DWBA_SEPA results, this is seen to be the case as the absorption potential brings the present results in closer agreement with the DCS of Buckman *et al.* (1979). For complete agreement at intermediate scattering angles $60^\circ \le \theta \le 110^\circ$, all the inelastic processes should be fully accounted for in the absorption potential.

In figure 4.32, the OP_SEP integral cross sections for electron-potassium elastic scattering are in good agreement with the Unitarized distorted wave Born approximation (UDWBA) of Mitroy *et al*. (1993), and the 17-state coupled channels optical method (17CCO6) of Bray *et al*. (1993) at all electron-impact energies considered. Agreement with the experimental results of Vuskovic and Srivastava (1980) is also good except at 100 eV. The DWBA_SEP results are consistently higher than the OP_SEP results due to the additional direct and exchange terms in the DWBA_SEP T-matrix element. Addition of the absorption potential has the effect, in both the OP_SEPA and DWBA_SEPA calculations, of decreasing the integral cross sections as shown in figure 4.32.

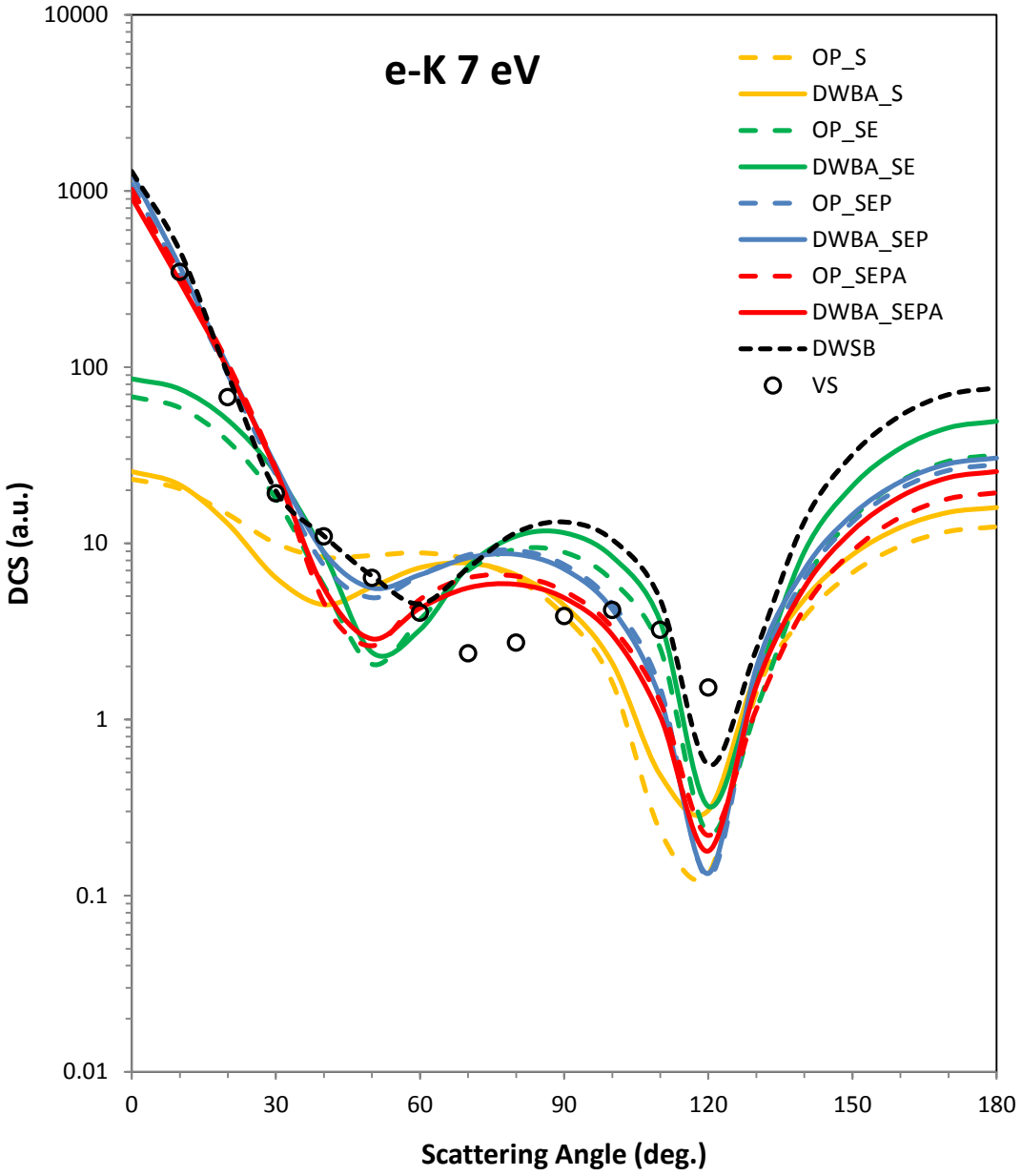

Figure 4.27: Differential cross sections for elastic scattering of electrons by potassium atom at 7eV impact energy. Experimental data: VS, Vuskovic and Srivastava (1980). Calculations: OP_SEP, present optical potential method with static-exchange-polarization potential, DWBA_SEP, present first order distorted wave Born approximation with static-exchange-polarization potential, OP_SEPA, present optical potential method with static-exchange-polarization-absorption potential, DWBA_SEPA present first order distorted wave Born approximation with static-exchange-polarization-absorption potential, DWSB, second order distorted wave Born approximation (Madison *et al.*, 1995)

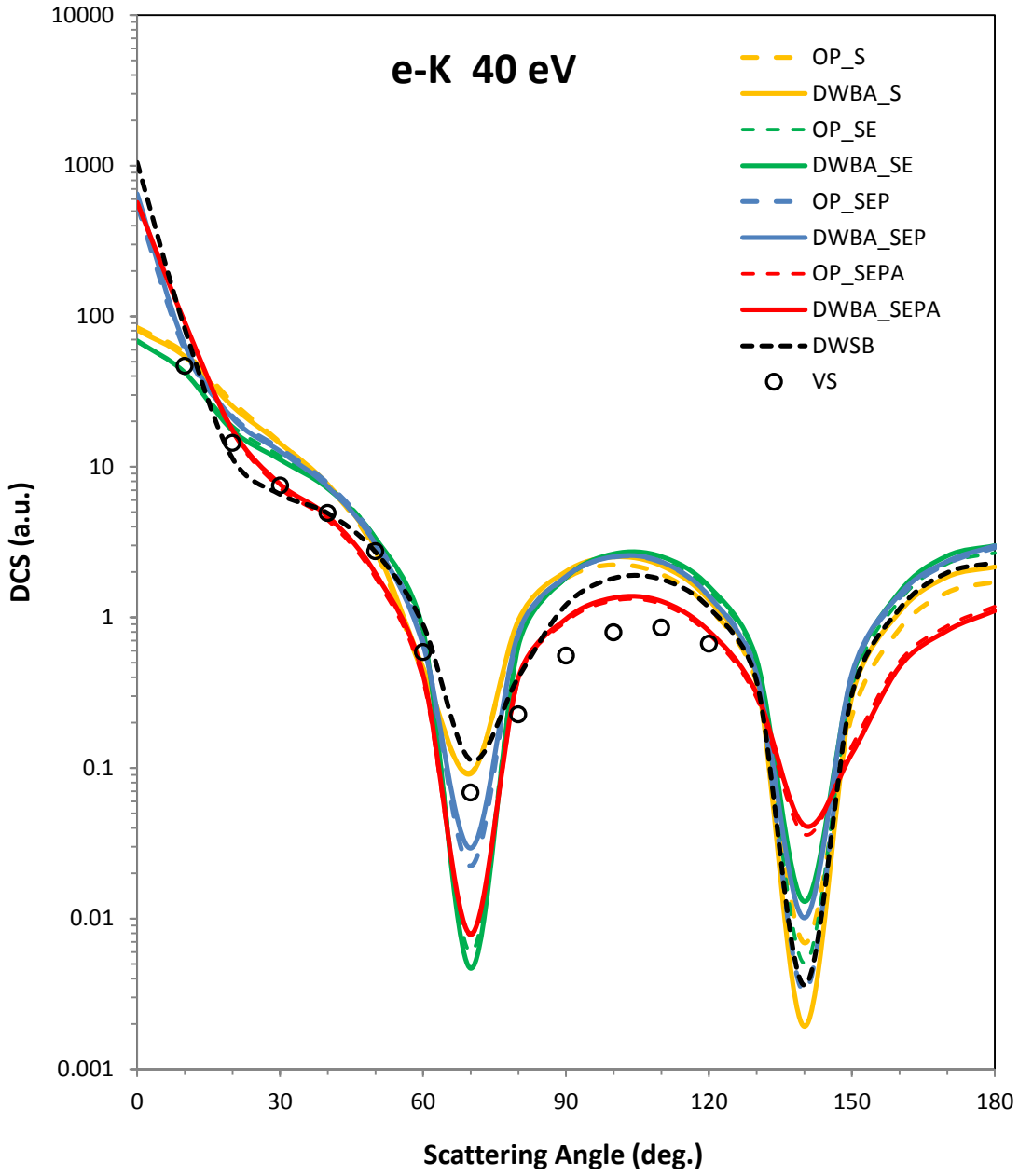

Figure 4.28: Differential cross sections for elastic scattering of electrons by potassium atom at 40eV impact energy. Experimental data: VS, Vuskovic and Srivastava (1980). Calculations: OP_SEP, present optical potential method with static-exchange-polarization potential, DWBA_SEP, present first order distorted wave Born approximation with static-exchange-polarization potential, OP_SEPA, present optical potential method with static-exchange-polarization-absorption potential, DWBA_SEPA present first order distorted wave Born approximation with static-exchange-polarization-absorption potential, DWSB, second order distorted wave Born approximation (Madison *et al*., 1995).

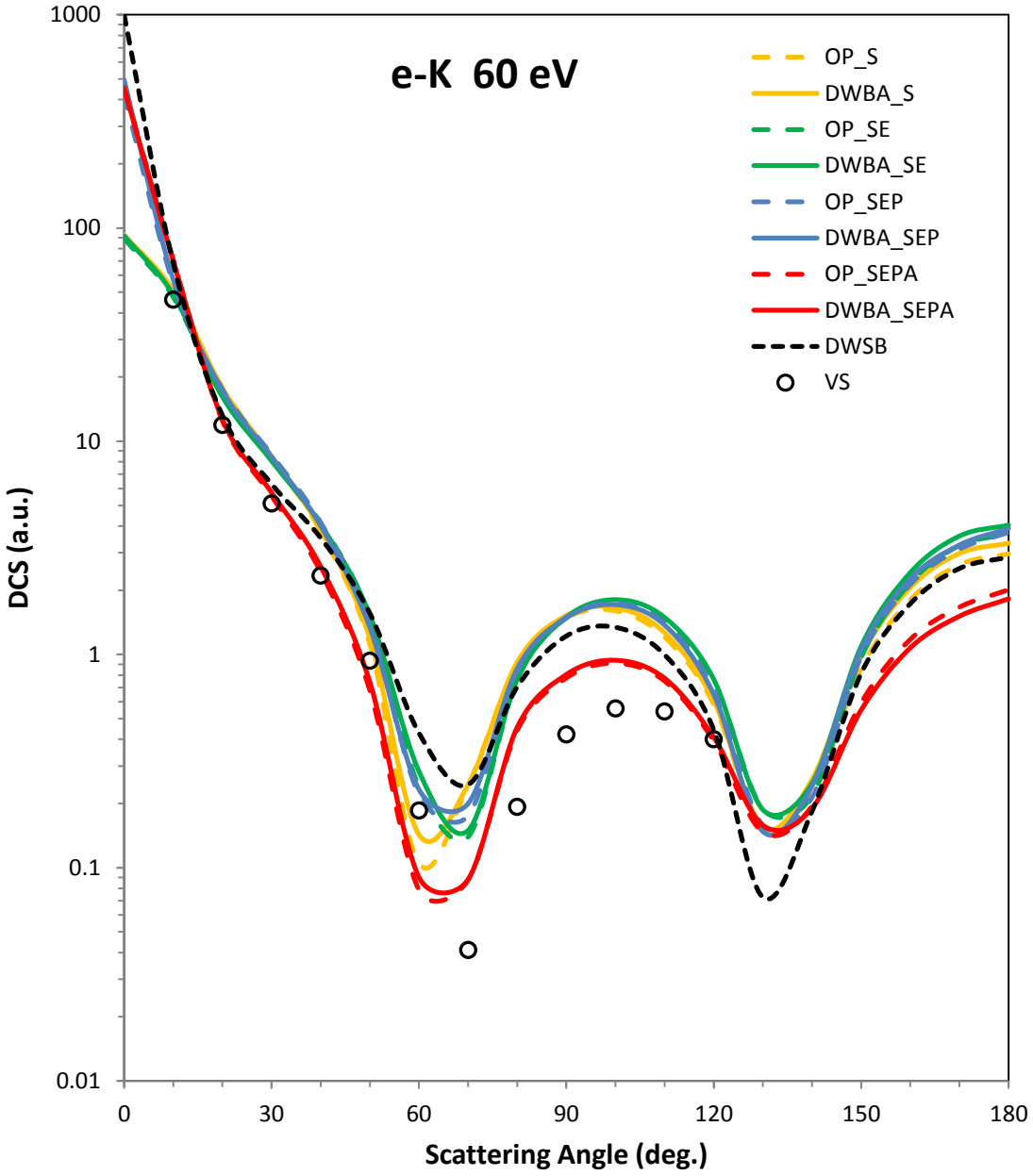

Figure 4.29: Differential cross sections for elastic scattering of electrons by potassium atom at 60eV impact energy. Experimental data: VS, Vuskovic and Srivastava (1980). Calculations: OP_SEP, present optical potential method with static-exchange-polarization potential, DWBA_SEP, present first order distorted wave Born approximation with static-exchange-polarization potential, OP_SEPA, present optical potential method with static-exchange-polarization-absorption potential, DWBA_SEPA present first order distorted wave Born approximation with static-exchange-polarization-absorption potential, DWSB, second order distorted wave Born approximation (Madison *et al*., 1995).

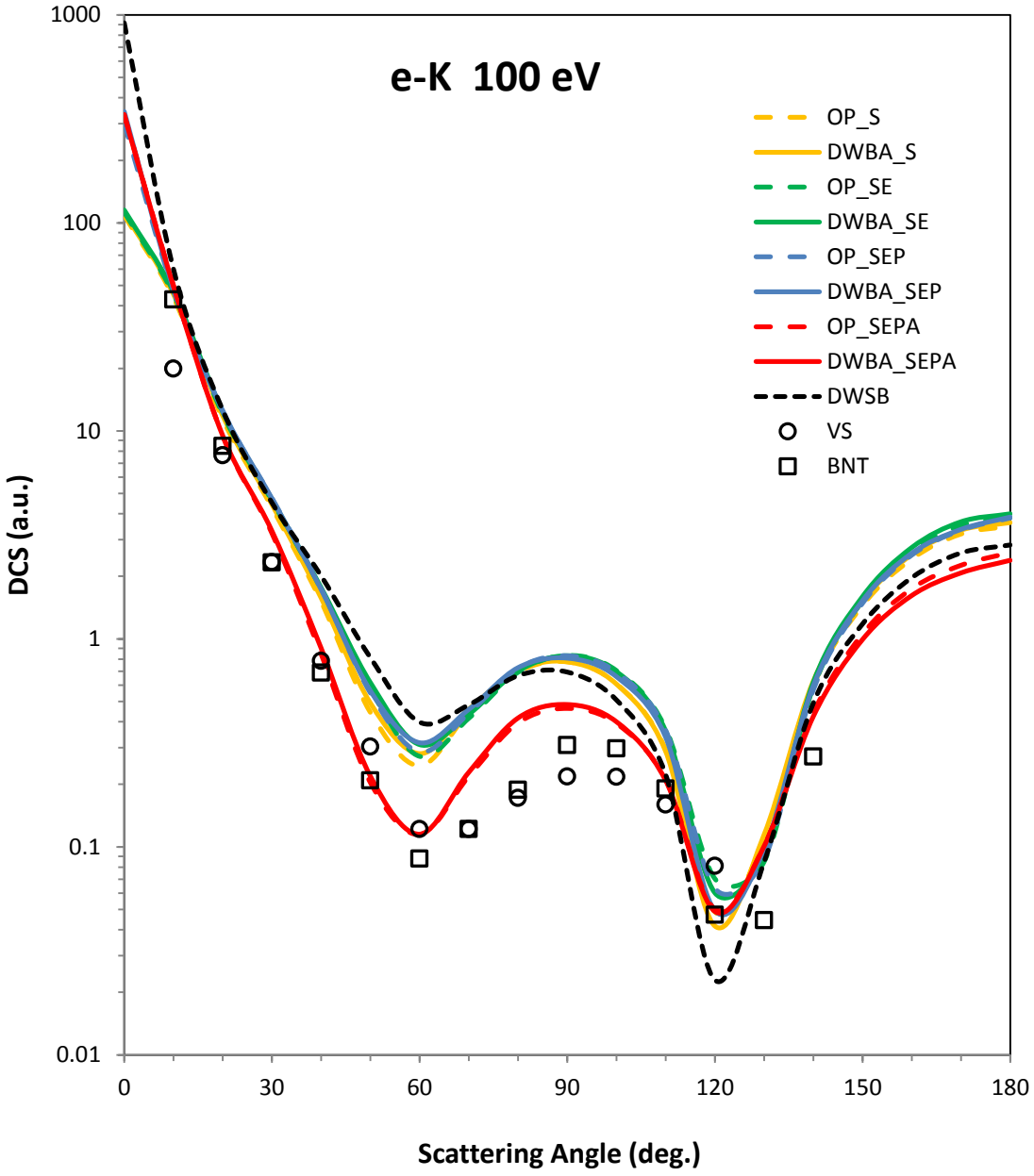

Figure 4.30: Differential cross sections for elastic scattering of electrons by potassium atom at 100eV impact energy. Experimental data: BNT, Buckman *et al*., (1979), VS, Vuskovic and Srivastava (1980). Calculations: OP_SEP, present optical potential method with static-exchange-polarization potential, DWBA_SEP, present first order distorted wave Born approximation with static-exchange-polarization potential, OP_SEPA, present optical potential method with static-exchange-polarization-absorption potential, DWBA_SEPA present first order distorted wave Born approximation with static-exchange-polarization-absorption potential, DWSB, second order distorted wave Born approximation (Madison *et al*., 1995).

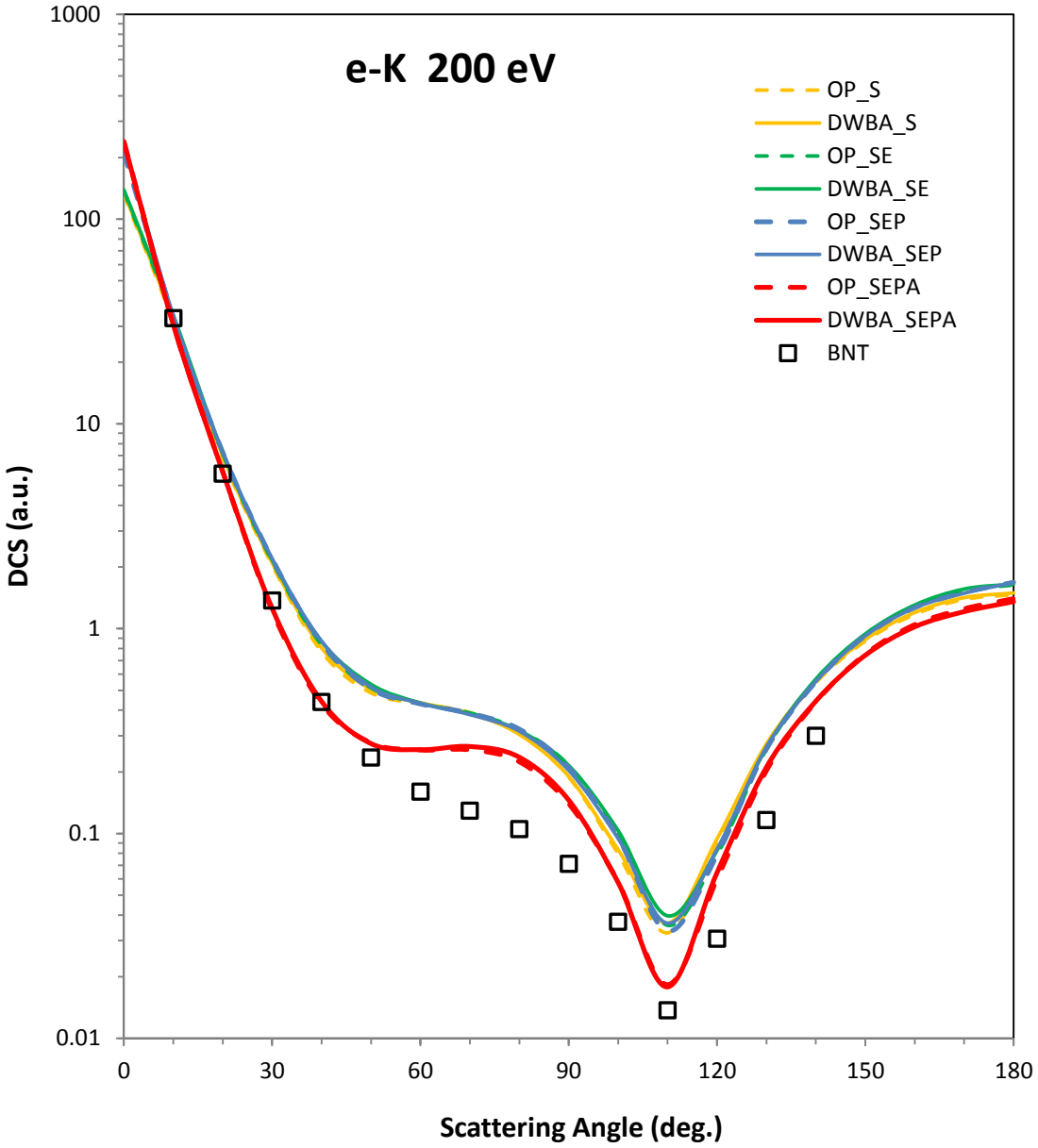

Figure 4.31: Differential cross sections for elastic scattering of electrons by potassium atom at 200eV impact energy. Experimental data: BNT, Buckman *et al*., (1979). Calculations: OP_SEP, present optical potential method with static-exchange-polarization potential, DWBA_SEP, present first order distorted wave Born approximation with static-exchange-polarization potential, OP_SEPA, present optical potential method with static-exchange-polarization-absorption potential, DWBA_SEPA present first order distorted wave Born approximation with static-exchange-polarization-absorption potential.

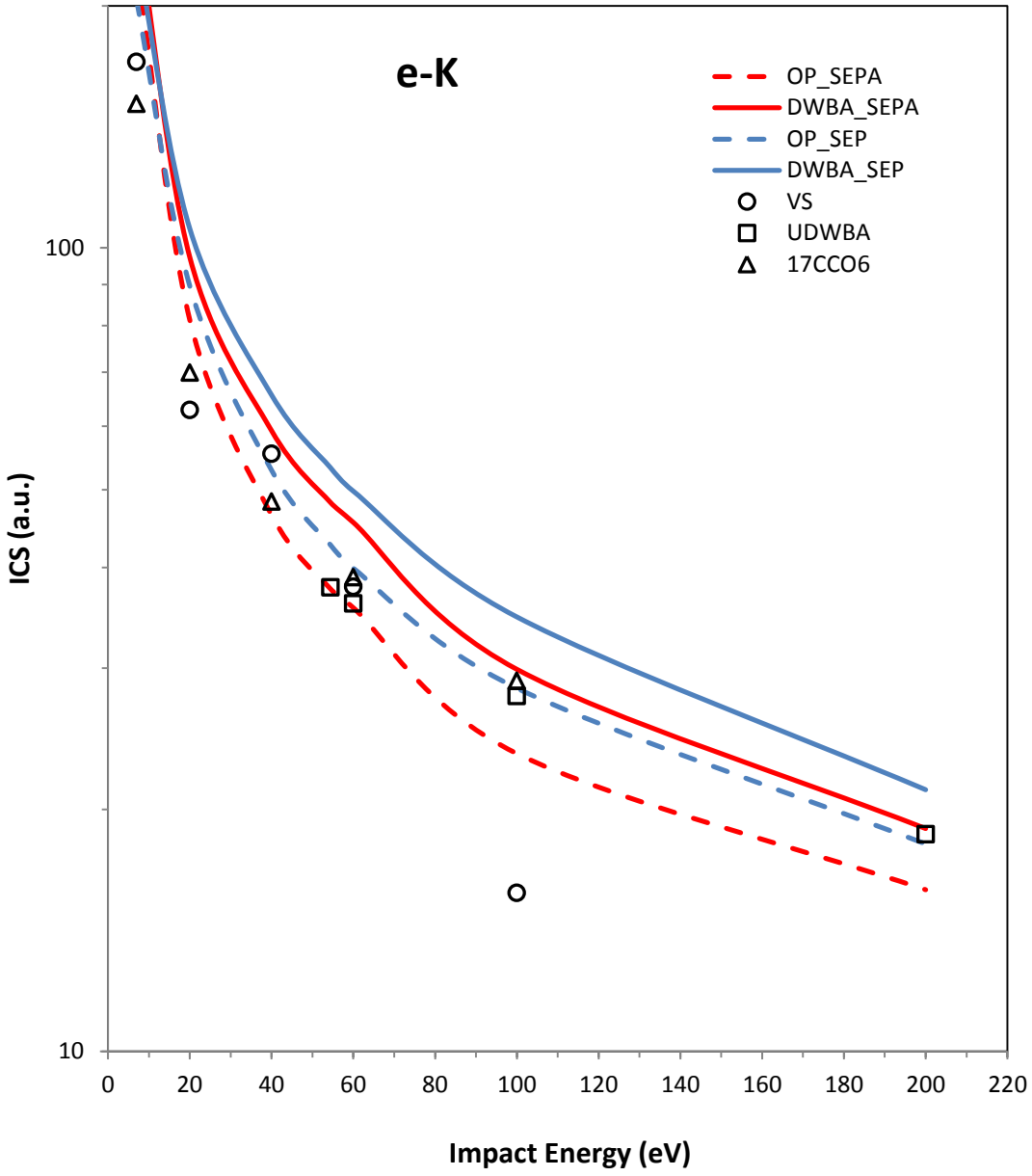

Figure 4.32: Integral cross sections for elastic scattering of electrons by potassium atom at 7 - 200eV electron impact energies. Experimental data: VS, Vuskovic and Srivastava (1980). Calculations: OP_SEPA, present optical potential method with static-exchange-polarization-absorption potential, DWBA_SEPA, present first order distorted wave Born approximation with static-exchange-polarization-absorption potential, OP_SEP, present optical potential method with static-exchange-polarization potential, DWBA_SEP, present first order distorted wave Born approximation with static-exchange-polarization potential, UDWBA, Unitarized distorted wave Born approximation (Mitroy *et al*., 1993), 17CCO6, 17-state coupled channels optical method (Bray *et al*., 1993).

Table 4.2: OP and DWBA integral cross sections for elastic scattering of electrons by potassium atom using static-exchange-polarization potential. VS, Vuskovic and Srivastava (1980). UDWBA, Unitarized distorted wave Born approximation (Mitroy *et al*., 1993). 17CCO6, 17-state coupled channels optical method (Bray *et al*., 1993).

Integral Cross Sections (a.u.)

eV	OP_SEPA	DWBA_SEPA	OP_SEP	DWBA_SEP	VS	UDWBA	17CCO6
7	225.32	255.39	203.44	233.51	170.35		151
40	46.50	59.22	52.87	65.59	55.42		48.3
60	35.65	45.52	39.92	49.79	37.85	36.07	38.9
100	23.47	29.88	28.31	34.72	15.75	27.67	28.9
200	15.89	18.93	18.11	21.16		18.62	

Table 4.3: OP differential cross sections for elastic scattering of electrons by sodium atom using static-exchange-polarization-absorption potential.

Differential Cross Sections (a.u.)

θ	10 eV	20 eV	40 eV	54.4	100
0	381.4986	299.6372	241.3788	208.5116	145.7053
10	141.4392	77.02651	48.29676	39.90179	25.87881
20	44.17949	17.53592	8.089752	6.212118	3.956908
30	10.24094	1.943914	1.025341	1.331733	1.581345
40	1.039255	0.150901	0.687755	1.010631	0.864268
50	0.081804	0.546139	0.842153	0.867435	0.473282
60	0.643022	0.866323	0.842283	0.691232	0.30191
70	0.995107	0.942875	0.682677	0.481196	0.183749
80	1.051894	0.840242	0.461482	0.27748	0.090361
90	0.952571	0.646634	0.254028	0.120499	0.03048
100	0.774641	0.423904	0.097518	0.030364	0.01281
110	0.573499	0.2562	0.056444	0.051315	0.056855
120	0.397795	0.203698	0.160752	0.195071	0.159146
130	0.271731	0.27233	0.400862	0.452315	0.319628
140	0.208083	0.439537	0.737263	0.787196	0.518133
150	0.199548	0.653259	1.093364	1.127959	0.709505
160	0.222812	0.853317	1.412997	1.434372	0.884472
170	0.248028	0.994014	1.635511	1.654497	1.013556
180	0.264847	1.037903	1.673025	1.678616	1.0054

Table 4.4: DWBA differential cross sections for elastic scattering of electrons by sodium atom using static-exchange-polarization-absorption potential.

	Differential Cross Sections (a.u.)				
θ	10 eV	20 eV	40 eV	54.4 eV	100eV
0	390.3318	311.1423	246.9728	211.6661	146.3754
10	152.8998	82.94488	49.91785	40.65523	25.95781
20	48.13642	18.76918	8.417705	6.36669	3.949675
30	10.72948	2.098043	1.083253	1.36786	1.580712
40	0.935891	0.156165	0.689221	1.020317	0.884993
50	0.116567	0.53919	0.822945	0.871317	0.497971
60	0.752469	0.821316	0.812254	0.687522	0.313906
70	1.037664	0.861942	0.648685	0.468378	0.180571
80	0.991227	0.755993	0.432427	0.26213	0.080681
90	0.832662	0.592501	0.239416	0.111279	0.024662
100	0.66106	0.420701	0.100566	0.030393	0.016113
110	0.512099	0.30252	0.066168	0.052248	0.065107
120	0.402858	0.279578	0.156988	0.180971	0.161106
130	0.336424	0.351926	0.36312	0.406525	0.303104
140	0.32038	0.507408	0.654809	0.69963	0.47449
150	0.354361	0.712445	0.97104	1.000359	0.637461
160	0.419963	0.912569	1.261411	1.274126	0.787731
170	0.478936	1.058972	1.467496	1.47296	0.899893
180	0.511631	1.113992	1.507052	1.496015	0.889627

From figure 4.33 and table 4.5 the OP_SEPA and DWBA_SEPA calculations give very similar total (elastic + inelastic) cross sections. Both sets of data are however much lower than the B-DWBA (Balashov *et al*., 1989), 3CCO (Bray *et al*., 1991) and CCC (Bray, 1994) calculations and the experimental results of Srivastava and Vuskovic (1980) and Kwan *et al*. (1991). This shows that the absorption potential of Staszewska *et al*. (1984) as used does not adequately describe small-angle scattering since this process has a large effect on total cross sections. Consequently, as previously noted, the average excitation energy in the absorption potential of Staszewska *et al*. (1984) should be determined using an *ab initio* method.

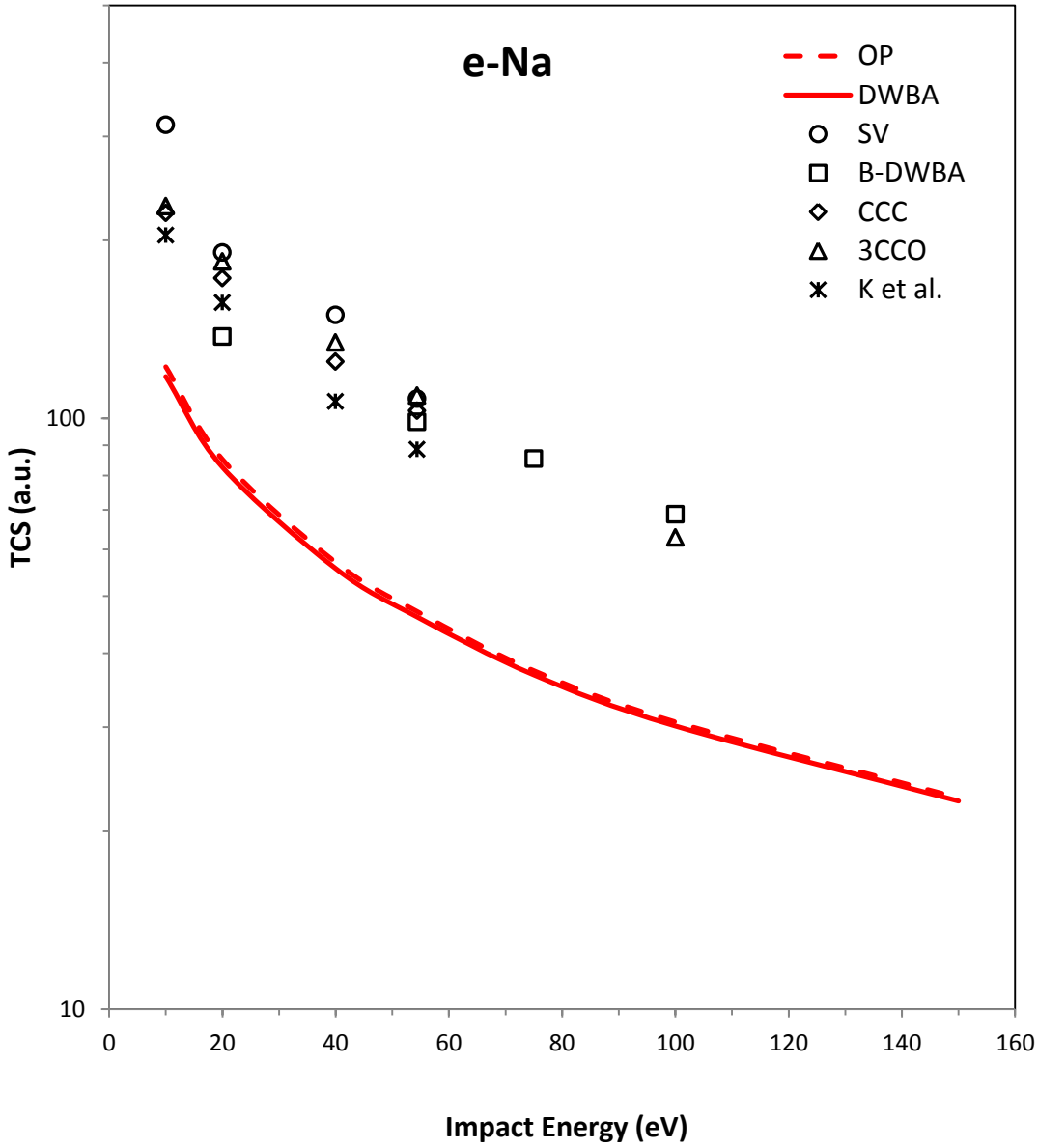

Figure 4.33: Total Cross Sections for electron scattering by sodium atom at 10 – 150 eV electron impact energies. Calculations: OP_SEPA, present optical potential method with static-exchange-polarization-absorption potential, DWBA_SEPA present first order distorted wave Born approximation with static-exchange-polarization-absorption potential, B-DWBA, distorted wave Born approximation (Balashov *et al*., 1989), 3CCO, 3-state coupled channels optical method (Bray *et al*., 1991), CCC, convergent close-coupling method (Bray, 1994). Experiment: SV, Srivastava and Vuskovic (1980); K et al, Kwan *et al*. (1991).

Table 4.5: OP and DWBA Total (elastic + inelastic) cross sections for elastic scattering of electrons by sodium atom using static-exchange-polarization-absorption potential. Srivastava and Vuskovic (1980). B-DWBA, distorted wave Born approximation (Balashov *et al*., 1989). CCC, convergent close-coupling method (Bray, 1994). 3CCO, 3-state coupled channels optical method (Bray *et al*., 1991). K et al, Kwan *et al*. (1991).

Total Cross Sections (a.u.)

eV	OP	DWBA	SV	B-DWBA	CCC	3CCO	K et al.
10	122.191	117.630	313.928		222.626	228.592	204.1
20	85.200	82.657	190.714	137.532	172.7	184.318	157
40	57.042	55.675	149.642		124.658	134.392	106.76
54.4	47.077	46.100	107.857	98.596	102.992	109.272	88.548
100	30.609	30.137		68.766		62.8	

Table 4.6: OP differential cross sections for elastic scattering of electrons by potassium atom using static-exchange-polarization-absorption potential.

Differential Cross Sections (a.u.)

θ	7 eV	40 eV	60 eV	100 eV	200 eV
0	1021.973	574.9038	454.9059	332.2473	239.3648
10	337.0276	91.31822	70.68968	50.08963	30.69047
20	104.9769	17.07516	12.46713	9.479702	5.849196
30	26.37479	7.215662	5.541341	3.224808	1.224837
40	4.588915	4.416231	2.441879	0.846166	0.429809
50	2.617777	1.833803	0.678638	0.204015	0.277193
60	4.802106	0.381495	0.078751	0.114684	0.255885
70	6.355162	0.00772	0.08776	0.218327	0.256144
80	6.503771	0.384447	0.440534	0.394166	0.223988
90	5.357659	0.936708	0.775763	0.463385	0.139836
100	3.333662	1.290972	0.909071	0.392116	0.057989
110	1.254692	1.227141	0.750629	0.210783	0.018277
120	0.219594	0.772355	0.392939	0.050251	0.059926
130	1.141021	0.291271	0.146695	0.100764	0.202965
140	4.27938	0.036267	0.194232	0.440463	0.439125
150	9.015198	0.139473	0.592852	1.055482	0.750771
160	14.05684	0.508988	1.176411	1.742848	1.046734
170	17.90181	0.876009	1.6659	2.259252	1.250781
180	19.3346	1.180927	2.01056	2.602613	1.402052

Table 4.7: DWBA differential cross sections for elastic scattering of electrons by potassium atom using static-exchange-polarization-absorption potential.

	Differential Cross Sections (a.u.)				
θ	7 eV	40 eV	60 eV	100 eV	200 eV
0	916.2131	568.4208	450.8236	329.7256	238.2172
10	306.0117	91.12301	70.33232	49.73396	30.51211
20	97.00463	17.60873	12.65655	9.49485	5.847574
30	25.93348	7.665956	5.744097	3.307549	1.257819
40	5.547847	4.692802	2.583368	0.903335	0.441751
50	2.865528	1.96226	0.741531	0.218954	0.27472
60	4.280676	0.415937	0.090126	0.115175	0.256592
70	5.582441	0.007898	0.087983	0.228422	0.265956
80	5.844133	0.396544	0.4554	0.416502	0.235836
90	4.899288	0.976339	0.804963	0.48371	0.145541
100	3.022049	1.347257	0.939019	0.399835	0.057617
110	1.042283	1.280776	0.772602	0.208809	0.017825
120	0.17903	0.810973	0.408632	0.048993	0.064362
130	1.551891	0.312859	0.157911	0.100783	0.210678
140	5.610825	0.041511	0.190139	0.424125	0.442835
150	11.74576	0.124676	0.548675	0.99359	0.742093
160	18.39538	0.470504	1.073935	1.616413	1.021354
170	23.57332	0.817015	1.511049	2.076748	1.211452
180	25.52555	1.107933	1.823218	2.388434	1.355918

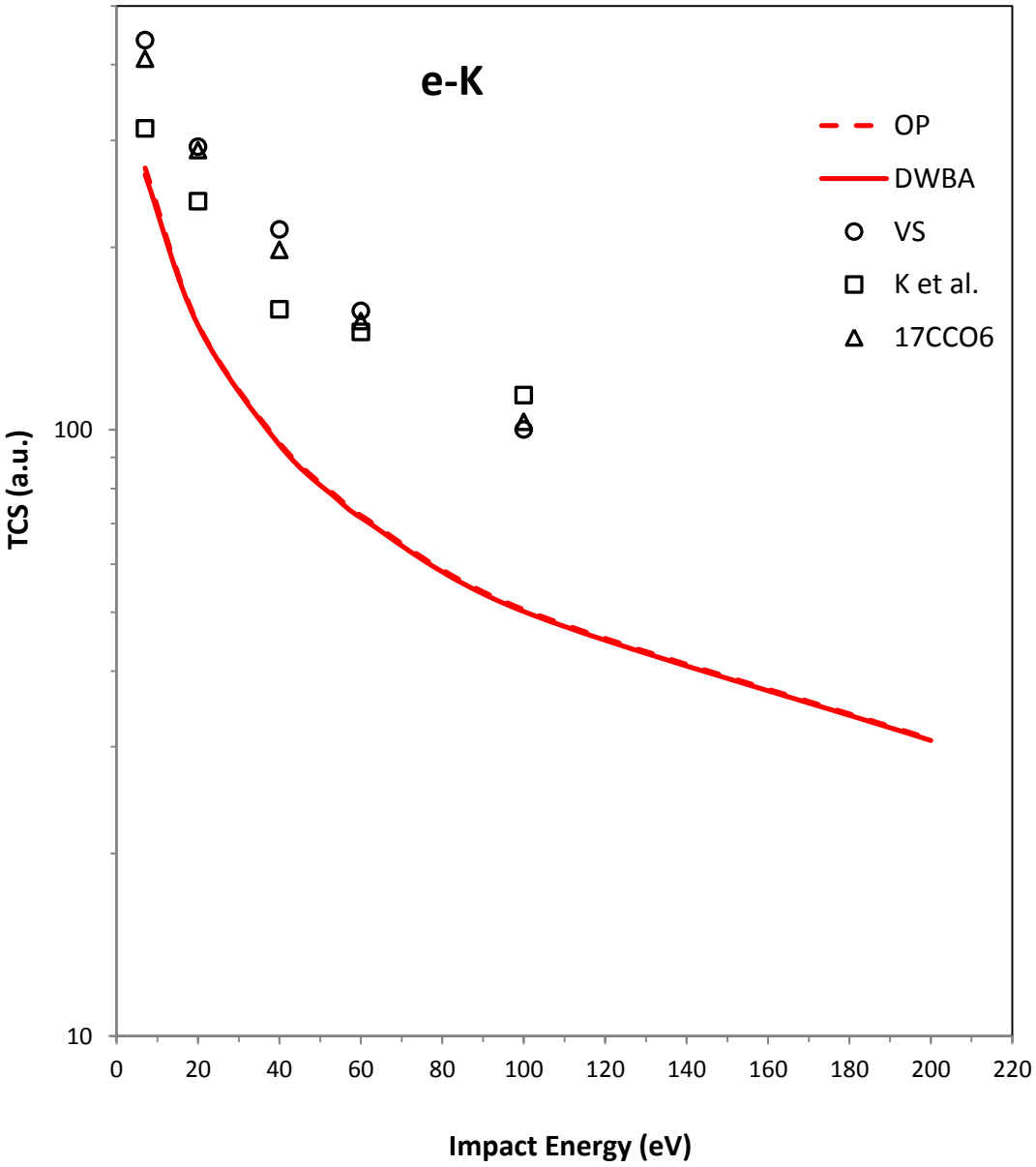

Figure 4.34: Total Cross Sections for electron scattering by potassium atom at 7 – 200 eV electron impact energies. Calculations: OP_SEPA, present optical potential method with static-exchange-polarization-absorption potential, DWBA_SEPA present first order distorted wave Born approximation with static-exchange-polarization-absorption potential, 17CCO6, 17-state coupled channels optical method (Bray *et al*., 1993), Experiment: VS, Vuskovic and Srivastava (1980); K et al, Kwan *et al*. (1991).

Table 4.8: OP and DWBA Total (elastic + inelastic) cross sections for elastic scattering of electrons by potassium atom using static-exchange-polarization-absorption potential. VS, Vuskovic and Srivastava (1980); K et al, Kwan *et al*. (1991). 17CCO6, 17-state coupled channels optical method (Bray *et al*., 1993).

Total Cross Sections (a.u.)					
eV	OP	DWBA	VS	K et al.	17CCO6
7	270.144	263.232	439	314	409
40	95.163	94.374	214	158	198
60	72.196	71.594	157	145	151
100	50.503	50.141	100	114	103
200	30.88	30.732			

Figure 4.34 and table 4.8 show that, as in the case of sodium atom, the absorption potential of Staszewska *et al.* (1984) yields small total cross section values for electron-potassium scattering compared to the 17CCO6 calculation of Bray *et al*.(1993) and the experimental results of Vuskovic and Srivastava (1980) and Kwan *et al*. (1991). This confirms that for alkali atoms the absorption potential of Staszewska *et al*. (1984) as used in the present calculations does not adequately describe small-angle scattering.

CHAPTER 5

CONCLUSIONS AND RECOMMENDATIONS

In this study the optical potential (OP) and first order distorted wave Born approximation (DWBA) methods have been systematically compared in the problem of elastic scattering of intermediate-energy electrons by the alkali atoms of sodium and potassium using various distorting potentials. Based on the results of the study the following conclusions and recommendations can be made:

5.1 Conclusions

- Since for a given distorting potential the OP method gives DCS and ICS results that have converged to infinite order of perturbation series, the very close agreement between the OP and DWBA results when a complex static-exchange-polarization-absorption potential is used indicates that the distorted wave series converges to first order for a complex potential. If the absorption potential is omitted, the DWBA method does not yield converged results.

- Exchange effects can be incorporated in the DWBA method in the form of the exchange T-matrix element as well as the through the exchange distorting potential. In the OP method only the distorting potential can be used. For a static potential the DWBA and OP methods yield quite different DCS at electron impact energies close to the ionization threshold for both sodium and potassium atom. It can therefore be

concluded that the exchange T-matrix element is important at these energies only. The distorting exchange potential is important at all intermediate electron impact energies.

- The non-local polarization potential proposed in this study yields ICS results that are in good agreement with measured and other calculated results. It can be concluded that this polarization potential gives an accurate description of small-angle scattering for electron-alkali atom elastic scattering.

- The absorption potential of Staszewska *et al.* (1984) yields DCS that are generally in good agreement with experimental data for potassium atom. The potential therefore describes fairly accurately inelastic processes in electron-potassium atom scattering. The total cross sections predicted using the absorption potential are however much lower than the values obtained from measurement and other calculations. This indicates the need to improve the determination of the average excitation energy used in the potential instead of taking the average of the first excitation energy and the ionization potential energy as done in this study.

5.2 Recommendations

- For electron-atom elastic scattering calculations at intermediate energies using the DWBA method, a complex distorting potential should be applied instead of a real potential as is routinely done.

- At electron impact energies close to the ionization threshold, the DWBA method, or some other momentum space method, should be applied in elastic electron-atom

scattering to take advantage of the exchange T-matrix element which is not present in the OP method.

- The non-local complex polarization and absorption potential proposed in this work should be tested fully on alkali atoms. This would require use of powerful computers as the memory and speed needed are not available on a personal computer.

- More experimental data especially for electron-sodium atom should be made available in order to resolve the existing discrepancy between measured and theoretical results.

REFERENCES

Allen L.J., Brunger M.J., McCarthy I.E., and Teubner P.J.O. (1987). A complex phaseshift analysis for elastic scattering of 54.4 eV electrons from sodium**.** *Journal of Physics B: Atomic and Molecular Physics.* **20**, 4861 – 4868.

Balashov V.V., Grum-Grzhimailo A.N., and Klochkova O.I. (1989). Inelastic and Superelastic Scattering of Electrons by Sodium: the role of the Imaginary part of the Optical Potential in the DWBA analysis of the 3S – 3P transition. *Journal of Physics B: Atomic and Molecular Physics*. **22**, L699 – L674.

Madison D.H. and Bartschat K. (1996). The Distorted-Wave Method for Elastic Scattering and Atomic Excitation. In Bartschat K. (Ed.) Computational Atomic Physics: Electron and Positron Collisions with Atoms and Ions. (pp. 67 – 86). Berlin: Springer

Bartschat K., McEachran R.P., and Stauffer A.D. (1988). Optical Potential Approach to Electron and Positron Scattering from Noble Gases: 1. Argon. *Journal of Physics B: Atomic, Molecular and Optical Physics.* **21**, 2789 – 2800.

Bray I., Konovalov D.A, and McCarthy I.E. (1991). Electron Scattering by Atomic Sodium: $3^2S – 3^2S$ and $3^2S – 3^2P$ Cross Sections at 10 to 100 eV. *Physical Review A.* **44**, 7179 – 7184.

Bray I. (1994). Convergent Close – Coupling Method for the Calculation of Electron Scattering on Hydrogenlike Targets. *Physical Review A*. **49**, 1066 – 1082.

Bray I., Fursa D.V., and McCarthy I.E. (1993). Calculation of Electron – Potassium Scattering. *Physical Review A.* **47**, 3951 – 3960.

Bray I., Konovalov D.A, and McCarthy I.E. (1991). Electron Scattering by Atomic Sodium: $3^2S – 3^2S$ and $3^2S – 3^2P$ Cross Sections at 10 to 100 eV. *Physical Review A.* **44**, 7179 – 7184.

Bray I., McCarthy I.E., Mitroy J., and Ratnavelu K. (1989). Coupled Channels in the Distorted – Wave Representation. *Physical Review A.* **39**, 4998 – 5009.

Buckman S.J. (1979). PhD Thesis. Electron Collisions with Alkali Atoms. Flinders University.

Buckman S.J., Noble C.J., and Teubner P.J.O. (1979). Intermediate Energy Electron Scattering from Potassium. *Journal of Physics B: Atomic and Molecular Physics.* **12**, 3077 – 3091.

Bunge C.F., Barrientos J.A. and Bunge A.V. (1993). Roothaan-Hartree-Fock Ground-state Atomic Wave Functions: Slater-Type-Orbital Expansions and Expectation Values for $Z = 2 – 54$. *Atomic Data and Nuclear Data Tables.* **53**, 113 – 401.

Chen S., McEachran R. P., and Stauffer A. D., (2008). Ab initio Optical Potentials for Elastic Electron and Positron Scattering from Heavy Noble Gases. *Journal of Physics B: Atomic, Molecular and Optical Physics.* **41,** 025201 (10pp).

Cowan R.D. (1981). The Theory of Atomic Structure and Spectra. Berkeley: University of California Press.

Deitel H.M. and Deitel P.J. (2004). C: How to Program. New Jersey: Prentice-Hall Inc.

Fischer C.F., Brange T. and Jonsson P. (1997). Computational Atomic Structure. London: Institute of Physics.

Furness J.B. and McCarthy I.E. (1973). Semiphenomelogical Optical Model for Electron Scattering on Atoms. *Journal of Physics B: Atomic and Molecular Physics.* **6**, 2280 – 2291.

Fursa D.V. and Bray I. (2012). Convergent Close-Coupling Method for Positron Scattering from Noble Gases. *New Journal of Physics*. **14,** 035002 (18 pp).

Gehenn W. and Reichert E. (1972). Differential Cross Sections for Elastic Scattering of low energy electrons by Sodium. *Zeitschrift fur Physik A*. **254**, 28 – 34.

Gell-Mann M. and Goldberger M. L. (1953). The Formal Theory of Scattering. *Physical Review*. **91**, 398 – 408.

Itikawa Y. (1986). Distorted-wave Methods in Electron-Impact Excitation of Atoms and Ions. *Physics Reports*. **143,** 69-108.

Jabloski A., Salvat F. and Powell C.J. (2004). Comparison of Electron-Elastic-Scattering Cross Sections Calculated from Two Commonly used Atomic Potentials. *Journal of Physical Chemistry*. **33**, 409- 451.

Joachain C.J. (1975). Quantum Collision Theory. Amsterdam: North-Holland.

Kwan C. K., Kaupilla W. E., Lukaszew R. A., Parikh S. P., Stein T. S., Wan Y.J., and Dababneh M. S. (1991). Total Cross-Section Measurements for Positrons and Electrons Scattered by Sodium and Potassium Atoms. *Physical Review A.* **44**, 1620.

Madison D. H., Bartschat K., and McEachran R.P. (1992). Second – Order Distorted Wave Calculation for Elastic and Inelastic Electron – Sodium Scattering. *Journal of Physics B: Atomic, Molecular and Optical Physics*. **25**, 5199 – 5221.

Madison D.H., Lehmann M., McEachran R.P., and Bartschat K. (1995). Elastic and Inelastic Scattering of Electrons from Potassium. *Journal of Physics B: Atomic, Molecular and Optical Physics*. **28**, 105 – 119.

Marinkovic B., Pejvec V., Filipovic D., Cadez I., and Vuskovic L. (1992). Elastic and Inelastic electron Scattering by Sodium at 10, 20 and 54.4 eV. *Journal of Physics B: Atomic, Molecular, and Optical Physics.* **25**, 5179 – 5197.

McEachran R.P. and Stauffer A.D. (2009). An Optical Potential Method for Elastic Electron and Positron Scattering from Argon. *Journal of Physics B: Atomic, Molecular and Optical Physics.* **42,** 075202 (6pp).

McCarthy I.E. and Weigold E. (2005). Electron-Atom Collisions. Cambridge: Cambridge University Press.

McCarthy I.E., Mitroy J.D., and Stelbovics A.T. (1985). Electron Scattering from alkali atoms in the one – electron model. *Journal of Physics B: Atomic and Molecular Physics.* **18**, 2509 – 2517.

McCarthy I.E. and Stelbovics A.T. (1983). Momentum – Space Coupled – Channels Optical Method for Electron – Atom Scattering. *Physical Review A.* **28,** 2693 – 2707.

McMillen (1934). Elastic Electron Scattering in Potassium. *Physical Review*. **46**, 983–988.

Mertzbacher, E. (1970). Quantum Mechanics. New York: John Wiley and Sons Ltd.

Mitroy J. (1993). Electron Scattering from Potassium at Intermediate Energies. *Journal of Physics B: Atomic, Molecular and Optical Physics.* **26,** 2201 – 2215.

Mitroy J., McCarthy I.E., and Stelbovics A.J. (1987). Electron Scattering from Sodium at Intermediate Energies. *Journal of Physics B: Atomic and Molecular Physics*. **20**, 4827 – 4850.

Mittleman M.H. and Watson K.M. (1959). Scattering of charged Particles by Neutral atoms. *Physical Review*. **113**, 193-211.

Press W.H., Teukolsky S.A., Vetterling W.T., and Flannery B.P., (1992). Numerical Recipes in C: The Art of Scientific Computing. Cambridge: Cambridge University Press.

Ryzhikh G. and Mitroy J. (1997). Positron Scattering from Atomic Sodium. *Journal of Physics B: Atomic, Molecular and Optical Physics.* **30,** 5545 – 5565.

Schiff L.I. (1968). Quantum Mechanics. Singapore: McGraw-Hill Co.

Srivastava S.K. and Vuskovic L. (1980). Elastic and Inelastic Scattering of Electrons by Na. *Journal of Physics B: Atomic and Molecular Physics*. **13**, 2633 – 2643.

Staszewska G., Schwenke D.W. and Truhlar D.G. (1984). Investigation of the Shape of the Imaginary part of the Optical – Model Potential for Electron Scattering by Rare Gases. *Physical Review A.* **29**, 3078 – 3091.

Teubner P.J.O., Buckman S.J., and Noble C.J. (1978). Differential Cross Sections for the Elastic Scattering of Intermediate Energy electrons from Sodium. *Journal of Physics B: Atomic and Molecular Physics.* **11**, 2345 – 2354.

Thirumalai D., and Truhlar D.G. (1982). Application of the Matrix – Effective – Potential Formalism to Electron – Neon Scattering at 150 – 700 eV Impact Energy and Comparison to Optical – Potential Calculations. *Physical Review A.* **25**, 3058 – 3071.

Thompson W.J. (1992). Computing for Scientists and Engineers. New York: John Wiley and Sons Ltd.

Shertzer J. and Temkin A., (2006). Direct Calculation of the Scattering Amplitude without Partial-Wave Analysis III. Inclusion of Correlation Effects. *Physical Review A.* **74,** 052701.

Valone S.M., Truhlar D.G., and Thirumalai D. (1982). Localised Second – Order Optical Potential for Electron Scattering in terms of Imaginary – Frequency Susceptibilities. *Physical Review A.* **25**, 3003 – 3014.

Vuskovic L., and Srivastava S.K. (1980). Scattering of Intermediate Energy Electrons by Potassium. *Journal of Physics B: Atomic and Molecular Physics.* **13**, 4849 – 4863.

Yaqiu Liang, Zhangjin Chen, Madison D.H., and Lin C.D. (2011). Calibration of Distorted wave Born approximation for Electron Impact Excitation of Ne and Ar at Incident Energies below 100 eV. *Journal of Physics B: Atomic, Molecular and Optical Physics.* **44**, 085201 (6pp).

Zatsarinny O. and Bartschat K. (2013). The B-spline R-matrix Method for Atomic Processes: Application to Atomic Structure, Electron Collisions and Photoionization. *Journal of Physics B: Atomic, Molecular and Optical Physics.* **46,** 112001 (39pp).

APPENDIX: Computer Program OPDWBA

The following are the descriptions of the computer program OPDWBA used to determine the differential cross sections, integral cross sections, and total cross sections for electron-sodium and electron-potassium elastic scattering.

main ( )

This is the driver function which calls functions HS_MESH and CROSS_SECT.

void HS_MESH(double R[ ])

Sets up the Hermann-Skillman mesh array R[ ]. This mesh is a linear approximation to a logarithmic mesh as described by Madison and Bartschat (1996). In total 1500 mesh points are used with an initial step size given by $h_1 = \left(2.2133535 \times 10^{-3}\right) Z^{-1/3}$ where Z is the nuclear charge of the target atom.

void CROSS_SECT(double *tcsop, double *tcsdw, double DCS_op[ ], double DCS_dw[ ], const double R[ ], double E_eV)

Receives the electron-impact energy, E_eV, in electron volts, and the Hermann-Skillman mesh R[ ] from function main ( ) and returns the differential, integral, and total (elastic + inelastic) cross sections by calling the following functions:

void RHFS_WFUNC(double p_1s[ ], double p_2s[ ], double p_3s[ ], double p_4s[ ], const double R[ ])

Receives the Hermann-Skillman mesh R[ ] from function CROSS_SECT and returns Roothaan-Hartree-Fock ground state atomic radial wavefunctions for orbital angular momentum quantum number $l = 0$ as tabulated by Bunge *et al.* (1993).

void RHFP_WFUN(double p_2p[ ], double p_3p[ ], const double R[ ])

Receives the Hermann-Skillman mesh R[ ] from function CROSS_SECT and evaluates the 2p and 3p Roothan-Hartree-Fock ground state atomic wavefunctions for $l = 1$ using the Slater-type-orbital expansions of Bunge C.F. *et al*. (1993).

void RHFE_WFUNC(double p[ ], const double R[ ])

Receives the Hermann-Skillman mesh R[ ] from function CROSS_SECT and evaluates an excitated-state Slater-type-orbital atomic wavefunctions p[ ] as tabulated by Mitroy (1993), and Ryzhikh and Mitroy (1997).

double MULTI_POT(double V[ ], const double R[ ], const double x1[ ], const double x2[ ], int l)

Receives the mesh and radial wavefunctions from CROSS_SECT and STATIC_POT and evaluates the multipole integrals V[ ] in the static potential (equation 86), and in the direct matrix elements of the polarization potential (equation 99) for the atomic orbitals x1[ ] and x2[ ] using the quadrature rules given in equations (116) and (117). For the static potential $l = 0$, while for the polarization potential $l = \lambda$.

double STATIC_POT(double V_st[ ], const double P_10[ ], const double P_20[ ], const double P_30[ ], const double P_40[ ], const double P_21[ ], const double P_31[ ],const double R[ ])

Evaluates the static potential V_st[ ] (equation 86) by calling MULTI_POT to evaluate the multipole integrals. The inputs to this function are the mesh R[ ], and the ground state atomic orbitals 1s, 2s, 3s, 4s, 2p, and 3p stored in the arrays P_10[ ], P_20[ ], P_30[ ], P_40[ ], P_21[ ], and P_31[ ], respectively.

void EXCHANGE_POTFM(double V_ex[ ], const double V_st[ ], const double p_10[ ], const double p_20[ ], const double p_30[ ], const double p_40[ ], const double p_21[ ], const double p_31[ ], const double R[ ], double E, int S)

Evaluates the exchange potential given in equation (87). The inputs to this function are the static potential V_st[ ], the ground state atomic orbitals 1s, 2s, 3s, 4s, 2p, and 3p stored in the arrays P_10[ ], P_20[ ], P_30[ ], P_40[ ], P_21[ ], and P_31[ ], respectively, the mesh R[ ], the electron-impact energy E, and the total spin S of the electron-atom system.

void POL_POT(double V_pol[ ], const double V1_4p[ ], const double V1_5p[ ], const double V1_3d[ ], const double V1_5s[ ], const double W_l[ ], const double R[ ], const double FACTL[ ], double kl, int l)

Evaluates non-local polarization potential V_pol[ ] which is the real part of equation (102). The inputs to this function are the multipole integrals V1_nl[ ], given by equation (99) obtained using the valence orbital and the various excited states $P_{n_\beta l_\beta}$ considered in the summation in equation (102), the radial scattering electron wavefunction W_l[ ], the mesh points R[ ], the factorials needed in evaluation of the 3-j symbols in equation (102), the momentum kl of the scattering electron, and the orbital angular momentum l of the electron.

void RICATTI_BESSEL (int l, double x, double *fl, double *gl)

Calculates Ricatti-Bessel functions needed in equations (102) and (114) by calling the spherical Bessel function SPHBES written by Press *et al.* (1992). The inputs to RICATTI-BESSEL are the orbital angular momentum l, the product $x = kr$ of the momentum k of the scattering electron and the radial position r of the electron. The function modifies the values of the regular Ricatti-Bessel function fl, and the irregular Ricatti-Bessel function gl in the calling function by use of pointers.

void DWAVE(double P[ ], const double V_HOMS[ ], const double V_INHS[ ], const double R[ ], int l, double E, double v)

Evaluates the radial wavefunction in equation (38) for the real part of the optical potential in equations (86) – (88) using Numerov's method (Thompson, 1992) for $l \leq 3$. The inputs are the sum of the static and exchange potential stored in the array V_HOMS[ ], the non-local polarization potential stored in V_INHS[ ], the mesh R[ ], the orbital angular momentum of the projectile electron l, the electron-impact energy E, and a parameter v related to the value of the static potential near the origin (Fischer *et al.*,1997).

void RE_SHIFT(double *ps, const double R[ ], const double W[ ],double kl, int l)

Extracts the real part of the phase shift ps from the radial wavefunction for $l \leq 3$ using equation (113). The inputs are R[ ], the radial projectile orbital W[ ], the momentum kl, and the orbital angular momentum l.

void QFABS_POT(double V_abs[ ], const double rho[ ], const double V_se[ ], double kl, double I_mean)

Evaluates the quasi-free absorption potential V_abs[ ] given by equations (103) – (109). The inputs are the target-atom electron charge density rho[ ], the static-exchange potential V_se[ ],the momentum kl, and the mean excitation energy, I_mean, in equation (109).

double PS_IM(const double V_abs[ ], const double W_l[ ], const double R[ ], double kl, double rphase, int l)

Returns the imaginary part of the phase shift for the absorption potential of Staszewska *et al.* (1984) using the Hulthen-Kato formalism (Chen *et al.,* 2008) for $l \leq 3$. The inputs are the

absorption potential V_abs[ ], the projectile radial orbital W_l[ ], the mesh R[ ], the momentum kl, the real part of the phase shift rphase, and the orbital angular momentum l.

void PWAVE(double W_l2[ ], double Z_l2[ ], const double W_l[ ], const double Z_l[ ], const double V_SE[ ], const double V_pol[ ], const double V_abs[ ], const double R[ ], double kl, int l)

Evaluates the radial wavefunction satisfying the integral equation (114) iteratively for $4 \le l \le l_{\max}$ where $l_{\max}$ is chosen to ensure convergence of the phase shift. The output arrays are the current real and imaginary parts of the radial wavefunctions stored in arrays W_l2[ ] and Z_l2[ ] respectively. The input arrays and parameters are the previous real and imaginary parts of the radial wavefunction W_l[ ] and Z_l[ ] respectively, the static-exchange potential V_SE[ ], the polarization potential V_pol[ ], the absorption potential V_abs[ ], the mesh R[ ], momentum kl, and orbital angular momentum l.

void KMTXEL(double *kmtx_r, double *kmtx_i, const double W_l[ ], const double Z_l[ ], const double R[ ], const double V_SE[ ], double V_pol[ ], double V_abs[ ], double kl, int l)

Determines the K-matrix element from the radial wavefunction using equation (115) for $4 \le l \le l_{\max}$. The output values are the real and imaginary parts of the K-matrix element kmtx_r and kmtr_i respectively. The input arrays are the real and imaginary parts of the radial wavefunctions W_l[ ] and Z_l[ ] respectively, the mesh R[ ], the static-exchange potential V_SE[ ], the polarization potential V_pol[ ], the absorption potential V_abs[ ], the momentum kl, and the orbital quantum number l.

void CMPLX_PS(double *Re_w, double *Im_w, const double x, const double y)

Extracts the complex phase shifts from the K-matrix element given in equation (115) for $4 \le l \le l_{\max}$. The output values are the real and imaginary phase shifts Re_w and Im_w respectively. The input is the real and imaginary parts of the K-matrix element x and y respectively.

void DIR_TMXEL1(double *dtm_r, double *dtm_i, const double Re_ps, const double Im_ps)

Evaluates the first direct T-matrix given by equation (44). The input values are the real and imaginary phase shifts Re_ps and Im_ps respectively.

void DIR_TMXEL2(double *dtm_r, double *dtm_i, const double Ub_ex[ ], const double VR_Inh[ ], const double VI_Inh[ ], const double W_l[ ], const double Z_l[ ], const double R[ ])

Evaluates the second direct T-matrix given by equation (50). The output values are the real and imaginary parts of the matrix element. VR_Inh[ ] and VI_Inh[ ] are obtained by multiplying the polarization potential and absorption potential by the projectile radial wavefunction.

void EXCH_CORE_TMXEL(double *rtm, double *itm, const double W_l[ ], const double Z_l[ ], const double P[ ], const double R[ ], int lb, int l, double FACTL[ ])

Evaluates the exchange T-matrix element given by (72) for the core target electrons. The input are the real and imaginary parts of the exchange matrix element, the real and imaginary parts of the radial wavefunctions, the target electron wavefunction, the mesh , the orbital

angular momenta of the target and projectile electrons respectively, and factorials need in calculation of 3-j symbols.

void EXCH_VALENCE_TMXEL(double *rtm,double *itm, const double W_l[ ], const double Z_l[ ], const double P[ ], const double R[ ], int S, int l, double FACTL[ ])

Evaluates the exchange T-matrix element given by (85) for the valence target electron. It is similar to EXCH_CORE_TMXEL but involves the total spin S of the electron-atom system.

double DCS_OP(const double d1[ ], const double d2[ ], double kl, int lmx, int deg)

Determines the differential cross sections in the OP method using equations (9) and (44). The input arrays contain the real and imaginary phase shifts. The input values include the momentum of the projectile, the maximum orbital angular momentum $l = 60$ of the projectile and the scattering angle θ.

double DCS_DWBA(const double d1[ ], const double d2[ ], const double DTM_R[ ], const double DTM_I[ ], const double RTM[ ], const double ITM[ ], double kl, int lmx, int deg)

This function determines the differential cross sections in the DWBA method using equations (9), (44), (50), (72), and (85). The input arrays contain the real and imaginary phase shifts, the direct and exchange T-matrix elements, the momentum of the scattering electron, the maximum l value, and the scattering angle.

double TCS_OP(const double d1[ ], const double d2[ ], double kl, int lmx)

Calculates the total cross sections in the OP method based on equation (112). The input arrays are the real and imaginary phase shifts, the momentum of the projectile and the maximum l value. For a real potential, this function returns the integral cross section, defined by equation (110), for the OP method.

double TCS_DWBA(const double d1[ ], const double d2[ ], const double DTMR[ ], const double DTMI[ ], const double ITM[ ], double kl, int lmx)

Calculates the total cross sections in the DWBA method in accordance with equation (112). The input arrays are the real and imaginary phase shifts, the direct and exchange T-matrix elements, the momentum of the projectile and the maximum l value. For a real potential, this function returns the integral cross section, defined by equation (110), for the DWBA method.